

Alma Mater Studiorum – Università di Bologna

DOTTORATO DI RICERCA IN

CHIMICA

Ciclo: XXVIII

Settore Concorsuale di afferenza: 03/A2

Settore Scientifico disciplinare: CHIM/02

**Electrochemistry of molecular systems for
new nanostructured materials and
bioelectronic devices**

Presentata da: Eleonora Ussano

Coordinatore Dottorato

Prof. Aldo Roda

Relatore

Prof. Massimo Marcaccio

Esame finale anno 2016

Contents

Preface	I
Chapter 1:	
1 Introduction	1
1.1 Top-Down and Bottom-Up Approach towards miniaturization	4
1.2 Supramolecular approach towards nanodevices	5
1.3 Electrochemistry role	6
1.4 How to investigate nanoworld	8
1.4.1 Optical techniques	8
1.4.2 Electron Microscopy	8
1.4.3 Scanning probe microscopy	9
1.5 Uses and benefits of nanotechnology	10
1.5.1 Life Science and Medicine	10
1.5.2 Information and comunication	11
1.5.3 Energy conversion and storage	12
1.6 Safety of nanomaterials	15
1.7 Highlight on selected Carbon Materials	16
1.7.1 Graphene	16

1.7.2 Graphene synthetic strategies	18
<i>Top-Down</i>	18
<i>Bottom-Up</i>	19
<i>Bottom-Up</i> through Chemical Synthesis	20
1.7.2 Graphene derivatives	23
1.7.3 Other nano-allotropic forms of Carbon	23
Fullerenes and Carbon Nanotubes	24
1.8 The aim of this work	25
References	27

Chapter 2:

2 Graphenic structure formation through electrochemistry	30
2.1 Corannulene	30
2.1.1 Electrochemical behavior	32
Corannulene Reduction	32
Corannulene oxidation and polymerization	33
Electrochromism	35
2.1.2 Determination of deposit mass	36
2.1.3 X-ray Photoemission Spectroscopy of poly-Corannulene	37
2.1.4 Morphological investigation by SEM and AFM	38

2.1.5 Theoretical Calculations	40
2.2 HexaBenzoCoronene	42
2.2.1 Voltammetric Properties	43
2.2.2 Investigation on the chemical nature of the deposit	44
2.2.2.1 Absorbance spectroscopy	45
2.2.2.2 LD-TOF	45
2.2.2.3 Raman	46
2.2.3 Morphological investigation of the deposit	47
2.2.3.1 AFM	47
2.2.3.2 TEM Investigation of aggregates	48
TEM Instrumental Equipment	50
2.2.3.3 X Ray Diffraction	50
2.3 Triphenylene	52
2.3.1 Electrochemical oxidation of O-Terphenyl	53
2.3.2 Chemical and morphological composition of Triphenylene-based deposit	56
2.3.2.1 LD-TOF Spectrum of deposited film	56
2.3.2.2 Absorbance and Raman Spectra	57
2.3.2.3 AFM	59
2.3.3 Carbons substrates for enzymatic catalysis	60
2.3.3.1 Basic enzymatic working mechanism	61

2.3.3.2 Nanostructured Carbons for Enzyme studies	64
References	68

Chapter 3:

3 Doped and functionalized Nanocarbons for energy conversion	70
3.1 Oxygen Reduction Reaction	70
3.1.1 Nanocarbons for ORR	73
3.1.2 Nitrogen doped reduced Graphene Oxide (rGO- N)	74
3.1.2.1 Synthesis and characterization of rGO-N	76
3.1.2.2 Electrochemical characterization	80
3.1.2.2.1 Cyclic Voltammetry	80
3.1.2.2.2 Rotating Disc Electrode Voltammetry	82
3.1.2.3 Scanning electrochemical microscopy	88
Generation-Collection SECM mode on rGO-N	88
Kinetic electron transfer constant	92
3.2 Fullerene based photoelectrochemical conversion system	93
3.2.1 Absorption and fluorescence measurements	93
3.2.2 Electrochemistry of Bodipy-C ₆₀	94
3.2.2.1 Voltammetric Investigation	94
3.2.2.2 UV-Vis-NIR Spectroelectrochemistry	98

3.2.3 Time resolved spectroscopy 100

References 104

Chapter 4:

4.1 Principles of Electrochemistry 105

4.1.1 Electron Transfer 105

4.1.2 Kinetic and Mass transport at the Electrode Surface 106

Kinetic at the electrode surface 106

Mass Transport 107

4.1.3 Techniques and equipments 108

4.1.3.1 Voltammetry 108

Linear Sweep Voltammetry 109

Cyclic Voltammetry 110

Rotating Disc Electrode Voltammetry 112

Electrochemical Induced Reactions 115

4.1.3.2 Electrochemical equipment 116

Electrochemical cell 117

Solvent and electrolyte treatment 117

4.1.4 Spectroelectrochemistry 118

4.1.4.1 SEC Equipment 119

4.2 Raman Spectroscopy	119
4.2.1 Raman Spectroscopy equipment	120
4.3 LD-TOF Mass Spectroscopy	120
4.3.1 LD-Tof Equipment	121
4.4 Atomic Force Microscopy	121
4.4.1 AFM Equipment	123
4.5 Scanning electrochemical Microscopy	123
4.5.1 SECM Equipment	126
4.6 X-ray Photoemission Spectroscopy	126
4.6.1 XPS Equipment	127
References	128
Chapter 5:	
5 Conclusions	129

Preface

Nanomaterials have a tremendously increasing importance in our daily lives, probably much more than we can imagine, for the great number of ripple effects they can produce. The reason for such importance is due to the size depending properties of the *infinitely small* that are completely different than that of large scale objects. Part of these properties are intrinsic of nanometric dimension particles while some others depend on the interaction between nanomaterials and incident energy.

In order to deal with nanomaterials and nanotechnology, chemistry has adapted and contributed with new theories and tools, trying to meet also the incoming necessity for cleaner technologies. Electrochemistry, in particular, dealing with fundamental electronic processes, can deeply investigate nanomaterials catalytic properties or provide new synthetic strategies.

Nanomaterial world is extremely wide and the main aim of this work is to implement the knowledge about these materials, focusing in particular on some of the nano allotropic forms of Carbon. This precise choice is consequence of their promising properties for electronic, energetic and biological applications.

Nanocarbons are extremely robust and versatile and, thanks to their low-dimension charge carrier transport, can be used as nanometric electrodes. Nanocarbons surface properties are enhanced compared to bulk materials and can be further improved by functionalization.

The first chapter of this dissertation introduces nanomaterials, highlighting their importance, recent developments in their study and application as well as future perspectives.

The second chapter reports the investigation and the proposal of a new synthetic pathway for nano-Graphene production. The principal building blocks for Carbon based nanomaterials are polyaromatic hydrocarbons that, through chemical dehydrogenation, can be intramolecularly or intermolecularly oxidatively cyclized in order to create extended conjugated structures.

Using electrochemistry I have been able to oxidize polyphenylene (HexaPhenylBenzene, O-Terphenyl) and polyaromatic hydrocarbons (Corannulene) which leads to the deposition of an insoluble films on the electrode. In order to confirm their structures and clarify their morphologies, a variety of techniques from mass detection to spectroscopy or surface microscopy have been used. The results of this work are the proof that electrochemistry can be used as an alternative method for building up Graphenic structures following a bottom-up strategy. The first visible advantage of this approach, compared to chemical synthesis, is that such films, directly deposited on the working electrode surface, are ready to be used without any further purification. To have an idea of the possible bio-applications of such Carbon nanostructures, an enzyme adhesion experiment has been performed, during the period spent in the group of professor Armstrong in Oxford.

The third chapter of this thesis has a more applicative perspective, focusing on the study of some energy uses of doped and functionalized nanocarbons.

With the purpose of finding a valid alternative to metal catalysts for Oxygen reduction reaction (ORR), the electrocatalytic properties of Nitrogen-doped Graphene have been tested. This property is probably due to two cooperative effects: the notable difference of density of states with respect to Graphene, introduced by the foreign atom in the lattice, and the different local surface electronegativity, which seems to promote local dipole formation with an increase of substrate binding. The results

obtained in this part are promising for application of this class of nanocarbons as catalysts for Oxygen Reduction Reaction in fuel cells or lithium-air batteries.

In this framework, also a system for photoelectrochemical conversion has been investigated. In such a trendy topic for green energy production, the coupling of a light-catching moiety with a charge delocalizing one, in order to avoid fast electronic recombination, is required. Among all the extraordinary properties of nanocarbons there is also their capability to delocalize electrons, thanks to their sp^2 structure, and, as a consequence, their optimal use in charge separation devices. In order to find a suitable alternative, a dyad formed by a Bodipy chromophore and a Fullerene has been studied. The investigation of its electronic properties was carried out by performing electrochemical and photophysical measurements, in order to understand the photoinduced electron transfer. The cross-checking of data demonstrates the effective charge separation between donor and acceptor and opens the way for the application of such supramolecular assembly in photoelectrochemical devices.

This work does not claim to be comprehensive but it wants to give a contribution to the knowledge on such a complex topic and to explain some fascinating results obtained for the systems and nanostructures that have been studied.

1 Introduction

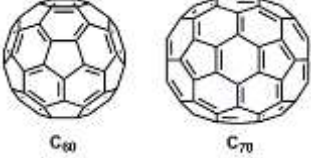
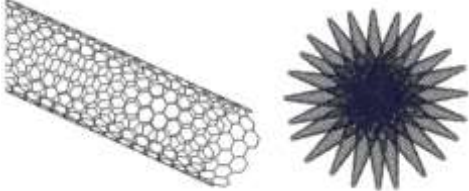

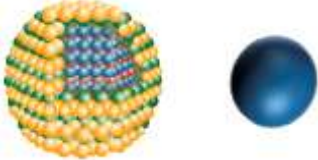
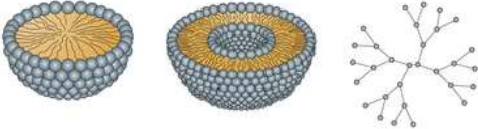
In the last few years technology is undoubtedly become the main engine of our daily life, pushing the development of our society and helping science with new equipment that transformed assumptions in discoveries, making for example possible for scientists to see and manipulate the infinitely small. On the other side no technological development would be possible without science, that provides new materials and solutions to nowadays problems.

Great part of scientific studies and financing all around the world are addressed to the possible discovery and applications of nanomaterials that have surely given new input to material science. The term nanomaterials indicates extended molecules or materials, generally having at least one size, internal or in the surface structure, in the nanoscale. ^[1] The reason why nanometric size objects are so interesting is due to their special features; size affects material properties and the way external inputs interact with these materials can be completely opposite with respect to conventional bulk materials. Size depending properties have great scientific relevance and have been deeply investigated in the last few years. As meaningful examples are quantum confinement, surface plasmon resonance and superparamagnetism, respectively for semiconductor, metal and ferromagnetic nanomaterials.

Actually nanomaterials is not a human invention, nature has surely the primary merit of using nanometric scale objects to reach performances that would not be possible in any other way, making possible the slow continuous steps of evolution through million years adaptation. A clear example of natural functional nanomaterials is the gecko toes structure, thanks to its hierarchically organized β -keratin. Every gecko toe is covered by lamellae made of micrometric size setae ending in nanometric spatulae.

Every single spatula interacts with surface through attractive Van Der Waals forces that multiplied for the great number of spatulae guarantees adhesion. ^[2] Contrary to gecko super adhesion, nature shows also superhydrophobic surfaces. Lotus effect, from the name of the plant that primary shows this behaviour, is due to the presence of a great number of hydrophobic nanostructures on the leafs. The high surface tension of water drops and this peculiar nanostructures makes water contact angle higher than 90 degrees, typical threshold value between hydrophilic and hydrophobic surfaces, preventing water to remain and wet its leafs. As a consequence, dirty particles eventually deposited on the leaf are easily entrapped by falling water drops with a self-cleaning effect, a natural, safe, clean and no-cost strategy to protect against pathogens. ^[3]

From the observation and study of nature phenomena science has taken inspiration to design new molecules, materials and new functions, using them for its own advantage. The first scientist who understood the importance of nanoworld and the possibility to drastically decrease size was surely Richard Feynman, in the late fifties of last century, many years before nanotechnology development. Even if he never used the word “nano”, during his famous talk “There’s plenty of room at the bottom” he prophetically predicted the possibility of directly “manipulating and controlling things on a small scale”. He suggested that dealing with small scale objects has nothing in common with large scale, as they follow quantum mechanics laws, and thus their manufacturing would be possible using, for example, quantized energy levels or interactions of quantized spins. Feynman imagined and predicted a number of phenomena, some of them actually have become common nowadays, but the great hope and purpose of his talk was to suggest physics to enter a new field. He compared the nanoscale study to a new scientific revolution and encouraged his audience to serve scientist from other fields, like biology and chemistry, providing them with new tools to see and handle microscopic objects. ^[4]

Material	Particle	Dimension in the nanoscale
Carbon	<p data-bbox="396 278 533 305">Fullerenes</p>  <p data-bbox="396 498 899 566">Nanotubes, nanohorns, nanooxions, nanodiamods</p>  <p data-bbox="396 862 821 893">Graphene, Graphene derivatives</p> 	<p data-bbox="924 278 963 305">3D</p> <p data-bbox="924 511 963 538">2D</p> <p data-bbox="924 902 963 930">2D</p>
QDs (Zn, Cd, Pb / S, Se,Te), Au, Ag, Pt, SiO ₂	<p data-bbox="396 1106 705 1137">Inorganic Nanoparticles</p> 	<p data-bbox="924 1106 963 1133">3D</p>
Organic Molecules	<p data-bbox="396 1361 825 1392">Micelles, Liposomes, Dendrimers</p> 	<p data-bbox="924 1361 963 1388">3D</p>

Tab. 1 example of various nanomaterials, their composition, and dimensions

Science contribution has brought in our daily life some nanometric objects, as Titanium Dioxide nanoparticles in sunscreens or Carbon Nanotubes (CNT) in high performance sport equipment. ^[5] Despite their trivial use there is still a lot of room for studying nanomaterials properties and their possible innovative applications. The most interesting application would surely be the technological one that implies the use of such materials in complex systems, able to perform specific operations. Likewise in macroscopic devices, each nanosized component would perform a simple act contributing to the complex whole function. This is of great interest and stimulus for scientist and investors especially because it intrinsically means miniaturization. Bulky materials can be used in microscopic devices through top-down scaling processes but the size of products obtained with this kind of approach is limited to hundreds of nanometres while the possibility of using nanomaterials could permit the bottom-up realization of devices.

1.1 Top-Down and Bottom-Up Approach towards miniaturization

As the name implies, Top-Down approach means decomposing something big to obtain smaller size parts. In material science and technology top-down consists in providing microdevices manipulating bulky materials. Silicon industry and all kind of micromachines are nowadays possible thanks to lithography that uses light (photolithography) or electron beams to modify the starting material. This technique has been largely implemented trough years and nowadays it is possible to have patterns in the tents of nanometers using, for example, two-photon lithography ^[6], X-ray lithography or extreme ultraviolet lithography. ^[7] Important strides have been done towards nanodevices production but it is still very difficult and expensive to overcome wavelength diffraction limit. A possible solution to obtain nanometric functional objects would be to change the scaling approach using bottom-up.

Bottom-up approach is quite the opposite respect top-down and builds up a structure starting from the lowest to the highest level of its hierarchic organization. In technology this approach implies the building up of devices from the littlest possible parts as atoms, molecules or nanostructures. Chemists are used to deal with some of the smallest components of matter, molecules, so they can easily imagine to build devices from the bottom. The construction strategy is clearly different respect the top-down, bypassing, for example, doping processes and obtaining directly the already doped material. Great advantages of bottom-up approach would reach smaller dimensions with respect to that obtained with lithographic techniques and an atomically precise control of the structure, with an increase of the amount of stored information and on the portability of crafts.

Atom by atom bottom-up seems to be almost impossible with current technology as atoms are not simple spheres that can be moved from one place to the other. Even though the idea of using nanotweezers to manipulate atoms is very fascinating it seems too much simplistic because it overlooks on the importance of molecular bonds. In fact, the risk is that once a nanotoll interact with atoms they would create bonds that could not be easily broken.^[8]

1.2 Supramolecular approach towards nanodevices

A more realistic step towards bottom-up nanodevices production would be the use of molecular building blocks that are undoubtedly more stable and easily to manipulate with respect to atoms. Another great advantage of molecules is that they can show well defined properties as a consequence of external inputs (i.e., light or electrons), giving a functional response. Nature shows a wide range of bionanodevices, which functioning is possible thanks to *unusual* bonds. Enzyme-substrate recognition, neurotransmission, genetic code transcription and mitochondrial electron

transport chain are only some of the supramolecular based processes in life. Differently than molecular chemistry, which is based on covalent bonds, supramolecular is “chemistry beyond the molecules”, based on conventional bonds but, above all, on intermolecular forces (electrostatic interactions, Hydrogen bonds and Van Der Waals forces) that drives molecular self-assembly.

This makes Self-Assembly complementary to common synthetic strategies and enables molecules to interact even without chemical bonds to create higher structures. This is used since the beginning of time by nature to build up and select the best structures but it can be used also by scientists for creating highly organized structures from molecular building blocks.

Chemists have a big challenge in taking nature’s example, designing molecules capable to interact specifically with each other, combining molecular chemistry knowledge with non-covalent architecture ^[9] in order to improve knowledge and progress.

1.3 Electrochemistry role

Electrochemistry is the part of chemistry that deals with electron transfer (ET) and it has a primary role in life because is used by several natural nanomachines to operate. One of the most relevant and beautiful examples of such ET driven nanomachines is given by the mitochondrial respiratory chain that produces ATP. ^[10]

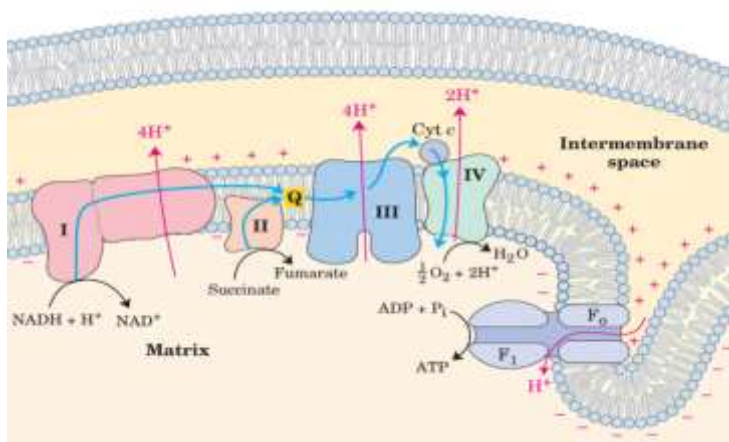


Fig. 1 Representation of ET (blue arrows) in mitochondrial respiratory chain. The coupled electrical and chemical potential drive the proton motive ATP synthesis

Taking advantage by nature's example, scientists can investigate the complexity of nanoworld and use electrochemistry to drive or check electronic and catalytic properties of these novel materials.

Electron transfer is, as the name implies, the transfer of one or more electrons between two redox active species, an electron-donor and an electro-acceptor. The great potential of electrochemistry is due to the bi-directionality of electron exchange that makes these reactions reversible. In some cases, chemical reactions can subtract the reactive reduced acceptor before the reverse electron transfer can happen. This phenomenon is not always undesired, in fact, in this way electrochemistry is exploited as a synthetic tool to build up structures.

The only possible problem in applying electrochemistry to nanoparticles (NPs) is that their uncommon and fascinating properties can make their investigation non-trivial. Chemical and physical properties are often different from bulk material and therefore electrochemical response can be surprising; it has been demonstrated that NPs influence electric double

layer affecting interfacial ET, affect mass transport and in some cases also reproducibility because of their lack of stability. ^[11]

1.4 How to investigate nanoworld

Together with conventional analytical techniques, able to identify sample composition, there are many others able to see and manipulate NPs in order to understand their morphology and relate their structure to properties.

1.4.1 Optical techniques

As previously mentioned, optical techniques have resolution limitation by incident light wavelength but some interesting information can, however, be obtained. A simple but effective way to distinguish NPs by their size is possible simply looking at the colour of their solution, because of light-particles interaction. It is in fact possible to distinguish NPs suspension colour changes during the reaction, indicating NP growth. A useful optical technique used to determine NPs size is Dynamic Light Scattering that takes advantage of the capability of particles smaller than incident wavelength to elastically scatter light; the collected scattered light is elaborated and its angular dependence is used to go back to particle size distribution profile. ^[12]

1.4.2 Electron Microscopy

One of the most efficient technique for reaching atomic resolution is Transmission Electron Microscopy (TEM) that uses the dual nature (particle and wave) of electrons. An accelerated and focused electrons beam passes through a sample and the intensity of coming out electrons depends on the

interaction they had with the sample, its molecular composition and density but also information on the outcoming wavelength, its phase and period. Even if TEM has a considerable better resolution than optical techniques, because of the short wavelength of electrons, aberration problems still exist but can be corrected using phase contrast transfer function to resolve image. Such technique, called High Resolution Transmission Electron Microscopy (HRTEM), have become a fundamental tool in material science and it's commonly used to investigate Carbon materials, as Graphene or Carbon nanotubes; its impressive resolution, that can reach 0.05 Å, makes possible to see individual atoms or punctual defects of samples.

1.4.3 Scanning probe microscopy

The term scanning probe microscopy includes a series of techniques able to show the infinite small topography of nanosurfaces.

The image reconstruction of a nanometric surface needs to be done with probes that have the same order of magnitude of the sample. The first technique used to *see* nanoobjects, was Scanning Tunnelling Microscopy (STM), developed in 1982, that uses as probes electrons, flowing from a tiny and sharp tip, installed on a piezoelectric tube, to the sample. Such a current, promoted by an applied voltage, when the tip is sufficiently close to the substrate, is a quantum mechanical tunnelling current. During the scan of the area, the tip explores different morphologies and the tunnelling current is affected by the distance tip-sample surface underneath. STM can work in two different modes, constant high tip and constant current; in the first case the surface electronic density is given by changes in the registered tunnelling current, in the latter case it is given by the profile of the moving tip that adjusts its position from the surface with a feedback to keep current constant.

Between scanning probe technique a fundamental role is hold by Atomic Force Microscopy (AFM) that exploit Van Der Waals forces to follow the morphology of surfaces on the nanoscale.

1.5 Uses and benefits of nanotechnology

Nanotechnology would provide great benefits in several research areas especially in life science, communications and energy conversion.

1.5.1 Life Science and Medicine

In life science and medicine new diagnostic tools and new proficient technology to care diseases would be available. This application of nanotechnology was imagined in ninety eighties by Kim Eric Drexler, who also invented the name nanomachine. He imagined these curing devices, driven by an internal nanocomputer, which could travel through blood and tissues, analyze cellular content to identify diseases and then operate it. ^[13] Actually, this view is not completely science fiction, in fact, nanometric devices comparable in size with living cells could really help in studying them in their real environment, imaging, detecting and eventually curing. Sensing devices using nanomaterials for extracorporeal detection are extensively studied and great deal could be the application of surface plasmon resonance (SPR) together with electrochemistry. The coupled application of these two techniques started in late seventies ^[14] but the development of nanomaterials have recently brought new life to this field. When light interacts with metals there's a change in the refractive index due to the interaction between incident light and the oscillation of conduction electrons at the metal-air interface; if the component of the wavevector of incident light matches that of surface plasmon, resonant condition can be reached. The advantage of using nanometrical structures,

respect to bulk materials, is due to the formation of nano-resonant structures, in the order of magnitude of the wavelength, trapping plasmons and producing a huge enhancement of the optical resulting field. ^[15] Nanostructure-driven enhancement is an obvious advantage for sensing and biosensing as was demonstrated by Bartlett and co-workers who were able to discriminate polimorphic pathogens with an electrochemically driven denaturation coupled with surface enhanced Raman spectroscopy (SERS). ^[16] In the future nano-sensing devices could be used for *in vivo* detections or nano-drug carriers could be addressed directly to the target tissue. The last possibility would represent a revolution especially in cancer caring approach; the local release of functional molecules would, in fact, avoid safe tissues poisoning, with important consequences on patient life quality and hope of survival.

1.5.2 Information and communication

Concerning information and communication, incredible progresses have been done in the last forty years but at the moment semiconductor industry is at an impasse, limited by fundamental physical barriers. As previously mentioned, common technology production and reading of data are performed using electromagnetic radiation, with a dramatic dependence on size, preventing from using circuits smaller than the used wavelength. Bottom up, or at least hybrid bottom up/top down fabrication, could bypass this problem because functional building blocks would bring in the resulting nano-architecture their feature avoiding further processing steps, as lithography. Integrated circuits could be replaced by nanosized components able to perform binary logic and, if miniaturization would go hopefully down to molecular computers, single molecules would operate as circuit elements, increasing the information density with great advantages for memory devices. An example of future nanoelectronic is given by pioneering Carbon Nanotubes (CNTs) based devices; similarly to

conductive or semiconductive nanowires they can be assembled in arrays in which every crosspoint is controlled by voltage to form the base of a memory bit. ^[17] Several efforts are addressed to the production of flexible nanotechnological devices, which would join the advantages of lightness, low-cost and flexibility of organic polymers with the high-density area and the special properties of nanomaterials. CNTs, deposited by chemical vapor deposition on polymeric supports, behave as p-type field effect transistors but their chemical modification can also show n-type transistor behavior. ^[18] An example of hybrid organic-inorganic flexible device has been realized using cobalt ferrite semiconductor NPs and pentacene ^[19] but, if using NPs, it is relatively easy to achieve monodispersion, using Graphene is much complicated. Dispersion is fundamental to obtain uniform material and device properties, for this reason Eda and coworkers developed a simple solution-based method to control the deposition of single or few layers Graphene on large areas. Starting from Graphene Oxide (GO) solution, by vacuum filtration, they were able to obtain a GO modified substrate and, after its fundamental reduction, a dispersion of Graphene. This kind of approach demonstrates, together with the dispersion of an insoluble material as Graphene, also the possibility to tune opto-electronic properties through the tuning of material dispersion. ^[20]

1.5.3 Energy conversion and storage

Nanomaterials could give also an enormous help to energy conversion and storage. In the last decades pollution, energy crisis and the conscience that earth resources are not endless, have betrayed the urgency to find new valuable solutions to maintain the actual industrial development respecting our planet. In this view, energy conversion and storage could benefit of nanomaterials peculiar properties, providing cleaner, low cost and small size power suppliers.

Energy producing reactions are carried out thanks to catalysts that participate to reactions without being modified and accelerate slow reactions of several orders of magnitude. Their working mechanism provides, in fact, an alternative lower energy way respect to uncatalyzed reactions, causing a decrease of the rate constant. ^[21] The most used industrial catalysts are metals, like Platinum, Rhodium or Ruthenium, that are rare, costly and easily poisoned; for these reasons it is very difficult to massively use them and, in the aim of solve this problem, metallic NPs for catalysis or electrocatalysis have been used. Even if reduction of particle size increases dispersion, lowering costs, catalytic properties does not scale linearly with dimension and some particles lose their metallic behaviour or can be easily passivated, making the investigation of their behaviour really complex. ^[22]

There is an urgent need in using power sources alternative to fossil fuels. Some important alternatives already exist but the main problem in using them is their conversion and storage, as they are mostly uncontinuos sources. Sun and wind are subjected to daytime, seasonal variations or weather conditions while Hydrogen and Carbon Dioxide should be produced from eco-friendly processes.

In the aim of facing such a problem, a huge number of publications have been made in the last decades about functional nanomaterials. Important results in water splitting for molecular Hydrogen (H₂) production have been obtained using Carbon or Titanium Dioxide (TiO₂) based nanotubes. ^[23] Another possible way to produce *green energy* is the direct conversion of sunlight, imitating natural photosynthesys with antenna systems able to collect electromagnetic radiation and convert it to chemical or electrochemical energy. Solar driven H₂ production hybrid inorganic-organic-biological system has been realized using Ruthenium photosensitizer complexes adsorbed on Hydrogenase modified TiO₂ NPs. ^[24] Concerning photoelectrochemical conversion, several nanomaterials have been tested as quantum dots ^[25], dendritic structures ^[26] or

supramolecular systems based on light catching metalloporphyrins and fullerenes (C_{60}), which are very good in delocalizing and stabilizing charge, thanks to their extended charge delocalization capability. ^[27] The distinctive feature of this kind of systems, called *dyads*, is the capability to promote charge separation in the structure. This peculiar behaviour, fundamental for charge injection in external circuit, is due to the exceptionally high driving force of the reaction; the resulting decrease of the back electron transfer rate constant makes it extremely slow and the charge can be injected in the external circuit, useful for application. ^[28]

Also electrochemical energy storage, lithium batteries, fuel cells and supercapacitors, can surely take advantage from recent development of nanostructured electrodes and electrolytes. Especially for Lithium batteries the use of nanomaterials could bring several advantages as the possibility of exploiting reactions otherwise not possible with bulk materials, as well as higher charge rates and increased cycle lifetime. The improvement of such properties are direct consequences of NP surface area, high electrode/electrolyte surface contact area and a better resistance to intercalation-deintercalation stress. ^[29] There are of course some disadvantages that need to be overcome and further work is still required but there is room for advances.

All these efforts would hopefully bring to the reduction of environmental pollution problem, resources consumption and to the direct production of energy in areas where is not easily available; in any case, bottom-up fabrication would guarantee precise control of the growing structure with less wastes during the preparation process and clear benefits for the environment.

1.6 Safety of nanomaterials

The rise in the study and application of nanomaterials has obviously increased the attention to their safety. In fact, there are some concerns about their consequences on environment and human health. It is really difficult to find an accord in establishing nano-objects risks especially because there is still no accord on the parameters that every toxicological study should include. Due to their nanometric size they can accidentally enter organism through ingestion, inhalation or dermal absorption, passing through skin and other tissues. To understand NPs toxicity it is not possible to refer only to particle size or distribution; in fact, impurities, chemical composition, degree of aggregation and surface chemistry can play a fundamental role. Moreover, when nanosized object interacts with living tissues, proteins are rapidly absorbed on NP surface, forming a layer called protein corona that greatly influence their biological outcome. Nanoparticles interacting with tissues have a biological identity which is slightly different than their synthetic one; this has several consequences on the way nanoparticle-corona complex interacts with living matter, on the eventually change in their dispersion and on the damage they can induce. In some cases it has been demonstrated that NPs immediately acquiring protein corona in cell serum bind to cell membrane less tightly respect NPs that do not present a preformed corona. ^[30] Upcoming scientific studies should take in serious account also culture media, to avoid producing an incomplete idea of such a complex topic using only common *in vitro* essays. Further scientific and toxicology studies are necessary to join the great potential of nanomaterials with their safe application. Investigation and clarification of all the possible benefits and risks of NPs and nanotechnology should be placed side by side with a correct communication. Only caution and conscience could avoid people misinformation, fear and excessive restrictions, finding the right way for a real progress.

1.7 Highlight on selected Carbon Materials

1.7.1 Graphene

Among new materials one of the most promising for device application is Graphene, thanks to its strength and conduction properties it could be the ideal candidate for replacing Silicon or doped Silicon in devices. Silicon is the second most abundant element present on earth crust ^[31], its technology is widely used and efficient but its isolation, purification and doping processes require several expensive procedures. Studies on Graphene can pioneer the production of strong, flexible and low cost crafts.

Graphene is a bidimensional material, one of the Carbon allotropic forms, characterized by an sp^2 orbital hybridization. Crystalline structure reveals an hexagonal basic unit that is repeated ideally endlessly. Its unique structure is responsible for all Graphene properties, in fact, the entire lattice is formed by covalent bonds that gives an enormous strength along the Graphene sheet. Molecular orbitals π on the carbon hexagons which lay on both sides of the plane are available for electronic out-of plane conduction and eventual reactions. ^[32] In terms of electronic conduction single layer Graphene has a very peculiar behaviour, different than semiconductors or metals, in fact, the potential surfaces of valence (VB) and conduction band (CB) have a unique conical shape that meets in Dirac points. For its energy gap lack, Graphene is usually compared to metals even if at Dirac points its density of states vanishes, differently than metals that always keep a finite density of states, resembling more to relativistic particles rather than electrons. ^[33]

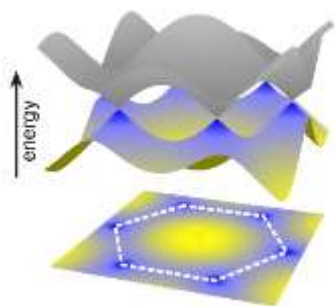


Fig. 2 Example of the potential energy surfaces of Graphene and Dirac points formation

As concerns the reactivity of Graphene, a very important role is played by the edges. In fact, it has been demonstrated that edges are more reactive than bulk respect to substitution and cycloaddition reactions. ^[34] Strano and co-workers deeply investigated the behaviour of single, multi-layer, bulk and edges Graphene using Raman and ET theory. They attributed the enhanced reactivity to the relative disorder reflected in D Raman peak. The decrease of Dirac point energy, consequent to the overlap between Graphene density of states and other reagents vacant oxidation states, seems to be responsible for this reactivity.

When Graphene is not ideal, due to the presence of defects, doping, non infinite extension of the sheet or multiple layers, its density of states is deeply affected and its properties change, especially conduction. Such factors obviously modify conjugation and aromaticity of the system which are proportional to the extension of the molecule and to the bulk-edge ratio. This complexity of structure and related properties is well exemplified by Graphene nanoribbons (GNRs). This two-dimensional structure consists in a Graphene portion with one finite width, that have differently occupied states than Graphene and whose conductive,

semiconductive or isolating behaviour depends on several factors as width and atom orientation at the edges. [35]

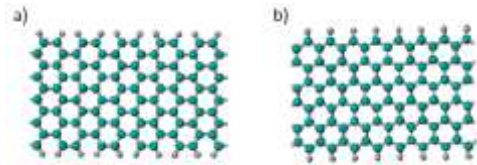


Fig. 3 a) Armchair and b) Zig-zag orientation of Carbon atoms at Graphene or GNRs edges

The modification of the properties does not necessarily imply a decline of its functions, Graphene continuous conduction can, in fact, impede its use as digital switch in electronics while *imperfect* materials can be modulated and their electronic conduction, when required, turned off. [36]

1.7.2 Graphene synthetic strategies

There are two main strategies for Graphene synthesis, *top-down* and *bottom-up*.

Top-Down

One of the possible top down approach consists in exfoliate Graphite with mechanical techniques or inserting some species in between the layers. For example, *electrolytes* or *intercalating ions*, often assisted by heat, enter Graphene layers, expanding and breaking π - π interactions, with the result of separating the sheets of graphite. Similar bond breaking mechanism happens with *scotch tape peeling*, the technique used by Geim and

Novoselov to isolate the first Graphene sheet. [37] While the use of ions or other chemical compounds can bring to a multilayer impure product [38], *Scotch tape* is extremely used because it gives pure, less defected Graphene. This method, suitable for large scale production of Graphene, has only a great disadvantage, it is not possible, in fact, to obtain standard dimension samples.

Another top down technique is *Chemical Graphite peeling* divided in a sequence of steps; the first is Graphite oxidation that brings to isolated oxidized-Graphene sheets. [39] This product, called Graphene Oxide (GO), is characterised by the presence of hydroxyl and epoxy groups on its basal plane and carboxyl groups at its edges. [40] Such Oxygenated groups make the sheets highly hydrophilic and dispersible, at the expense of its conductivity that is lost. To regain excellent electronic properties it is necessary to reduce GO producing reduced Graphene-Oxide (r-GO) which regain most of the properties of Graphene. Reduction is made mainly through the use of hydrazine hydrate, even if recent studies have tried to replace it using environmental friendly reducing agents. [41] The big defect of this production method consists in the difficult control of the achievement of GO total reduction and of the number of defects.

Several other techniques have been tried, for example oxidative or laser induced CNTs unzipping that produce GNRs [42], but they are not massively used, especially in the first case that gives Graphene defected by oxygen functionalities.

Bottom-Up

Bottom up Graphene production is performed in different ways exemplified in Fig. 4.

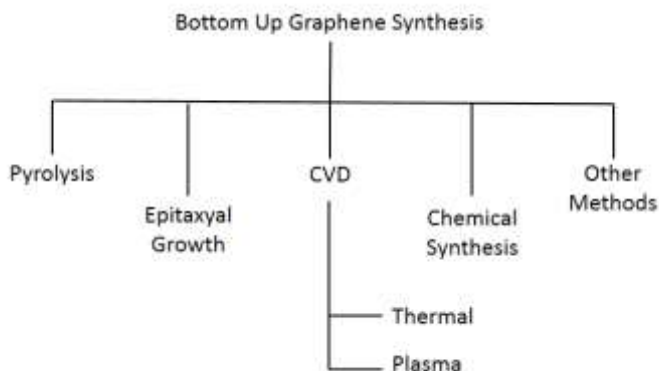


Fig. 4 Possible pathways for Bottom up Graphene synthesis

Even if, generally, bottom-up methods are promising there is not a definitive synthetic pathway yet. None of this methods can, in fact, give pure, not defective, Graphene sheets with a narrow range of flake sizes. An example of defected multilayer structures, more similar to nano-Graphite than to Graphene, are produced during pyrolysis. ^[43]

The two most promising bottom up methods nowadays seems Chemical Vapour Deposition (CVD) and Chemical Synthesis. In CVD a gaseous hydrocarbon precursor is flown above an oportune heated substrate that promotes chemical reactions with the subsequent formation of single or few layers Graphene over the substrate. ^[44]

Bottom-Up through Chemical Synthesis

The *chemical synthesis* of Graphenic structures is possible thanks to the pioneer work of Roland Scholl at the beginning of last century and to the successful intuition of Klaus Müllen, who reported additional synthetic

strategies. Scholl reaction is a coupling reaction consisting in a catalyzed oxidative cyclodehydrogenation in presence of a protic acid and a Lewis acid. Its extreme relevance is due to the possibility of intra or intermolecular cyclization that couples arene compounds with consequent expansion of the graphenic structure. [45]

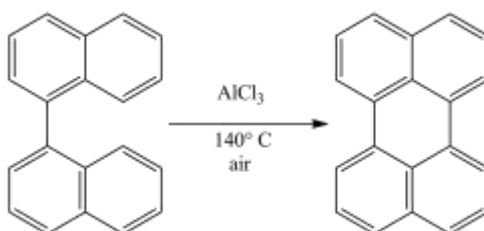


Fig. 5 First cyclodehydrogenation reaction of 1,1'-binaphthyl to perylene reported by R. Scholl and co-workers in 1910

The reaction mechanism is quite complicated and several studies have been done but the most reliable hypothesis consists in the formation of an arenium cation that generally has a free energy formation pathway which has a lower energy with respect to that of the radical cation. [46]

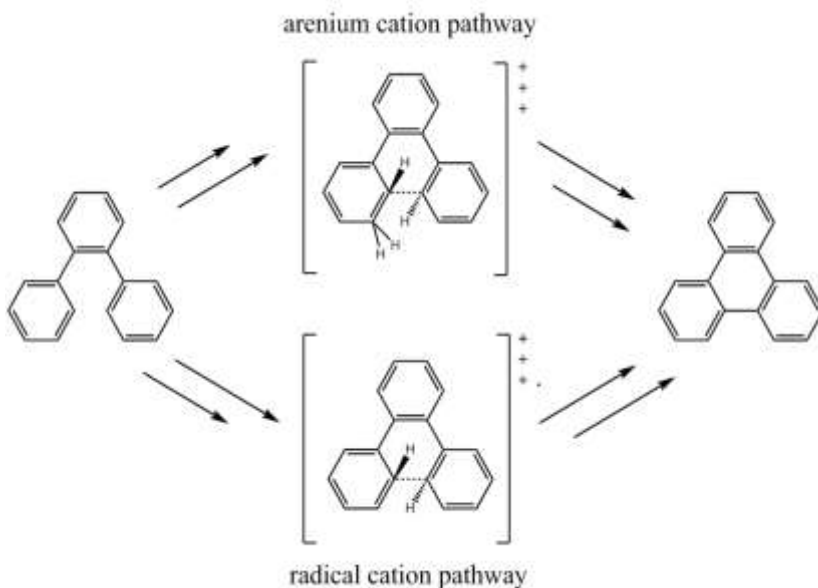


Fig. 6 Two possible alternative ways for cyclodehydrogenation of PAH, through arenium or radical cation formation

Scholl-like reactions provides the production of a wide range of nanographene molecules and extended GNRs that, together with the better control of the reactivity, is the main advantage of bottom-up cyclodehydrogenation compared to top-down synthesis. The chemical synthesis disadvantage is that the products need to be purified with further dissolutions. The obtained graphenic structures are no more soluble in conventional solvents and it is necessary to insert in the structures side alkyl chains that lowers π - π interaction between molecules, increasing their dispersion but diverging from the purpose of creating pure Graphene.

1.7.2 Graphene derivatives

The relative reactivity of Graphene permit the production of a wide range of derivatives. The aim of such modifications is to insert functionalities able to improve Graphene properties. One of the possible strategy is to insert in the lattice different atoms in order to maintain the main properties of the Graphene and providing new possible functions. The insertion of foreign atoms intrinsically modify its structure, tuning its electronic properties or locally creating chemical active sites. Doping can also increase the interaction of the material with other species and Nitrogen-doped Graphene has been tested in biosensing application. ^[47]

One of the most interesting future applications of doped Graphene is on Oxygen reduction reaction (ORR). In fact, it has been demonstrated that doping Graphene with Nitrogen or Boron gives good catalytic activity towards this reaction. These metal-free catalysts would be very challenging for the substitution of noble metals, improving the use of alternative, less rare and expensive, materials to support or substitute Platinum in fuel cells cathodes. ^[48]

The impact of any doping in Graphene electronic states can be huge and there is the risk to confuse changes in the properties due to impurity effect with doping derived properties; for this reason some researchers are convinced that the real responsible of catalytic behaviour of doped Graphene are impurities. ^[49]

1.7.3 Other nano-allotropic forms of Carbon

There are several nanometric allotropic forms of Carbon as *Nanohorns*, *Nanoonions*, *Fullerenes*, *Carbon Nanotubes* and *Nanodiamonds*. As all other nanometric objects their electronic, optical and physical properties are strictly related to their size and, similarly to Graphene, they have evident or

promising applications in molecular electronics and other technological advanced applications.

Fullerenes and Carbon Nanotubes

Fullerene (C_{60}), discovered by chance in 1985 during Graphite laser vaporization, was solubilised, studied and massively produced since the nineties. ^[50] C_{60} is a truncated icosahedron made all of 60 Carbon atoms with sp^2 hybridization but also *higher fullerenes*, with 70 or 84 Carbon atoms, are diffused. Differently than other nanocarbon species, Fullerenes in their neutral pristine forms are generally soluble in various organic solvents, giving coloured solutions that make UV-visible as well as ^{13}C NMR spectra easily recorded. ^[51] Even if C_{60} is stable at ambient conditions it can undergo various chemical reactions localized on double bonds; Buckyball is not, in fact, a *super aromatic* molecule. Electrons are not delocalized on the whole molecule but only extended onto six-membered rings. The spherical shape of the molecule forces Carbon orbitals to keep a pyramid shape and C-C bonds to be non-planar, deviating from the original Csp^2 - Csp^2 length. The consequent excess of strain is responsible of C_{60} reactivity that acts as an electron deficient olefine or shares its 2p orbitals in cycloadditions, with an associated relaxation of structural tension passing from an sp^2 to an sp^3 orbital hybridization. ^[52] C_{60} adducts in most cases retain its original properties, allowing to exploit all fullerene properties as well as new applications.

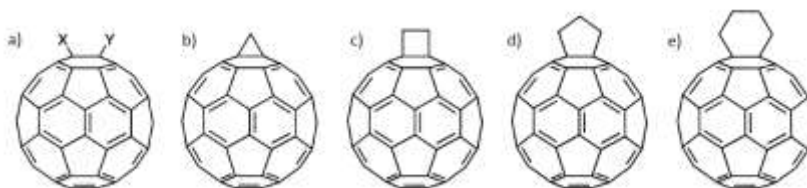


Fig. 7 Examples of C_{60} derivatives a) opened adducts, b) three-membered ring, c) four-membered ring, d) five-membered rings, e) six-membered ring

Carbon Nanotubes are one of the most studied nanocarbons, because of their versatility they are used in biosensing as well as in energetic. ^[53] They have a Carbon cylindrical structure with length that can be 500 hundred times their diameter and can be found as single or multi-walled. They can be considered as a rolled Graphene layer and the way C atoms are arranged along tubes main axes determine their chirality and their metallic or semiconductive behaviour. ^[54] CNTs great potential is in part eclipsed by their lack of solubility that often determines the formation of irregular bundles, differently than C_{60} they are not soluble both in inorganic or organic solvent. Suspending or solubilising strategies consist in sonication, the use of dispersing agents (surfactants) or through chemical reactions modification. ^[55]

1.8 The aim of this work

For the complexity of the topic, nanomaterials study and nanoscience development require cooperation of several science branches as chemistry, physics and engineering. Electrochemistry, in particular, can play a fundamental role, it can investigate properties, modify or synthesize new materials, in few words it represents the possible interface between

nanosystems and macroscopic world. It could be one of the possible ways to *decrease the size of our fingers* in order to *handle* such fundamental nanometric objects, to *extend our vision* in order to *see* this amazing world.

In this scenario the aim of my PhD thesis is to give a contribution to our knowledge about Graphene and other nanometric Carbon materials, of their possible synthetic strategies and less explored properties.

“Il mio mestiere vero, quello che ho studiato a scuola e che mi ha dato da vivere fino ad oggi, è il mestiere del chimico. Ci dividiamo in due rami principali, quelli che montano e quelli che smontano, e gli uni e gli altri siamo come dei ciechi con le dita sensibili. Dico come dei ciechi, perché appunto, le cose che noi manipoliamo sono troppo piccole per essere viste, anche coi microscopi più potenti; e allora abbiamo inventato diversi trucchi intelligenti per riconoscerle senza vederle. Tante volte, poi, noi abbiamo l’impressione di essere non solo dei ciechi, ma degli elefanti ciechi davanti al banchetto di un orologiaio, perché le nostre dita sono troppo grossolane di fronte a quei cosetti che dobbiamo attaccare o staccare.” [56]

References

- 1 Official Journal of the European Union, Commission Recommendations of 18 October 2011 on the definition of nanomaterial
- 2 Autumn K. et al. , *PNAS*, **2002**, *99*, 12252
- 3 Barthlott W., Neinhuis C., *PLANTA*, **1997**, *202*, 1
- 4 Feynman R. P., *CALTECH ENGINEERING AND SCIENCE*, **1960**, *23:5*, 22
- 5 <http://www.nanowerk.com/spotlight/spotid=30661.php>
- 6 a) Sun H., Matsuo S., Misawa H., *APPL PHYS LETT*, **1999**, *74*, 786 b) Kawata S. et al., *NATURE*, **2001**, *412*, 697
- 7 Harriott L.R., *MATER TODAY*, **1999**, *2*, 9
- 8 Balzani V., Credi A., Venturi M., **2003**, *Molecular devices and machines*, Weinheim, Wiley-VCH
- 9 Lehn J.M., *J INCLUSION PHENOM*, **1988**, *6*, 351
- 10 Nelson D.L., Cox M.M., **2004**, *Lehninger Principles of Biochemistry*, 4th ed., New York, W. H. Freeman
- 11 a) Watkins J.J., White H.S., *LANGMUIR*, **2004**, *20*, 5470; b) Kleijn S.E.F. et al., *ANGEW CHEM INT EDIT*, **2014**, *53*, 3558
- 12 R.Pecora, *J CHEM PHYS*, **1964**, *40*, 1604
- 13 Drexler K.E., *Engines of Creation*, Oxford, Oxford University Press, **1990**
- 14 a) Kötz R., Kolb M.D., Sass J.K., *SURF SCI*, **1977**, *69*, 359 b) Chao F. et al., *J ELECTROANAL CHEM*, **1977**, *83*, 65
- 15 a) Cole R.M. et al., *NANO LETT*, **2007**, *7*, 2094 b) Cintra S. et al., *FARADAY DISCUSS*, **2006**, *132*, 191
- 16 Papadopoulou E. et al., *ANAL CHEM*, **2015**, *87*, 1605
- 17 Lu W., Lieber C.M., *NAT MATER*, **2007**, *6*, 841
- 18 Bradley K., Gabriel J.-C. P., Grüner G., *NANO LETT*, **2003**, *3*, 1353
- 19 Jung J.H. et al., *SMALL*, **2015**, *11*, 4976
- 20 Eda G., Fanchini G., Chowalla M., *NAT NANOTECHNOL*, **2008**, *3*, 270
- 21 Atkins P., de Paula J., **2006**, *Atkins' Physical Chemistry*, 8th ed., New York, W.H. Freeman and Company
- 22 Proch S. et al., *JACS*, **2013**, *135*, 3073;
- 23 Park J.H., Kim S., Bard A.J., *NANO LETT*, **2006**, *6*, 24
- 24 Reisner E. et al., *JACS*, **2009**, *131*, 18457
- 25 Ellingson R.J. et al., *NANO LETT*, **2005**, *5*, 865

26 a) Dong R., Zhou Y., Zhu X., *ACC CHEM RES*, **2014**, *47*, 2006 b) Lee H. et al., *JACS*, **2015**, *137*, 12394

27 Krokos E. et al., *CHEM-EUR J*, **2012**, *18*, 1328

28 Marcus R.A., *J CHEM PHYS*, **1956**, *24*, 966

29 a) Aricò A.S. et al., *NAT MATER*, **2005**, *4*, 366 b) Yu S.-H. et al., *JACS*, **2015**, *137*, 11954

30 a) Lesniak A. et al. , *ACS NANO*, **2012**, *6*, 5845 b) Ge C. et al., *PNAS*, **2011**, *108*, 16968 c) Hu W. Et al., *ACS NANO*, **2011**, *5*, 3693

31 <http://www.britannica.com/science/silicon>

32 Diancov G., Neumann N., Goldhaber-Gordon D., *ACS NANO*, **2013**, *7*, 1324

33 a) Geim A.K., *SCIENCE*, **2009**, *324*, 1530; b) Fuhrer M.S., Lau C.N., MacDonald A.H., *MRS BULLETIN*, **2010**, *35*, 289

34 a) Sharma R. et al., *NANO LETT*, **2010**, *10*, 398; b) Cao J. et al., *JACS*, **2013**, *135*, 17643; c)

35 a) Brey L., Fertig H.A., *PHYS REV B*, **2006**, *73*, 235411; b) Sharma R., Nair N., Strano M.S., *J PHYS CHEM C*, **2009**, *113*, 14771

36 Fuhrer M.S.; *NAT MATER*, **2010**, *9*, 611

37 Novoselov K.S. et al., *SCIENCE*, **2004**, *306*, 666

38 Chung D.D.L., *J MATER SCI*, **202**, *37*, 1475

39 a) Brodie B.C., *PHIL TRANS R SOC LOND*, **1859**, *149*, 249 ; b) Hummers W.S., Offeman R.E., *JACS*, **1958**, *80*, 1339

40 Lorf A. et al., *J PHYS CHEM B*, **1998**, *102*, 4477

41 a) Stankovich S. et al., *CARBON*, **2007**, *45*, 1558 b) Abdolhosseinzadeh S., Asgharzadeh H., Kim H.S., *SCI REP*, **2015**, *5*, 10160

42 a)Kosinkin D.V. et al., *NATURE*, **2009**, *458*, 872; b) Kumar P., Panchakarla L.S., Rao C.N.R., *NANOSCALE*, **2011**, *3*, 2127

43 a) Hong N. et al., *MATER RES BULL*, **2012**, *47*, 4082; Zou B. et al., *CHEMM COMM*, **2015**, *51*, 741

44 a) Gamo Y. Et al., *SURF SCI*, **1997**, *374*, 61; b) Reina A et al., *NANO LETT*, **2009**, *9*, 30; b) Kim K.S. et al, *NATURE*, **2009**, *457*, 706

45 a) R.Scholl, J. Mansfeld, *BER DTSCHEM CHEM GES*, **1910**, *43*, 1734; b) Schwab M.G. et al., *JACS*, **2012**, *134*, 18169

46 a) Rempala P., Kroulík J., King, B.T., *JACS*, **2004**, *126*, 15002; b) Rempala P., Kroulík J., King, B.T. *J ORG CHEM*, **2006**, *71*, 50667; c) King B.T. et al., *J ORG CHEM*, **2007**, *72*, 2279

-
- 47 Wang Y. et al., *ACS NANO*, **2010**, *4*, 1790
- 48 a) Yu D. et al., *J PHYS CHEM LETT*, **2010**, *1*, 2165; b) Sheng Z.-H. et al., *J MATER CHEM*, **2012**, *22*, 390; c) Parvez K. et al., *ACS NANO*, **2012**, *6*, 9541
- 49 a) Giovannetti G. et al., *PHYS REV LETT*, **2008**, *101*, 026803; b) Ardenghi J.S. et al., *SUPERLATTICE MICROST*, 2016, *89*, 398; c) Wang L., Ambrosi A., Pumera M., *ANGEW CHEM INT ED*, **2013**, *52*, 13818
- 50 a) Kroto H.W. et al., *NATURE*, **1985**, *318*, 162; b) Krätschmer W. et al., *NATURE*, **1990**, *347*, 354
- 51 Marcaccio M. & Paolucci F. (Eds.), **2014**, *Making and exploiting fullerenes, Graphene, and Carbon Nanotubes*, Heidelberg, Springer
- 52 Prato M., *J MATER CHEM*, **1997**, *7*, 1097
- 53 a) Zamolo V.A. et al., *ACS NANO*, **2012**, *6*, 7989; b) Tuci G. et al., *ACS CATAL*, **2013**, *3*, 2108
- 54 a) Iijima S., *NATURE*, **1991**, *354*, 56; b) Iijima S., Ichihashi T., *NATURE*, **1993**, *363*, 603; c) Bethune D.S. et al., *NATURE*, **1993**, *363*, 605
- 55 a) Tasis D. et al., *CHEM REV*, **2006**, *106*, 1105; b) ref 47; c) Al-Hamadani Y.A.J. et al., *SEP PURIF TECHNOL*, **2015**, *156*, 861
- 56 Primo Levi, **2011**, *La chiave a stella*, Torino, Einaudi

2 Graphenic structure formation through electrochemistry

As previously mentioned, polycyclic aromatic hydrocarbons (PAHs) are extremely interesting for molecular electronic and biosensing application because they represent the basis to study Graphene properties and to implement its characteristics. The numerous advantages of bottom up chemical intramolecular cyclodehydrogenation have been already discussed in first chapter but in this section a possible alternative for bottom up synthesis will be shown. The basic idea is to replace chemical oxidizers, as FeCl_3 or AlCl_3 , with heterogeneous electron transfer. Electrochemical oxidation of the molecule can drive the one-pot formation of the unstable arenium cation that leads to C-C bonds formation. Moreover electrochemistry can drive intermolecular polymerization with subsequent bottom-up enlargement of the graphenic structure. Another important advantage of this approach, with respect to other synthetic methods, is represented by the formation of the required structure directly onto electrode surface. PAHs are, in fact, soluble in common organic solvents, like dichloromethane (DCM), but the planar, closed and extended structure which is formed during electrochemical oxidation is no more soluble and, immediately, after its generation tends to precipitate onto the surface. As a result, functionalization with aliphatic chains or any other dissolution and purification steps are unnecessary.

2.1 Corannulene

Corannulene (dibenzo[*ghi,mno*]fluoranthene; $\text{C}_{20}\text{H}_{10}$) is a bowl shaped molecule formed by a cyclopentane (*cor*) fused with five benzene rings (*annula*) that resembles to planar Coronene. The corannulene (C)

complicated synthesis was extremely simplified by Scott and co-workers in the nineties but its industrial production was possible only few years later, thanks to the work of Rabideau, Sygula. [1]

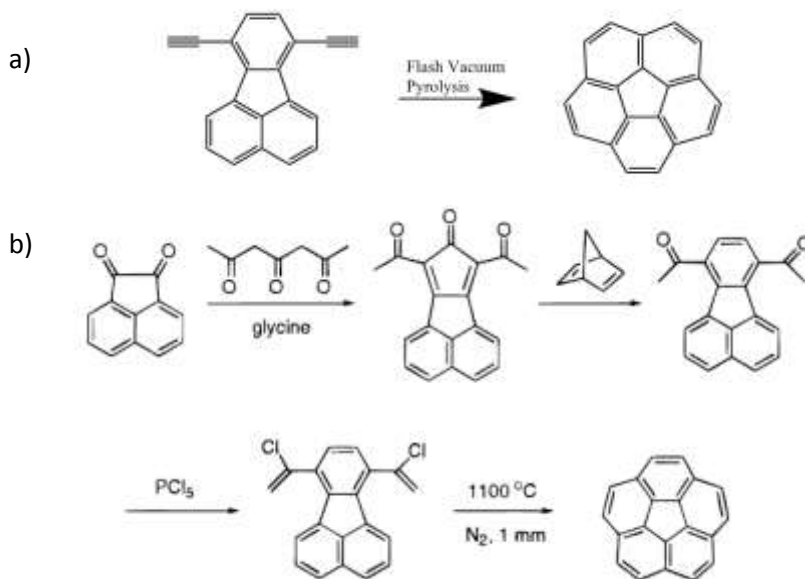


Fig. 8 a) Pyrolysis and b) three-step synthesis of Corannulene proposed by Scott

Such curved structure has a bowl depth (0,86 Å) lower than that of C_{60} , probably because of the minor tension of the opened structure. Another unexpected characteristic of this molecule is the absence of intramolecular π - π interactions that avoid bowl stacking. Its pyramidal structure has C_{5v} symmetry and is surprisingly flexible; bowl-to-bowl inversion, with an energy barrier of few Kcal/mol, has been demonstrated through Nuclear Magnetic Resonance. [2]

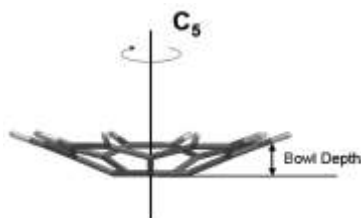


Fig. 9 Corannulene bowl shaped symmetry

One of the most interesting properties of C is its good luminescence and electroluminescence efficiency that makes it an ideal candidate for solid state light emitting devices or wavelength tunable electrochemiluminescent sensors. [3]

Moreover Corannulene and other *buckybowls* have motivated a great number of scientists because they represent a good model for C₆₀ reactivity, showing a good compromise between strain and conjugation, but above all because they represent the possible molecular *starters* for bottom up synthesis of C₆₀ and capped NTs. [4]

Even if a broad range of Fullerenes is commercially available their synthesis is still fundamental as only following this way it is possible to exploit and control several features as isotope labeling, exo or endohedral complexation or the formation of alkali-metallodoped superconductors. [5]

2.1.1 Electrochemical behavior

Corannulene Reduction

Corannulene reduction has been widely explored and it is characterized by four one-electron reductions. Each reaction occurs through an outer-sphere reversible ET process associated with a reduction standard potential. [6]

The use of carefully dried solvents and electrolytes (ultra-dry conditions) allows the potential window to extend up to -3.1 V. Anyway, even in these extraordinary conditions the number of reductions of C is not completely accessible. While the first two reductions are rather easily observable, the possibility to see the third is largely influenced by ion pairing stabilization between generated ions and supporting electrolyte counteranions. Trianion can be obtained in the available potential window only in the presence of high charge density alkylammonium salts (eg. tetramethylammonium) while tetra-reduced corannulene can be obtained only by a slow chemical reduction with metallic lithium.^[7]

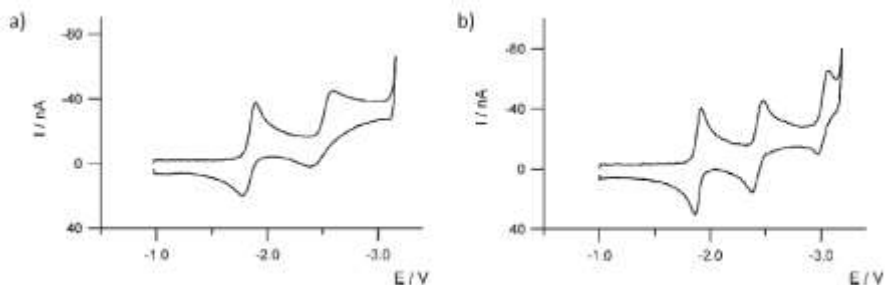


Fig. 10 Cyclic voltammetric curves of corannulene 1 mM in (a) 0.07 M TBAH/DMF solution ($T = 218$ K) and (b) 0.08 M TMAB/DMF solution ($T = 213$ K); WE Pt disk $125 \mu\text{m}$; reference electrode SCE; scan rate = 1 V/s

Corannulene oxidation and polymerization

Anodic behaviour of Corannulene has been rarely investigated until now and in all cases described as an irreversible process producing electrode fouling. Voltammetric experiments have been carried out using ultra dry DCM, which has very low nucleoficity, and carefully dried Tetrabutylammonium Hexafluorophosphate (TBAH). The choice of such a supporting electrolyte is due to its high resistance to oxidation and low nucleophilicity that does not interfere with highly reactive cations formed by electrochemical oxidation of C.

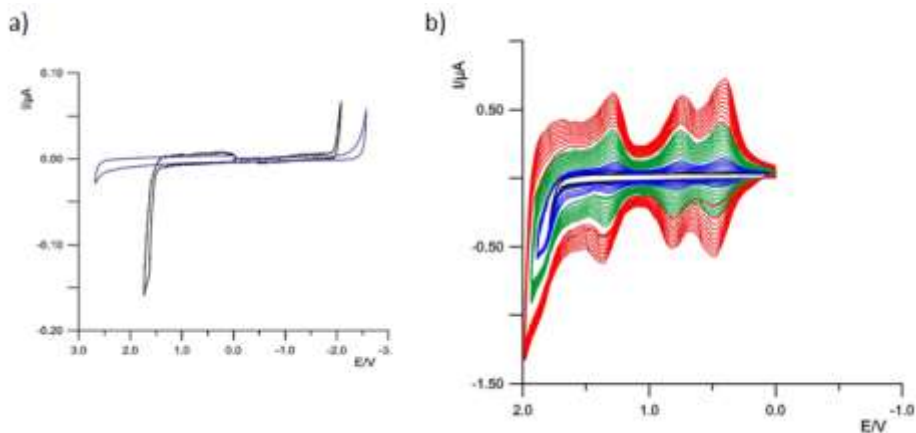


Fig. 11 a) Solvent baseline (blue) and first voltammetric cycle of Corannulene (black); b) following oxidations of Corannulene, the continuous current increase is highlighted by color sequence. 1mM in TBAH 0,08M/ultra dry DCM, Pt 125 μ M ultramicroelectrode, Ag QRE, Scan rate: 1V/s

Cycling the potential in the positive region causes the oxidation of monomers and the continuous increase in current, which usually implies the deposition onto electrodic surface of an insoluble conductive deposit. Generated oligomers, ^[8] with higher molecular weight with respect to monomers, tends, in fact, to precipitate forming a conductive film.

This result is very important because the observed voltammetric pattern is very similar to that previously reported for the C₆₀ polymerization and demonstrates the capability to drive the formation of C-C bonds through electrochemistry.^[9] The thin film thus formed on the electrode surface is a graphene-like nanostructure that could be very interesting in several technological fields, from catalysis to optoelectronics.

Electrochromism

When the deposition of such a film is made onto a transparent WE, as Indium Tin Oxide doped glass (ITO), the formation of an electrochromic film is eye-visible, as can be seen in Fig. 12.

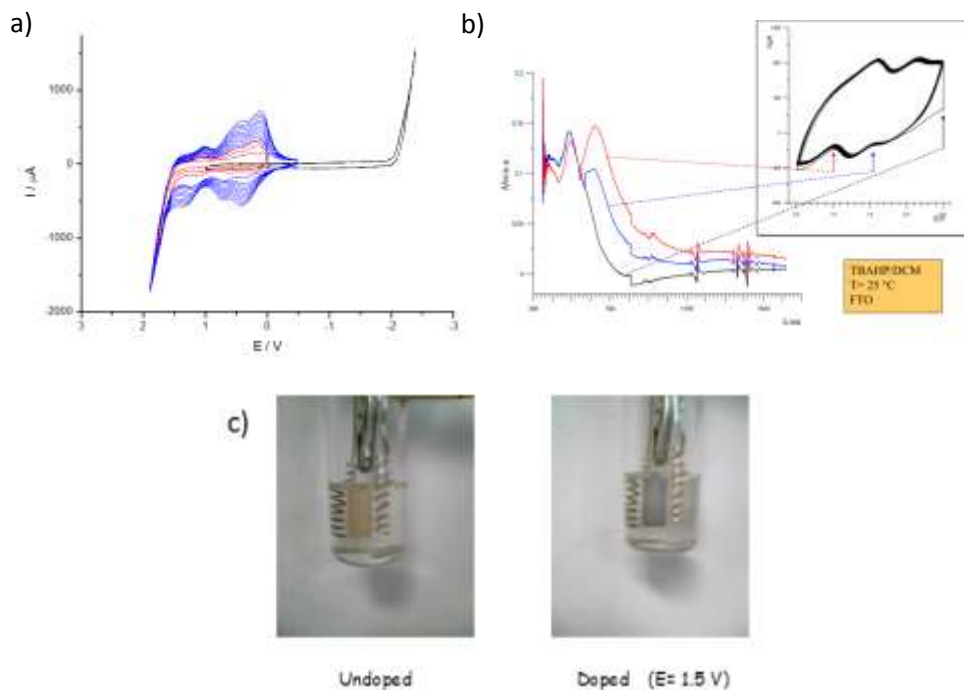


Fig. 12 a) Electrochemically induced oxidative intramolecular condensation of Corannulene to poly-C on ITO WE and b) Absorbance spectrum of the deposit in a blank TBAH/DCM electrolyte solution. Framed panel highlights three different potentials corresponding to different absorption spectra; c) undoped ($E=0\text{ V}$ vs SCE) and doped ($E=1.5\text{ V}$ vs SCE) polycorannulene film correspond to reduced and oxidized forms of the electrochemically deposited material.

This material, in fact, reversibly changes its colour depending on its oxidation state turning from yellow-brownish to blue.

2.1.2 Determination of deposit mass

In order to shed some light on the molecular structure of the oligomeric species produced by oxidation of corannulene, LD-TOF analysis was performed on the material deposited onto ITO surface. This ionization technique confirmed that the material comes, indeed, from an efficient intermolecular oligomerization by electrooxidation. The formation of oligomers is clearly shown by masses correspondent to dimers, trimers, tetramers and a very small quantity of pentamers at almost 1200 m/z.

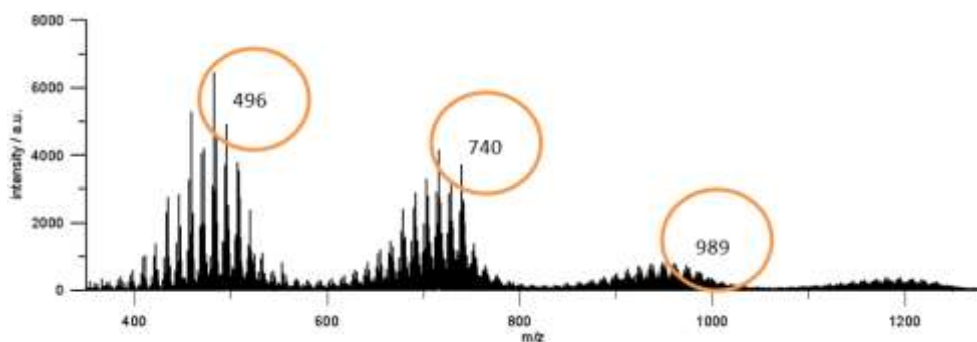
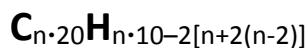


Fig. 13 LD-Maldi spectrum of poly-Corannulened obtained trough electrochemical oxidation of Corannulene monomer, m/z values correspond to that of dimers, trimers and tetramers

Corannulene monomer has a m/z of 250, its first three oligomers show a m/z loss of 4, 10 and 16. This means that oligomers do not have a simple multiple loss of Hydrogen atoms but the oligomerization behaviour is more complex. For n = number of corannulenyl unit, the first three oligomer ions have respectively m/z values of $2n-4$, $3n-10$ and $4n-16$. Using this values a formula to predict Corannulene electropolymerization behaviour can be extrapolated.



2.1.3 X-ray Photoemission Spectroscopy of poly-Corannulene

XPS measurement, performed on polycorannulene (Poly-C) on ITO, deposited under the same experimental conditions used for CV, clarify that the film is exclusively composed by Carbon.

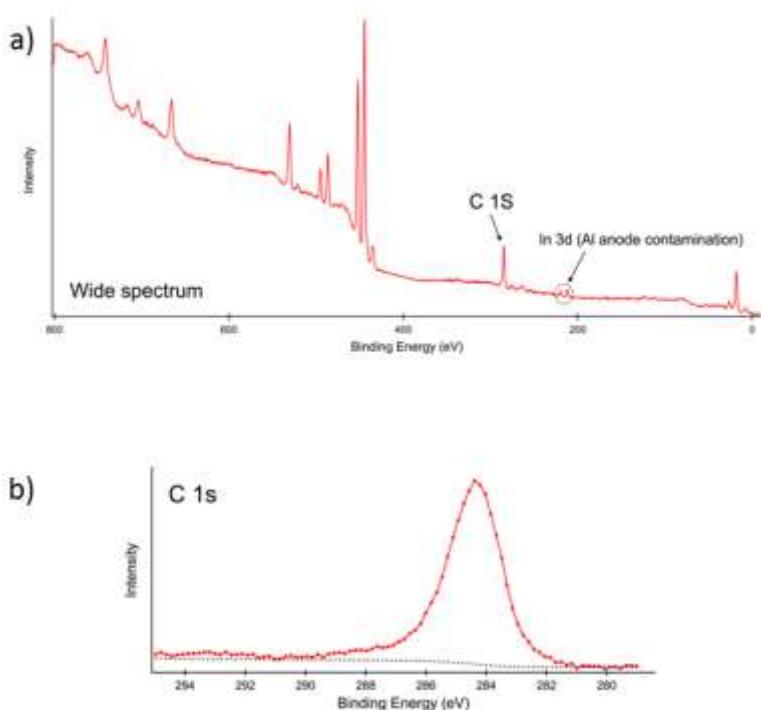


Fig. 14 XPS spectrum of poly-Corannulene electrodeposited on ITO

Apart from peaks corresponding to ITO material and to an anodic Aluminium contamination, only a peak at 284,4 eV is visible. This binding energy for C 1s is shifted with respect to the values of C₆₀ (285,1 eV) and the anodically obtained poly-C₆₀ (283,8 eV) and the result is very close to

that obtained for Graphene/Graphite (284.5 eV).^[10] The explanation for such a shift is due to the larger presence of sp² respect to sp³-hybridized carbon atoms; moreover, in Poly-C the investigation of core hole through XPS is easier because the asymmetry in the high binding energy side of the lineshape is not very large respect to poly-C₆₀. Moreover C1s peak is characterized by a small asymmetry that could be due to different reasons: a small density of states at the Fermi level; an overlap of different C1s peaks, each corresponding to Carbon atoms in different environment, as expected for different oligomers deposition; Oxygen accidental contamination.

2.1.4 Morphological investigation by SEM and AFM

Even if Corannulene molecules does not show π - π stacking, oligomers formation seems to improve this capability and the development of discrete aggregates onto the surface is visible using Scanning Electron Microscope (SEM).

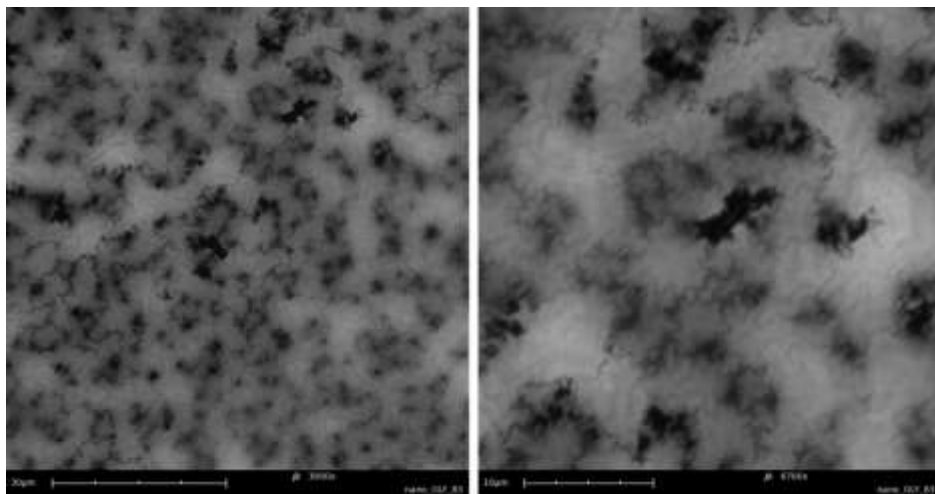


Fig. 15 SEM images of poly-Corannulene sample on ITO at two different magnifications 3000x (left) and 6700x (right) obtained using a Phenom G2 pure microscope

Further investigations on different samples with AFM, able of higher resolutions in comparison to SEM characterization, confirmed the surface film formation and its morphological evolution.

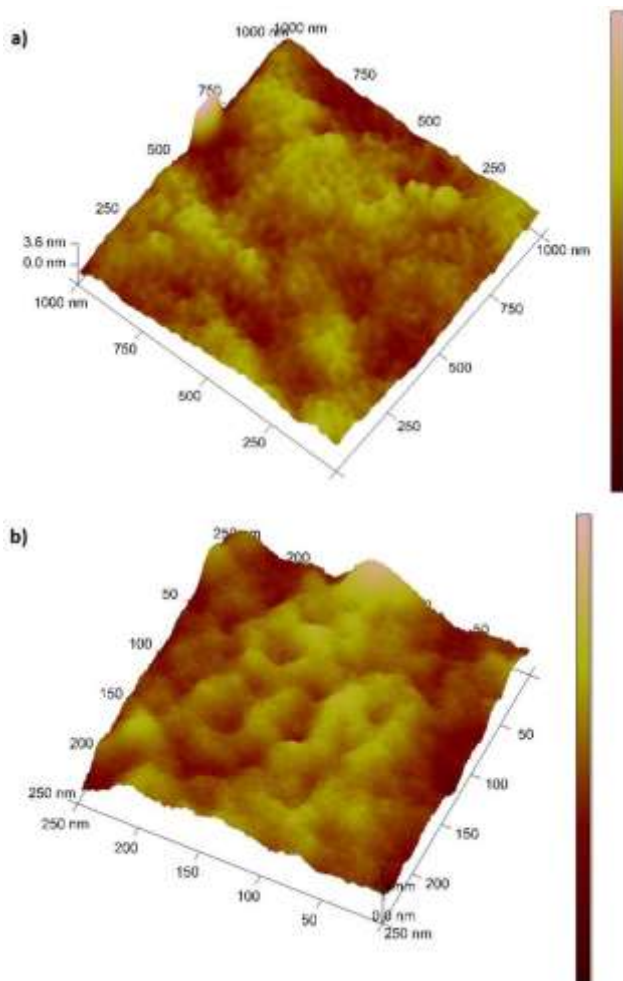
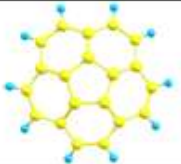
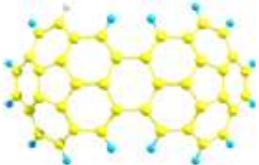
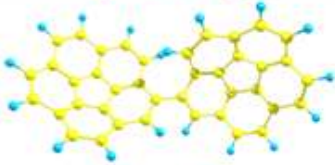
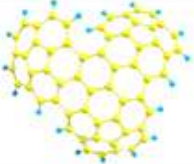
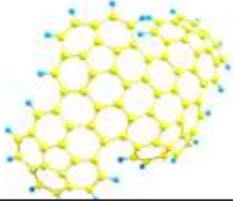
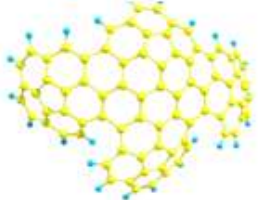


Fig. 16 AFM images of electropolymerized Corannulene on ultra flat ITO surface made with three subsequent voltammetric oxidative cycles, scan rate: 0, 4 V/s a) $1 \times 1 \mu\text{m}^2$ and b) $0,25 \times 0,25 \mu\text{m}^2$ areas

AFM revealed, in fact, the presence, onto ultra flat ITO surface, of a sort of self-assembled nanometric rings with an average diameter ranging from 30 to 40 nm.

2.1.5 Theoretical Calculations

The investigation of the reactivity of the electrochemically generated corannulenium and its oligomerization products has also been computationally tackled in collaboration with prof. Claudio Fontanesi of the University of Modena e Reggio Emilia. Some of the possible oligomers, especially dimers and tetramers, can have different 3D structures with different ionization energies. Calculations of the ionization energies have been performed as differences between neutral and oxidized forms, using B3LYP method. In Table are reported the lower energies obtained at two different level of the theory and hence the most probable structures.

<u>Corannulene</u>	<u>Structure</u>	<u>IP(eV)</u>
<u>Monomer</u>		7.49 7.73
<u>1,2 Dimer</u>		6.77 7.01
<u>2,0 Dimer</u>		6.90 7.16
<u>Trimer</u>		6.47 6.72
<u>Tetramer A</u>		6.18 6.44
<u>Tetramer B</u>		6.21 6.47

Tab. 2 Theoretically calculated structures and ionization energies obtained with B3LYP/6-31G* (red) and with the more extended B3LYP/cc-pVTZ basis set (black)

2.2 HexaBenzoCoronene

Hexaphenylbenzene (HPHB), composed by seven benzene rings, is the widely used reagent to obtain one of the most representative PAHs, Hexapery-hexabenzocoronene (HBC), through an intramolecular ring closing .

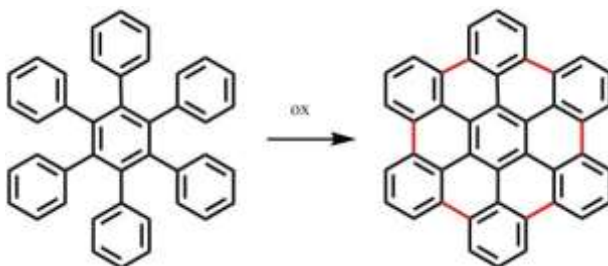


Fig. 17 Example of the supposed electrochemically driven HBC formation

In the last decade this class of molecules has attracted great attention among scientific groups because these species represent possible molecular building blocks for Graphene nanoribbons (GNRs) or Graphene nanosheets bottom-up synthesis. ^[11]

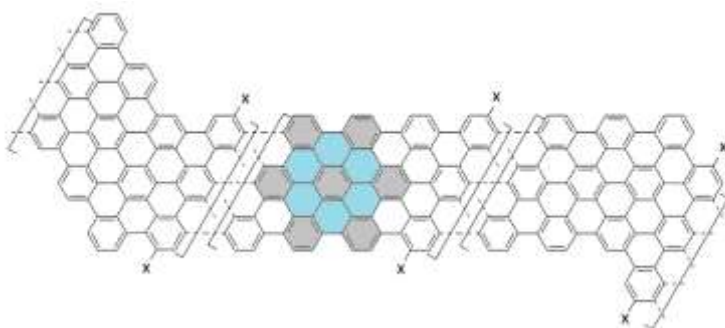


Fig. 18 One of the possible extended GNRs obtained with bottom-up chemical synthesis, the presence of eventual side chains is shown with x and HPHB and HBC building blocks are highlighted (grey and grey-pale blu)

2.2.1 Voltammetric Properties

The redox behaviour of HPhB has been investigated recording the voltammetric curve, in ultra dry DCM and TBAH, at 1 V/s (Fig. 19). The only remarkable voltammetric feature is a completely irreversible multielectronic oxidation peak at about 1.8 V. Subsequent voltammetric cycles evidence the growth of new peaks with a classic triangular shape, indicating that these new processes can be attributed to electron transfers of adsorbed species. With the increase of the number of cycles, peak current increases.

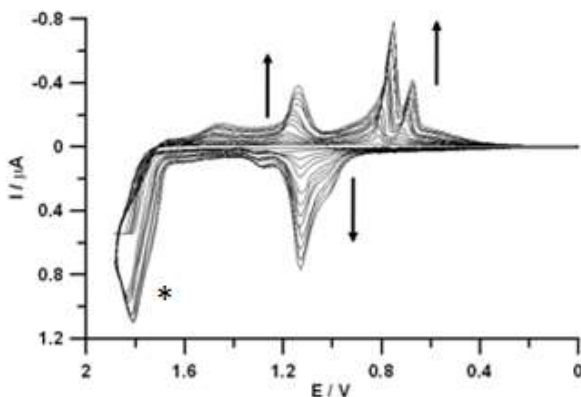


Fig. 19 Cyclic voltammetric curves of HPhB in the positive potential region. Working electrode Pt disk (diameter 125 μm), DCM, TBAH, scan rate: 1 V/s Reference electrode Ag wire (quasi reference electrode – QRE)

This can be rationalized by a continuous deposition of electroactive material. In fact, a thin film is deposited on the electrode surface also observed by visual inspection. Thus, the irreversible oxidation of HPhB

promotes the formation of a new specie, which is Hexabenzocoronene (HBC), as also evidenced by the spectroscopic characterization (vide infra).

Changing the working electrode material, similar results are shown. As matter of facts, deposition on Indium Tin Oxide (ITO) conductive glass or gold are reported below in Figure 20.

At opposite of the very interesting behaviour in positive potential region, no significant reduction peaks can be observed in the negative potentials.

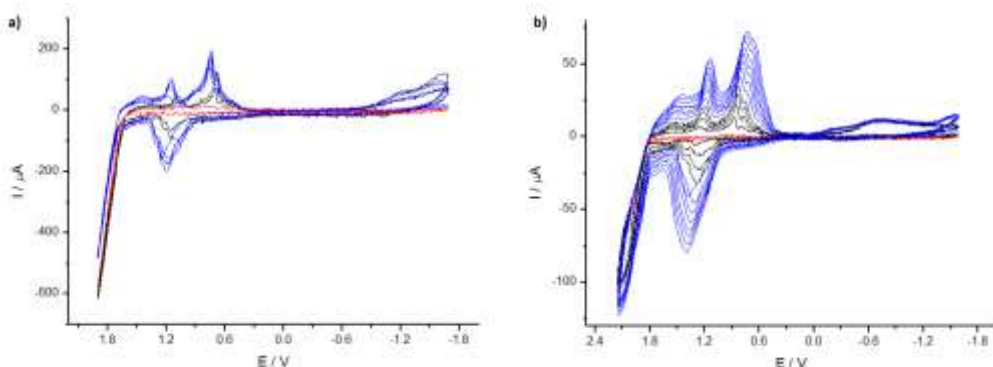


Fig. 20 Deposition from 1 mM of HPhB in 0.1 M TBAH/DCM solution. Scan rate 0.4 V/s, Ag QRE, on a) ITO glass and b) Gold electrode (supplied by Olivetti)

2.2.2 Investigation on the chemical nature of the deposit

Deposition on substrates with very low roughness, as ultraflat ITO gives the possibility to perform many investigations on the chemical nature and the three-dimensional structure of the deposit.

2.2.2.1 Absorbance spectroscopy

The insoluble deposit on ITO revealed an absorbance UV-Vis spectrum with a maximum at about 350 nm (Fig. 21). The comparison of this spectrum with that of a sample of HBC chemically synthesized and drop-casted on ITO (red trace in Fig. 21) highlights a close similarity. The little difference in shape consists in the coalescence of the vibrational structure for the spectrum relative to the electrochemically synthesized film (black trace, Fig. 21) and this can be attributed to the presence of molecular aggregates and to a higher thickness of the deposit. ^[12]

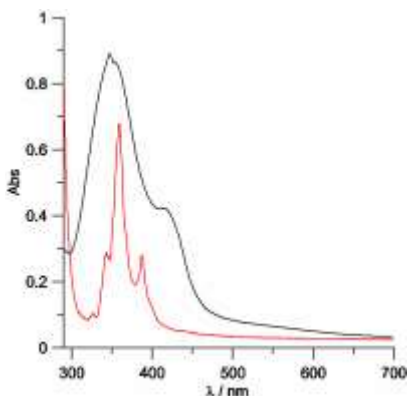


Fig. 21 Absorbance spectra of chemically synthesized HBC 1mM in DCM five times amplified (red) and of HBC eletrosynthesized and deposited on ITO conductive glass (black)

2.2.2.2 LD-TOF

The use of LD-TOF allowed to have a further evidence about the chemical nature of the film. Thus, the mass of the deposit confirmed the exclusive presence of the HBC closed monomer (HBC $m/z = 522,14$).

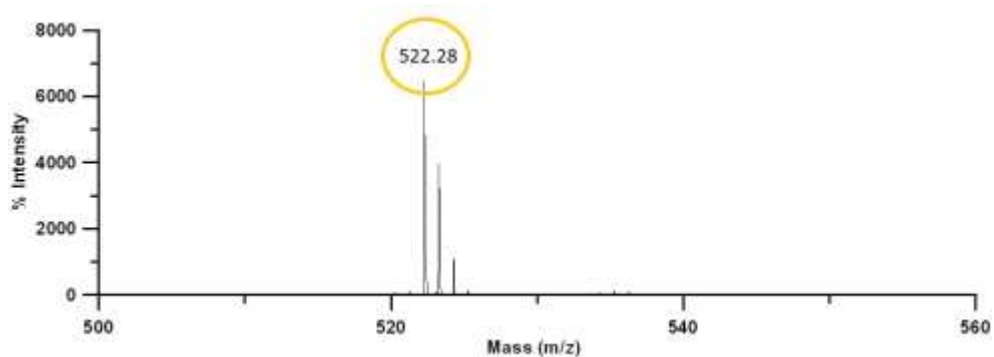


Fig. 22 LD-TOF Spectrum of electrooxidized HPhB on ITO glass shows the presence of an highest peak corresponding to HBC monomer mass

2.2.2.3 Raman

Raman measurements showed the typical G and D bands of carbon materials. The G band has a Raman shift which perfectly matches with the shift for HBC stretching modes.^[13] The D band, which is usually affected by molecular disorder, has a composed shape that can be attributed to the double peaked structure, usually visible in the Raman spectra of edge graphite.^[14]

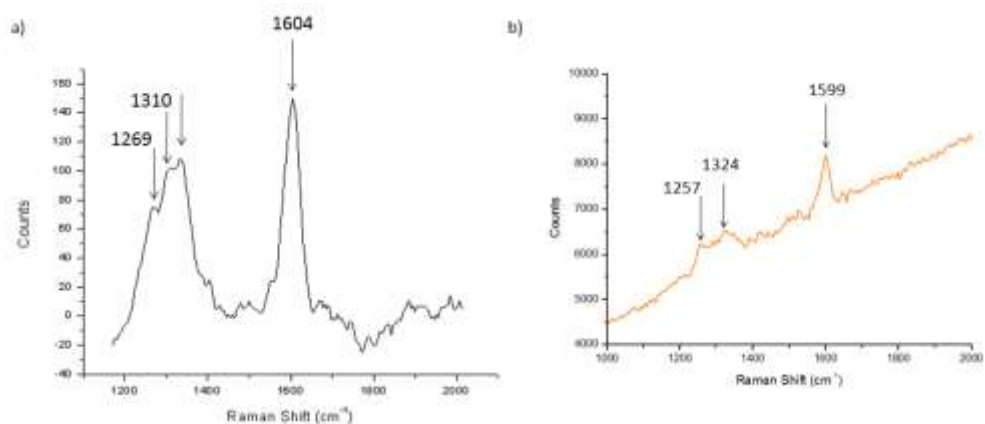


Fig. 23 Comparison between Raman spectra obtained for a) HCB electrodeposited on ITO substrate (Ventana 532 Raman Spectrophotometer of Ocean Optics) and b) chemically synthesized HBC (Horiba XploRA One Raman microscope)

2.2.3 Morphological investigation of the deposit

After the confirmation of the proficient electrooxidation, the morphological characterization of the deposit was performed, in order to control if any possible molecular arrangement exists, as the study and control of the 3D molecular arrangement is fundamental for technological application.

2.2.3.1 AFM

AFM measurements in tapping mode showed that HBC effectively self-assembles and, in contrast with any expectations, the organization is not parallelly stacked on the electrode surface, but the image clearly reveals the presence of columnar structures laying on the surface. The diameters of the *rods* thus formed is up to fifty nanometres and their lengths vary from one to few hundreds of nanometres.

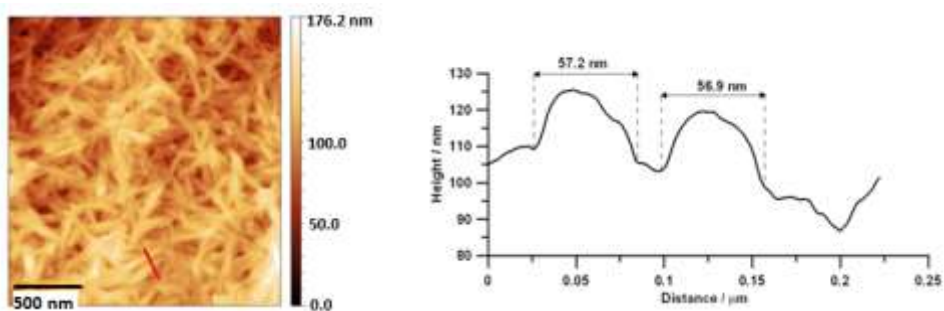


Fig. 24 left) AFM image of HBC deposit on ultraflat ITO, rod shaped assemblies are well visible; right) section obtained along the red line on the left image

2.2.3.2 TEM Investigation of aggregates

In order to deeply investigate the morphology of such aggregates an High Resolution Transmission Electron Microscope (HR-TEM) together with a High Angle Annular Dark Field Scanning Transmission Electron Microscopy (STEM-HAADF) were used. This particular equipment uses a *z-contrast* imaging mechanism, generated by the HAADF, in order to collect electrons which are not Bragg-scattered, with the great advantage of irrelevant diffraction effect.

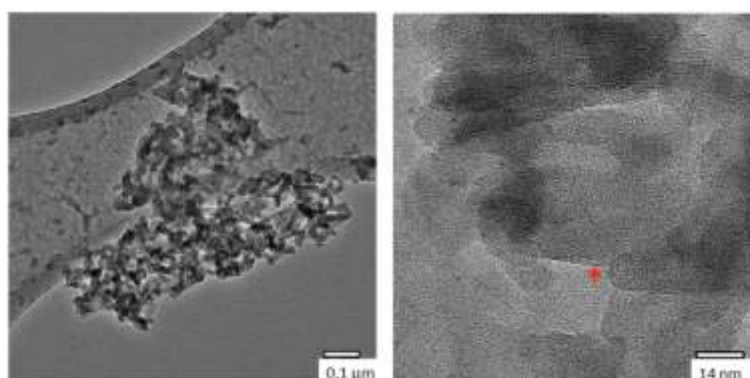


Fig. 25 left) TEM image of round shaped Carbon aggregates on the grid; right) an amplified detail of the sample, it is possible to see the amorphous nature of the sample, which present only few crystalline areas (*)

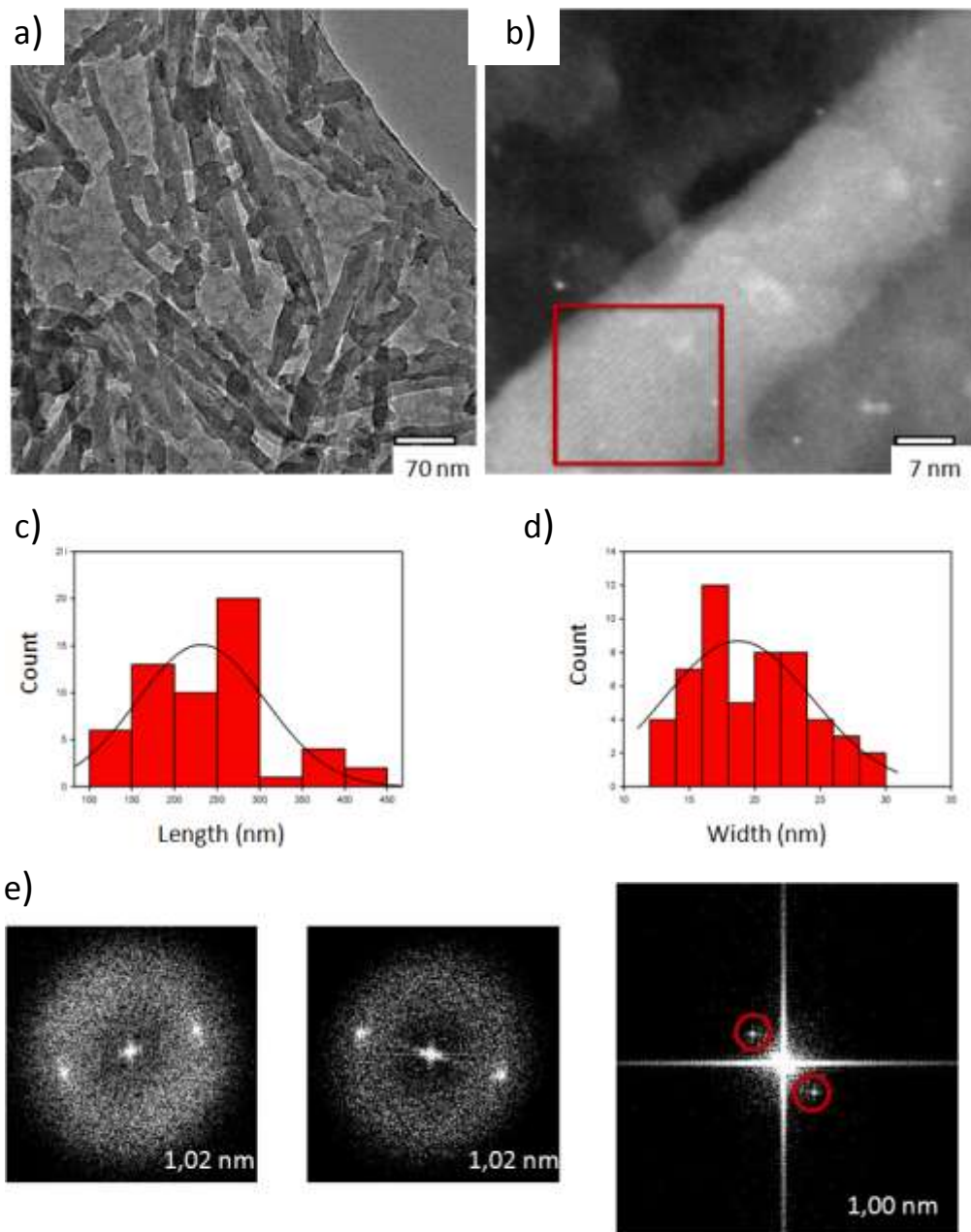


Fig. 26 a) TEM image of the rod shaped aggregates; b) amplified image of the rods with highlighted tubular structure (red square); in c) e d) is possible to see the distribution of lengths and widths of the aggregates; e) (left) diffraction fingers corresponding to an interplanar distance of 1,02 nm; (right) lattice fingers for an interplanar distance of 1 nm

The formed Carbon aggregates have an heterogeneous distribution of lengths and widths, with medium dimension of 231 and 18 nm respectively.

Diffraction fingers obtained with this measurement correspond to an interplanar distance of 1,02 nm (Fig.), comparable with Graphite values (1,04 nm) and further measurements of the lattice fingers, highlighted by FFT, give an interplanar distance of 1 nm. Such values correspond to an inter-planar distance compatible with the formation of regular supramolecular pillars made of packed HBC molecules.

TEM Instrumental Equipment

High Resolution TEM and STEM-HAADF micrographs were recorded using a Tecnai F205T TEM with a Schottky field emitter operating at 120 kV in order to minimize beam induced damage and a Fischione High Annular Dark Field STEM detector.

2.2.3.3 X Ray Diffraction

A further proof of the formation of these structures was given by X-ray diffraction patterns, obtained using a PanAnalytical X'pert Pro equipped with X'Celerator detector power diffractometer. XRD measurements show the presence of only one crystalline peak, correspondent to an inter-discotic distance of 0.305 nm, which is comparable to graphite interplanar distance (0.335 nm).

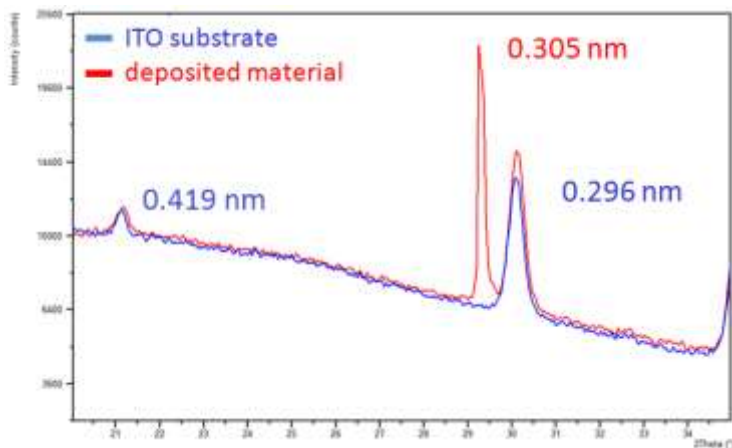


Fig. 27 X-ray diffraction of ITO glass (blue) and of HBC deposited on the same support (red) with the single crystalline peak

Similar results have been obtained by Müllen's with a value around 0.35 nm. In absence of side alchyl chain, HBC molecules are expected to have stronger π - π interactions that give closed packed structures. The insertion of side alchyl chains in the structure, necessary for chemical synthesis and processability of HBC, introduces steric hindrance and a certain disorder with an increase of interplanar molecular distance. ^[15]

The joined results of XRD and TEM analysis give a clear picture of the supramolecular assemblies thus obtained upon concomitant synthesis and self-assembly processes electrochemically driven. Such structures consist in a highly stable tridimensional array of HBC molecules.

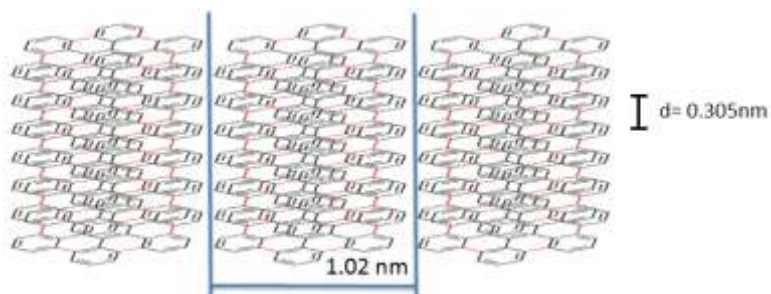


Fig. 28 Supposed structure for the formation of HBC columnar assemblies

Orbital overlap between closed molecules supports charge carrier mobility. Such HBC peculiar assemblies, thanks to their semiconductive properties and 3D closed packing, that enhances charge transport, could be the ideal candidate for replacing usual semiconductors in field effect transistors or photoelectrochemical devices.

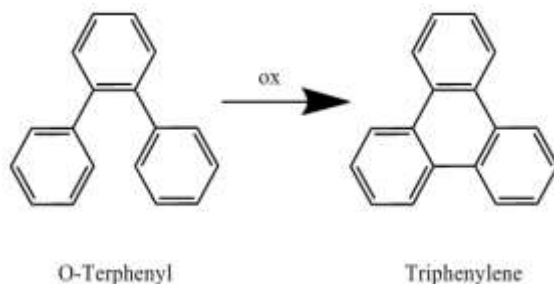
2.3 Triphenylene

Triphenylene (TPH) is an aromatic molecule composed by four benzene rings that can be used as a precursor to build up Graphene or GNRs from the bottom.

In the last years, Triphenylene molecules have been widely investigated especially for the very fascinating properties they share with other PAHs. Together with self-assembly, one-dimensional charge and energy migration, it shows also electroluminescence, ferroelectric switching and discotic liquid crystalline behavior that makes it an excellent candidate for the production of blue emitters in organic (OLED) or polymeric light emitting diodes (PLEDs).^[16]

2.3.1 Electrochemical oxidation of O-Terphenyl

O-Terphenyl is the precursor for Triphenylene and, as previously seen for other PAHs, also in this case the electrochemical cyclodehydrogenation pathway was investigated.



The electrochemical investigation of O-Terphenyl carried out in ultra dry DCM shows an irreversible multielectronic oxidation peak, at about +1,8 V. The subsequent cycles show a constant increase in current, at least for thirty cycles, due to the deposition of a conductive material onto the electrode surface. The voltammetric pattern develops similarly to that observed for the oxidation of HPhB and a yellowish film can be observed on the electrode, giving a first evidence of possible cyclooxidation.

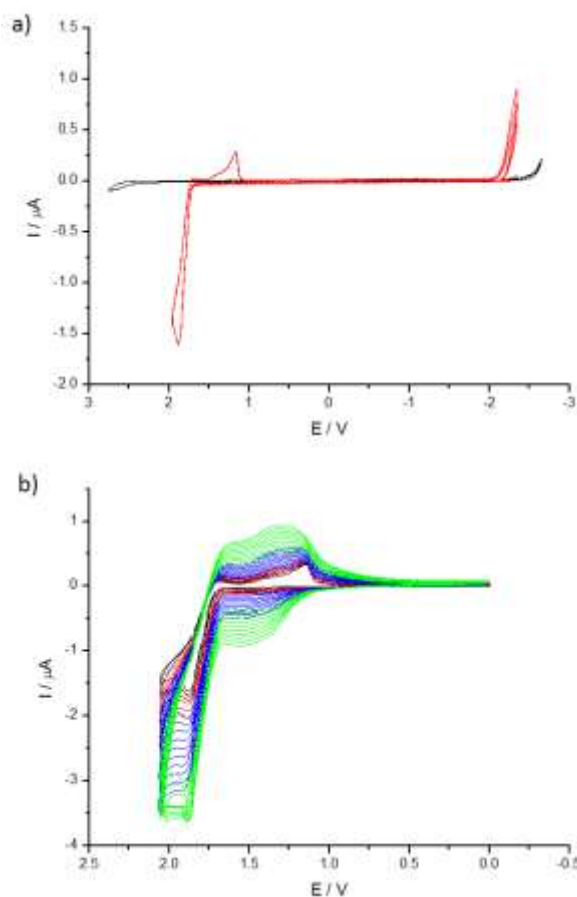
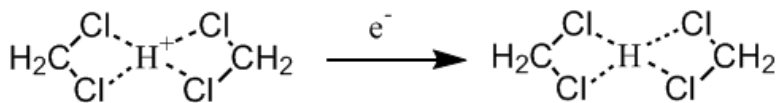


Fig. 29 Cyclic voltammetric curves. a) Comparison between DCM baseline (black) and the first three voltammetric cycles of O-Terphenyl (red); b) multiple oxidative cycles of O-Terphenyl 1mM in 0,08M TBAH/DCM, Pt 125 μ M ultramicroelectrode, Ag QRE, Scan rate: 1V/s

During voltammetric cycling an irreversible reductive process can also be observed at the edge of the negative discharge of the solvent/electrolyte system at about -2 V (see Fig. 29). Such a phenomenon can be attributed to the H^+ reduction in DCM; in fact, the reduction potential of the cluster H^+ -DCM (vide infra), calculated at B3LYP/cc-pVTZ level of the theory, including also the solvation contribution by the model C-PCM, is -2.18 V vs SCE.



Electrochemical oxidation of O-Terphenyl was performed also using an ultraflat ITO glass as working electrode, in order to obtain a flat substrate for the deposit, thus allowing an easily investigation of its morphological composition. An insoluble material is deposited onto the electrode surface, which has been further characterized.

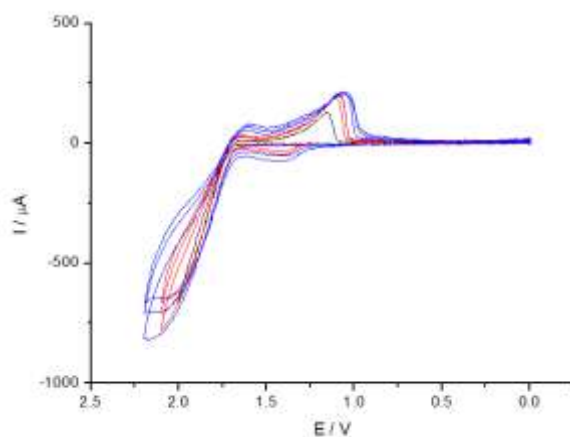


Fig. 30 Deposition onto ultra flat ITO glass; 1mM O-Terphenyl, TBAH 0,08M/ ultra dry DCM, Ag QRE, scan rate: 1V/s

2.3.2 Chemical and morphological composition of Triphenylene-based deposit

2.3.2.1 LD-TOF Spectrum of deposited film

Following a similar investigation and characterization protocol already seen for the previous carbon systems discussed above, the first step to determine the deposit composition was the analysis of LD-TOF spectrum. This clearly showed the presence of oligomers, as a consequence of the intramolecular and intermolecular processes of cyclodehydrogenation promoted by electrochemical oxidation. The value of m/z for O-Terphenyl is 228 and its dimers, trimers and tetramers formation is characterized by a linear hydrogen decrease; in fact, the oligomers lose two, six and eight Hydrogen atoms, respectively.

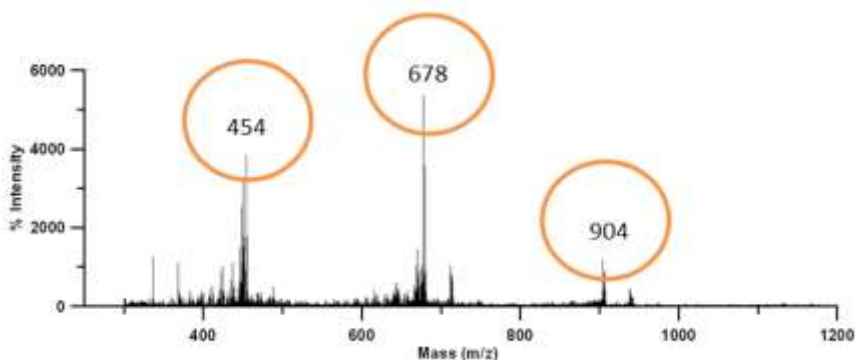


Fig. 31 LD-TOF Spectrum of the Triphenylene-based material deposited on ITO electrodic surface with highlighted dimers, trimers and tetramers

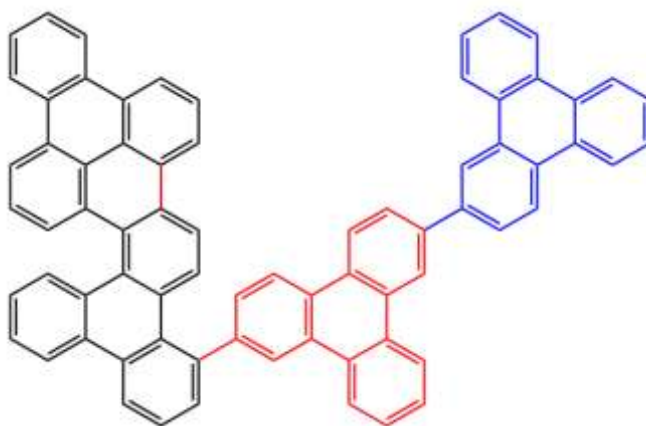


Fig. 32 One of the possible structures for dimer (black), trimer (red) and tetramer (blue) obtained by electrochemical inter-intramolecular O-Terphenyl oxidation

2.3.2.2 Absorbance and Raman Spectra

The yellowish deposit was then characterized by UV-Vis and Raman spectroscopy. The mixed oligomer deposit absorbance spectrum was compared with that of commercial Triphenylene, both in DCM solution and dropcasted onto ITO surface. The sample electrochemically obtained has some features in common with the dropcasted one, showing two large bands around 500 and 800-1000 nm, which are not present in solution and probably caused by charge transfer phenomena between packed molecules. A deeper investigation shows a correspondence between Triphenylene monomers spectra, despite a little red shift of the four little peaks, between 320 and 360 nm can be seen in the case of dropcasted sample, and which are substituted in our deposit by a single wide band centred at 330 nm.

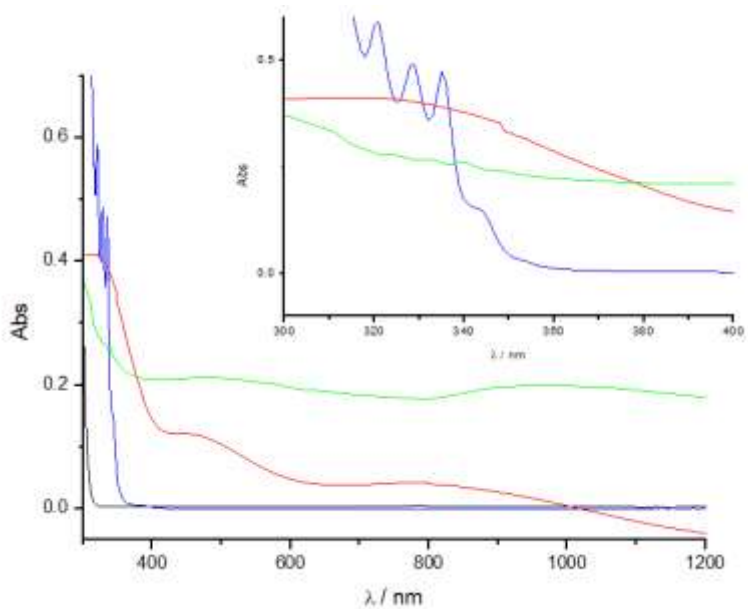


Fig. 33 Absorbance spectra of O-Terphenyl 1mm/DCM (black), of our film (red), chemically synthesized Triphenylene monomer both 1mm in DCM (blue) and dropcasted on ultra flat ITO surface (green), detail shows the transition from defined peaks to a single wide band going from monomer to the oligomeric deposit

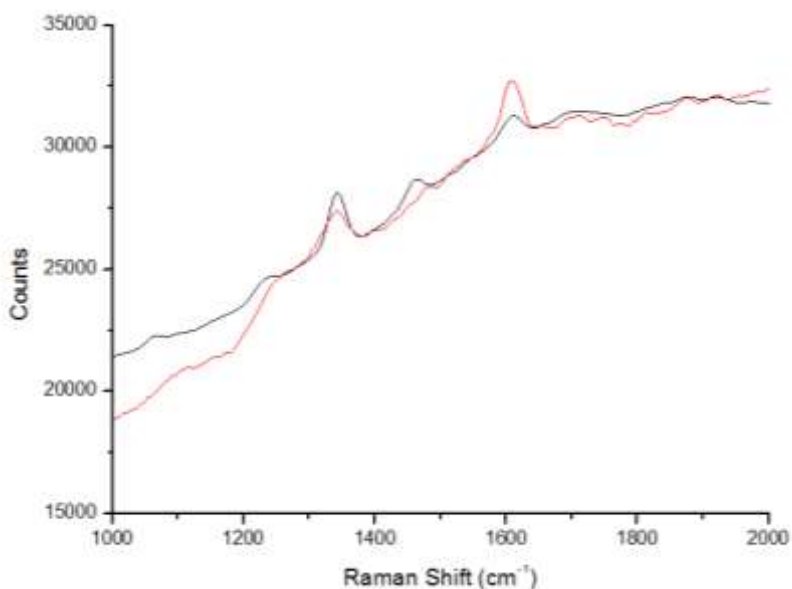


Fig. 34 Correspondence between Raman spectra of twenty times amplified oligomeric film on ITO glass (red) and purchased Triphenylene dropcasted onto ITO (black); (Ventana 532 Raman Spectrophotometer of Ocean Optics)

Raman spectrum of the film has some features in common with the Triphenylene obtained by chemical synthesis, especially D and G band at 1341 cm^{-1} and at 1608 cm^{-1} , even though there is not a total correspondance.

2.3.2.3 AFM

Atomic Force Microscopy of the deposit reveals the formation of a material which aggregates in little uniform grains of sub-micrometric dimension and this is commonly observed for polymeric material.

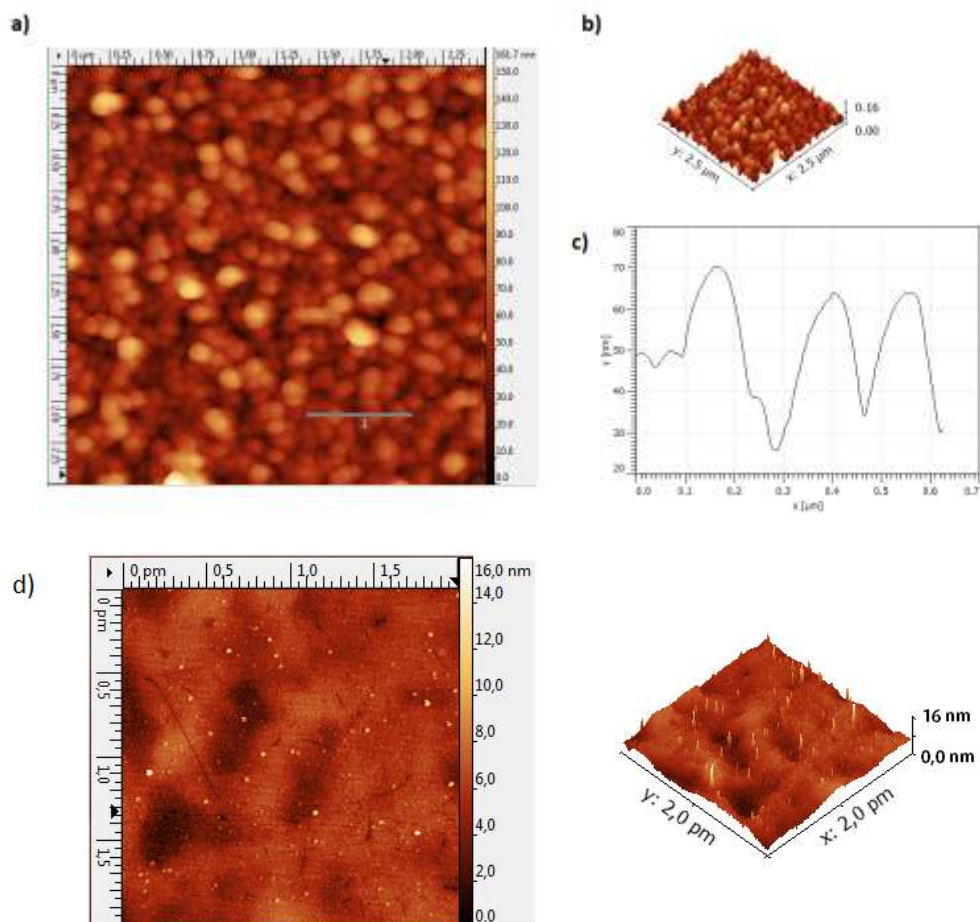


Fig. 35 a) AFM image of oligo-Triphenylene sample deposited on ITO glass and b) its three-dimensional vision, c) sample profile with relative height (grey line in fig.a), d) AFM image of ultra flat ITO used for oligomers deposition

2.3.3 Carbons substrates for enzymatic catalysis

Carbon structures are commonly used, in the form of Pyrolytic Graphite Edge Electrode (PGEE), as conductive supports for studying enzymes. Several proteins and enzymes, in fact, adhere to such scaffolds without

losing their catalytic activity, giving a good challenge to easily exploit much of their properties. [17]

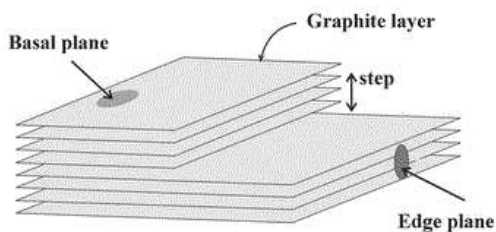


Fig. 36 a) Sketch of edge plane pyrolytic Graphite respect to basal plane that exposes Graphite layer

2.3.3.1 Basic enzymatic working mechanism

Enzymes are among the most studied energy producing systems but not all of their function mechanisms are completely understood. Enzyme operation is, in fact, very complicated, their catalytic activity is affected by activation, inhibition mechanisms and continuous three-dimensional conformational changes. The deep investigation of their function could help scientists to enhance their catalytic activity and their application in bio-based energy devices. Enzymes bound to a substrate is the key step for biocatalytic reactions as it allows the favorable alignment for the substrate to spontaneously react with its partner, with the lowest possible activation energy. The part of the enzyme responsible for the success of this reaction is the *active site* that specifically and sterically binds to the substrate.

One of the most studied class of enzymes is surely Hydrogenase, that catalyzes reversible H_2 production and represent an attracting option for replacing in the future fossil fuels that produce greenhouse gas .

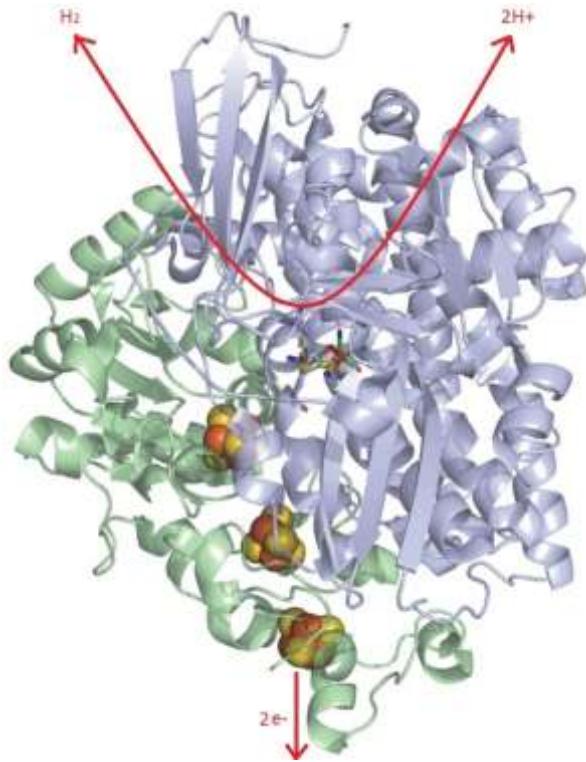


Fig. 37 Hydrogenase from *Ralstonia Eutropha* microorganism structure. In the centre of the protein is buried the Nickel-Iron active site; three iron-sulfur clusters provide a bridge for electron transfer to Cytochrome b (in nature) or to the electrode surface

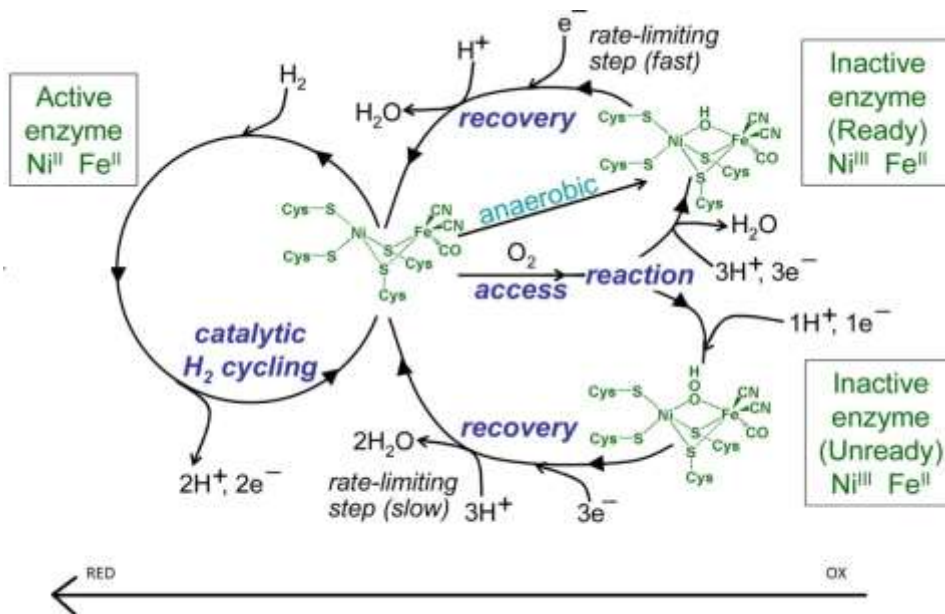


Fig. 38 Sketch of the complex working mechanism of Hyd with the role of NiFe active site highlighted

In order to maximize and uniform reaction rates, enzymes are subjected to activation cycles; when enzymes stick to the conductive support, reactions proceed with random kinetics, but if all molecules are in the same ideal configuration, aligned in order to have an accessible active site, reactions will be facilitate and proceed at the maximum rate.

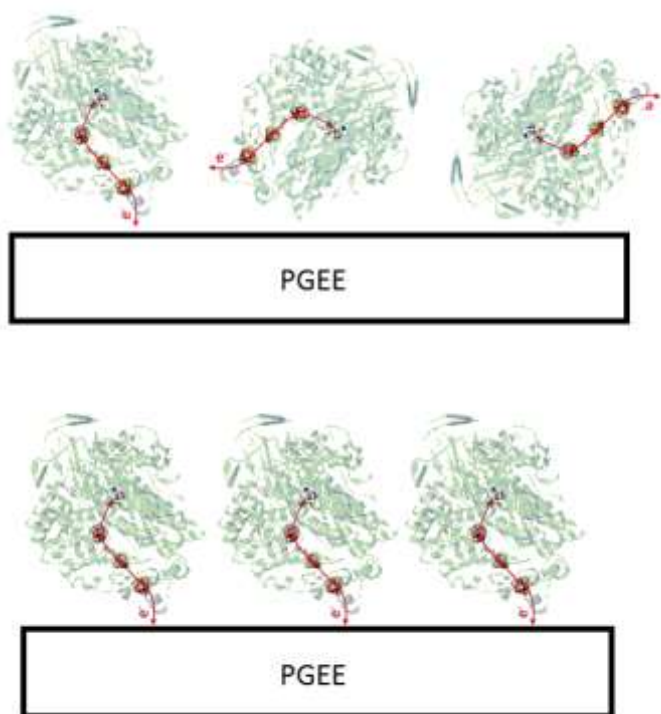


Fig. 39 Sketch of the effect of activation on enzymatic film (random (up) and ordered (down) enzymes distributions): the accessibility of the active site and the correct orientation of Fe-S clusters functioning as a bridge between the active site and the electrode guarantees the maximum rate constant and an increase in current

2.3.3.2 Nanostructured Carbons for Enzyme studies

Enzymatic activation and catalysis are commonly studied using chronoamperometry or cyclic voltammetry at PGEE rotating disc electrodes but the use of nanostructured carbon electrodes could be a good challenge to increase their activity in bioenergetic devices. ^[18]

For this reason we decided to test Hydrogenase1 wild type (Hyd1 WT) adhesion and activation onto nano-Graphenic Triphenylene-based film.

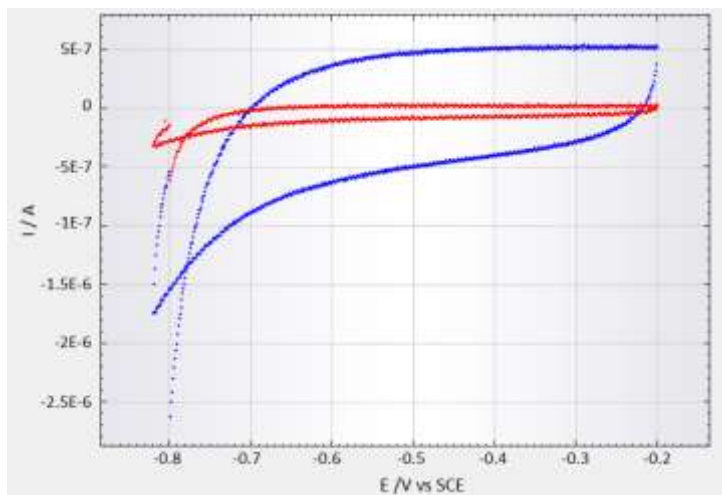


Fig. 40 Cyclic voltammeteries of the Triphenylene-based film on ITO surface at 1 mV/s (red) and 10 mV/s (blue) in mixed Hydrogenase Buffer (MHB) ^[19], CE: Pt, RE: SCE

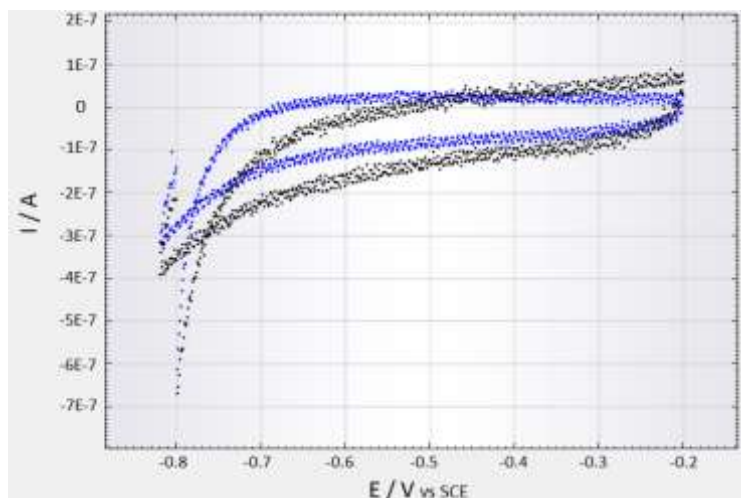


Fig. 41 The comparison between PGEE at 10 mV/s (black) and Triphenylene-based electrode at 1 mV/s (blue); MHB, CE: Pt, RE: SCE

The comparison between the electrochemical behaviour of our film, compared to that of PGEE, in the same potential range is similar even though current resulted to be higher due to the higher surface area of ITO deposit.

Before testing enzyme adhesion to our sample the eventual activity of Triphenylene oligomers towards H_2 reduction in enzyme absence was tested.

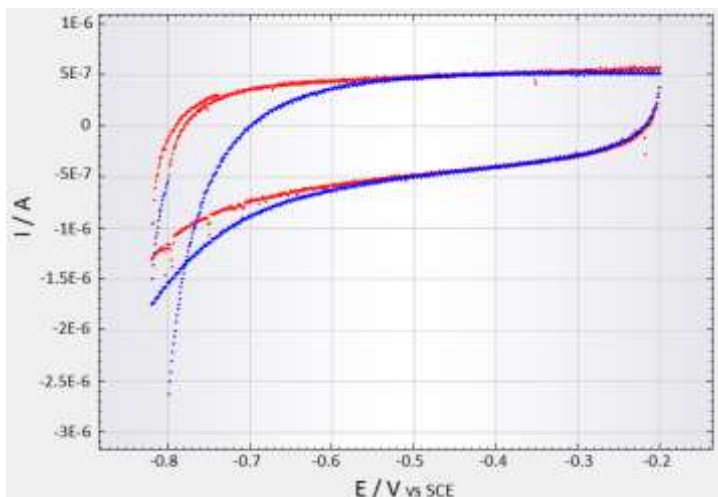


Fig. 42 Triphenylene film deposited on ITO in absence (blue) and presence (red) of H_2 ; scan rate: 1 mV/s, MHB, CE: Pt, RE: SCE

The voltammetric response of Triphenylene oligomeric film does not show any activity with respect to H_2 reduction, in fact, no change in current is obtained after bubbling it close to the WE surface. At this point, in order to verify if there is a certain degree of adhesion of the enzyme to the nanostructured substrate, Hydrogenase1 (Hyd1) from *Escherichia Coli* (E

coli) was dropcasted onto the modified ITO surface and cycled to verify if any current change was visible.

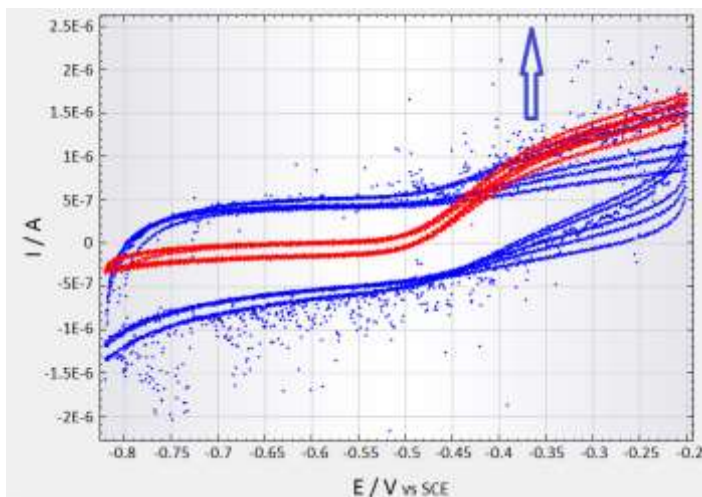


Fig. 43 Hyd1 WT on PGEE (red) and on Tryphenylene based film on ITO (blue); 10 μ l dropcast; scan rate: 1 mV/s, MHB, CE: Pt, RE: SCE

Multiple cyclic voltammetric curves of Hyd1, dropcasted onto Tryphenylene-based film on ITO, show a progressive increase in H_2 reduction current. This phenomenon gives an indication on the conversion from the inactive to the *active form* of proteins, which have metabolic activity and that effectively catalyze H_2 reduction. Importantly, the onset of the reduction current is practically the same as for the Hyd1 on PGEE. This demonstrates the efficient grafting of Hydrogenase on Triphenylene-based nanocarbon and hence that such nanostructured new materials could be possibly used as substrates for immobilizing catalysts and in particular biocatalyst for the exploitation of bioenergetic applications.

References

- 1 a) Barth W.E., Lawton R.G., *JACS*, **1966**, *88*, 380; b) Borchardt A. et al., *JACS*, **1992**, *114*, 1921; c) Scott L.T. et al., *JACS*, **1991**, *113*, 7082; d) Scott L.T. et al., *JACS*, **1997**, *119*, 10963; e) Seiders T.J. et al., *JACS*, **1999**, *121*, 7804; f) Sygula A., Rabideau P.W., *JACS*, **2000**, *122*, 6323
- 2 a) Lovas F.J. et al., *JACS*, **2005**, *127*, 4345; b) Petrukhina M.A. et al., *J ORG CHEM*, **2005**, *70*, 5713; c) Scott L.T., Hashemi M.M., Bratcher M.S., *JACS*, **1992**, *114*, 1920
- 3 a) Mack J. et al., *ORG BIOMOL CHEM*, **2007**, *5*, 2448; b) Valenti G. et al., *J PHYS CHEM C*, **2010**, *114*, 19467
- 4 a) Faust R., Vollhardt K.P.C., *J CHEM SOC, CHEM COMM*, **1993**, 1471; b) Sastry G.N. et al., *J CHEM SOC, PERKIN TRANS 2*, **1993**, 1863
- 5 Haddon R.C., *ACC CHEM RES*, **1992**, *25*, 127
- 6 Bard A.J., Faulkner L.R., **2001**, *Electrochemical Methods. Fundamentals and Applications*, 2nd ed., New York, Wiley
- 7 a) Bruno C et al., *J PHYS CHEM B*, **2009**, *113*, 1954; b) Ayalon, A. et al., *SCIENCE*, **1994**, *265*, 1065
- 8 Yanney M., Fronczek F.R., Sygula A., *ORG LETT*, **2012**, *14*, 4942
- 9 a) Eisenberg D. et al., *J ORG CHEM*, **2008**, *73*, 6073; b) Ref. 2 c) Riccò M. et al., *JACS*, **2010**, *132*, 2064; c) Ref. 45 Chap.1; d) Ref. 46 Chap. 1
- 10 a) Lichtenberger D.L. et al., *CHEM PHYS LETT*, **1991**, *176*, 203; b) Ref. 2
- 11 a) Wu J., Pisula W., Müllen K., *CHEM REV*, **2007**, *107*, 718; b) Chai J. et al., *NATURE*, **2010**, *466*, 470; c) Simpson C.D. et al., *CHEM EUR J*, **2002**, *8*, 1424
- 12 Simpson C.D. et al., *JACS*, **2004**, *126*, 3139
- 13 a) Castiglioni C. et al., *J CHEM PHYS*, **2001**, *114*, 963; b) Negri F. et al., *J CHEM PHYS*, **2004**, *120*, 11889
- 14 Casiraghi C et al., *NANO LETT*, **2007**, *7*, 2711
- 15 Wong W.W.H. et al., *J MATER CHEM*, **2012**, *22*, 21131
- 16 a) Marguet S. et al., *J PHYS CHEM B*, **1998**, *102*, 4697; b) Seguy I., Destruel P., Bock H., *SYNTHETIC MET*, **2000**, *111*, 15; c) Heppke G. et al., *J MATER CHEM*, **2000**, *10*, 2657; d) Kumar S., *LIQ CRYST*, **2005**, *32*, 1089; e) Feudenmann R., Behnisch B., Hanack M., *J MATER CHEM*, **2001**, *11*, 1618; f) Saleh M. et al., *MACROMOLECULES*, **2010**, *43*, 137

-
- 17 a) Sucheta A. et al., *BIOCHEMISTRY*, 1993, 32, 5455; b) Hexter S.V. et al., *PNAS*, 2012, 109, 11516
- 18 a) Lyon L.J., Stevenson K.J., *ELECTROCHIM ACTA*, 2008, 53, 6714; b) Quinson J. et al., *FARADAY DISCUSS*, 2014, 172, 473
- 19 Fourmond V. et al., *CHEM COMM*, 2013, 49, 6840

3 Doped and functionalized Nanocarbons for energy conversion

The concerns about the great incoming environmental and energy problems, have driven increasing scientific efforts towards the study and resolution of these issues. In this scenario doped and functionalized nanomaterials with their extreme flexibility have attracted the attention of scientific community.

3.1 Oxygen Reduction Reaction

Oxygen Reduction Reaction (ORR) is one of the most important reactions in life because it is involved in biological respiration but it is also one of the key process in fuel cells and lithium-Oxygen batteries. Fuel cells are devices, based on redox reactions, able to convert the chemical energy of specific fuels in flowing electrons that, directed trough the external circuit, supply it with energy. The most environmental friendly fuel cells are surely that based on H_2 oxidation and O_2 reduction half-reactions; when H_2 and O_2 are, in fact, used as fuels the only waste-product is water. ^[1]

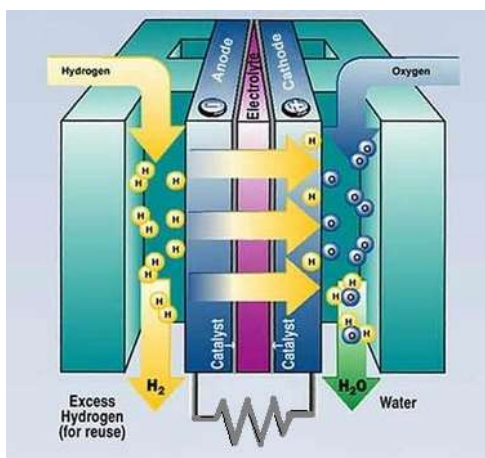


Fig. 44 Fuel Cell based on H_2 oxidation and O_2 reduction reactions.

Similarly, Li-O₂ rechargeable batteries are able to convert chemical energy in electric current, during discharge ORR, at Carbon cathode, transforms Li in peroxides and during recharge O₂ is given back to atmosphere and Li⁺ is reduced to metallic Li on anode surface. [2]

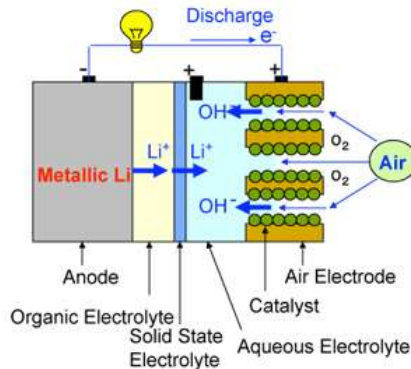


Fig. 45 General simplified sketch of one of the possible working mechanism of Li-O₂ battery

Oxygen reduction occurs via specific mechanisms: in aqueous solutions through the direct four-electrons reduction from O₂ to water (H₂O) or following the less efficient two-electrons process to hydrogen peroxide (H₂O₂) while in alkaline or non-aqueous solutions to superoxide (O₂⁻).

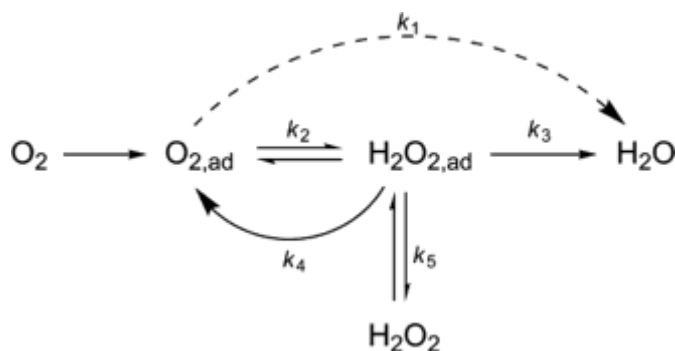


Fig. 46 Mechanism for ORR in aqueous solutions

Both half-reactions are possible thanks to O₂ adsorption on a suitable catalysts that permit to overcome the high energy barrier, thus providing the reaction with an alternative, low energy multi-step way.^[3]

Electrolyte	OR reactions	Thermodynamic electrode potential at standard conditions, V
Acidic aqueous solution	$O_2 + 4H^+ + 4e^- \rightarrow H_2O$	1.229
	$O_2 + 2H^+ + 2e^- \rightarrow H_2O_2$	0.70
	$H_2O_2 + 2H^+ + 2e^- \rightarrow 2H_2O$	1.76
Alkaline aqueous solution	$O_2 + H_2O + 4e^- \rightarrow 4OH^-$	0.401
	$O_2 + H_2O + 2e^- \rightarrow HO_2^- + OH^-$	-0.065
	$HO_2^- + H_2O + 2e^- \rightarrow 3OH^-$	0.867
Non-aqueous aprotic solvents	$O_2 + e^- \rightarrow O_2^-$	—
	$O_2^- + e^- \rightarrow O_2^{2-}$	—

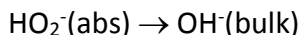
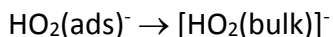
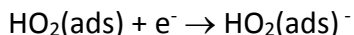
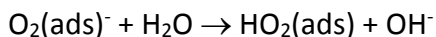
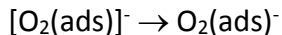
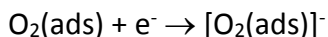
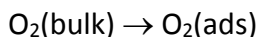
Tab. 3 Principal O₂ reduction reactions are listed together with their standard potentials in acid and alkaline media. Thermodynamic potentials in non-aqueous aprotic solvents, strictly depending on the specific solvent, are not indicated

The best catalyst for O₂ reduction, by now, is Platinum but it presents several problems, mainly due to poisoning and limited abundance that obviously influences its price and hence does not allow its massive use. The switching to non precious metals or even to metal-free catalyst could be a turning point in H₂ fuel cells and Li-air batteries massive application. In this scenario, nanomaterials as catalysts for ORR seem very promising; they have, in fact, uncommon and peculiar properties that could enhance H₂O₂ decomposition in favour of O₂ and H₂O production.

3.1.1 Nanocarbons for ORR

Among all nanomaterials the most promising to replace platinum and other precious catalysts seem to be Carbon based ones, especially for their conduction properties, resistance to corrosion and low production cost. Another great advantage of the Carbon nanomaterials (CNMs) is that they could work both as supports, electrodes and catalysts.

The catalytic mechanism of Carbon materials for the ORR is not completely clear yet but the most authoritative seems to be characterized by several basic steps that include (i) O₂ adsorption, (ii) electron transfers from CNMs to O₂ and (iii) the subsequent formation of high energy intermediates (Reactive Oxygen Species, ROS). This reaction step is very difficult to be followed because ROS have very short lifetimes and cannot be easily isolated.



The last reaction is that responsible for H₂O production that, for a maximized efficiency, should be enhanced to disadvantage of previous one, responsible for peroxide production.

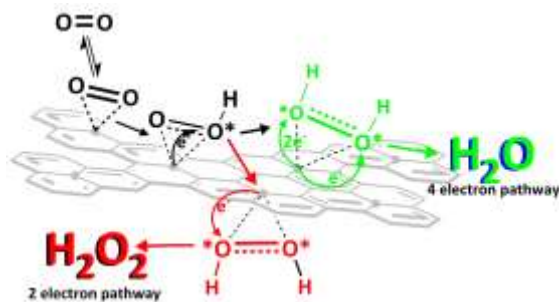


Fig. 47 Sketch of two reaction pathways on Graphene surface

Even though the 2-electrons pathway seems to be the major way for *Carbons* ORR ^[4], actually, there is no accord in the scientific community on the reasons for this enhanced electrocatalytic activity. Great part of the success of such systems seems to be due to the presence of doping atoms. It has been theoretically demonstrated that the voluntary or involuntary insertion of different atoms in the lattice alters Graphene electronic structure, thus modifying its energy potential surfaces. Several doping atoms and their combinations have been tested to find the most promising conditions for enhancing CNMs catalytic activity and give a definitive direction to this science branch. The most studied dopants are Sulphur, Boron, Phosphorus, Fluorine and Nitrogen. ^[5] Reduced graphene oxide (rGO) materials doped with Boron, Nitrogen and mixed Boron Nitrogen have been investigated. However, in this dissertation only the most efficient ORR catalytic systems will be discussed.

3.1.2 Nitrogen doped reduced Graphene Oxide (rGO- N)

Nitrogen doping seems very promising for Graphene based electrocatalysts for ORR. The efficiency of this strategy is due to the presence of Nitrogen itself that, thank to its electron accepting behaviour in the sp^2 lattice, withdraws electrons causing a relatively positive charge density on

adjacent Carbon atoms, promoting a local dipole formation. In such situation Yeager model for O_2 absorption seems to be privileged respect Pauling one; the parallel diatomic absorption affects substrate bonding, weakening O_2 double bond and promoting ORR with a probable higher efficiency of the 4-electrons reaction. [6]

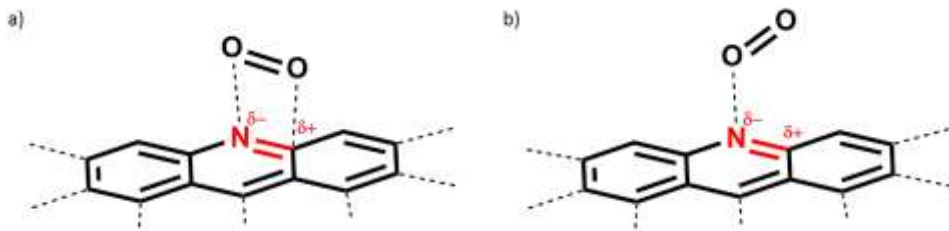


Fig. 48 Two possible mechanisms for interaction between substrate and catalyst; a) side-on mechanism, as assumed in Yeager model, seems to be privileged in N-doped Carbons respect to b) end-on mechanism as assumed in Pauling model

The situation is further complicated by Nitrogen hybridization; not all the Nitrogen atoms in the system show the same behaviour towards ORR and in order to perform it is necessary to point and maximize the N active form content respect to the non active ones. [7]

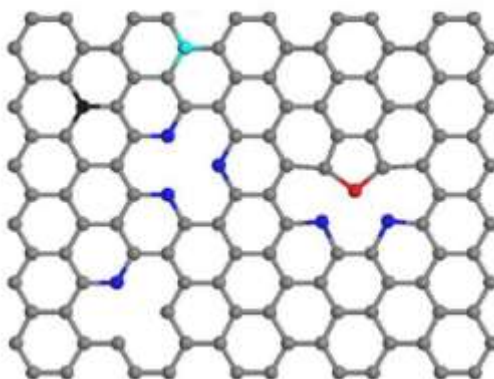


Fig. 49 Different kinds of Nitrogen hybridization in Graphene lattice; quaternary N in the basal plane (black), quaternary N in the edge plane (pale blue), pyrrolic N (red) and pyridinic N (blue) probably responsible for high and stable ORR.

Several other factors affect N-Graphene performances. It has been, in fact, demonstrated, by using digital simulation and hydroperoxide decomposition rate constant, that a specific role is performed by edge defects. ^[8]

Debate is still opened but surely the complexity of such a topic requires accurate studies and control of several factors. In this scenario our purpose is to give another contribution for the development of metal free, green and low cost catalysts.

3.1.2.1 Synthesis and characterization of rGO-N

Nitrogen doped Graphene Oxide (rGO-N) was prepared with a combined reductive amination of Graphene oxide, using Hydrazine (H_2N_4) in water solution.

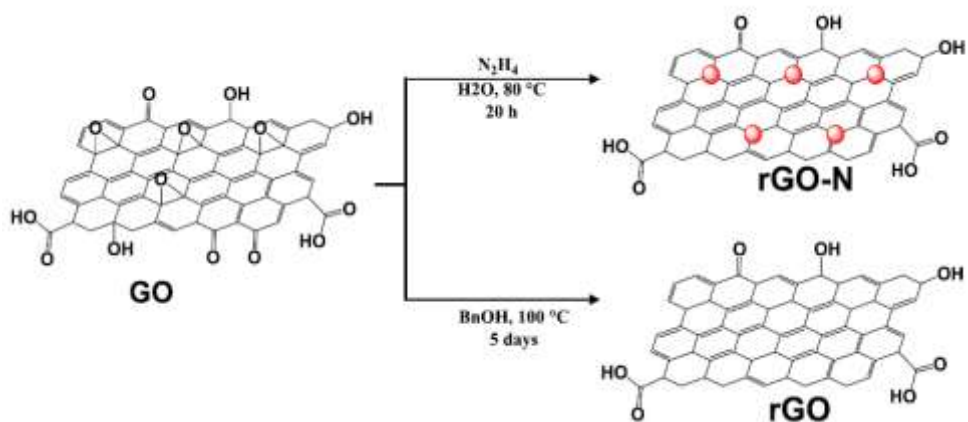


Fig. 50 Synthetic pathways for rGO and rGO-N

The obtained materials were characterized by elementary analysis and XPS in order to confirm the reduction and heteroatom insertion that is visible in the decrease of oxygen content and increase in Nitrogen, previously absent.

Sample	Elem. Anal (wt.%)		XPS (at.%)		
	C	N	C	N	O
Graphite	98,0	0,0	97,8	0,0	2,2
GO	48,0	0,0	69,1	0,0	30,4
rGO	83,5	0,0	87,6	0,0	12,4
rGO-N	77,6	1,9	84,1	1,8	12,9

Tab. 4 Elementary analysis and XPS measurements demonstrate the proficient insertion of Nitrogen in the lattice and the decrease in Oxygen content both for rGO and rGo-N

Comparing C1s XPS spectra of Graphene, GO, rGO and rGO-N, it is clear how reduction corresponds to a decrease of the components with high binding energy, corresponding to CO groups and a reconstruction of C sp² network; on the other side N1s spectrum of rGO-N shows the prevalence of pyrrolic or amminic groups at 400 eV and a minor component at 402 eV that can be attributed to nitro-oxidized species.

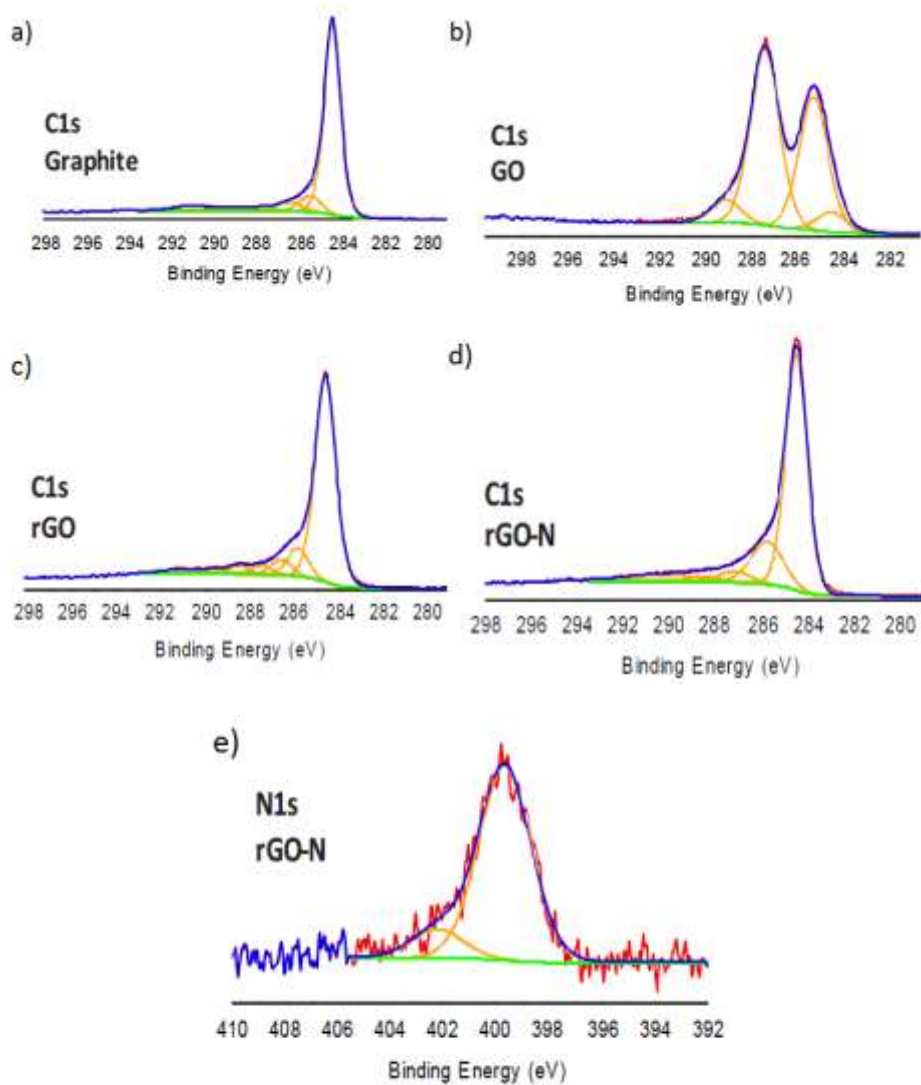


Fig. 51 C1s XPS spectra for a) Graphite, b) GO, c) rGO, d) rGO-N and e) N1s XPS spectrum for rGO-N

3.1.2.2 Electrochemical characterization

3.1.2.2.1 Cyclic Voltammetry

Electrochemical characterization was performed in alkaline solution in order to reproduce alkaline fuel cells conditions and to avoid proton coupled electron transfer (PCET), which would dramatically slow down the reaction kinetic. [9]

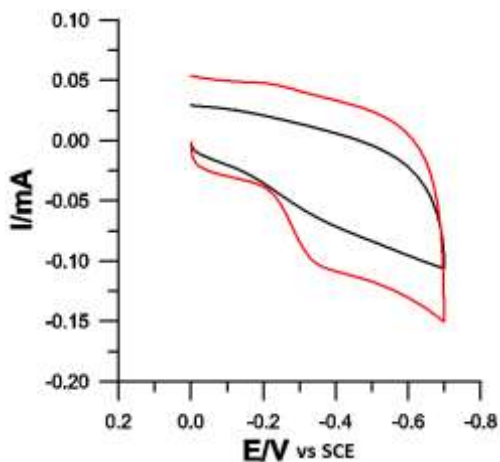


Fig. 52 Cyclic Voltammeteries of rGO-N 40 μ l of 1 mg/ml EtOH dispersion dropcasted onto Glassy Carbon (GC) WE in PBS 1x solution at pH=7 (black) and KOH at pH=13 (red); O₂ atmosphere; scan rate=0,05V/s

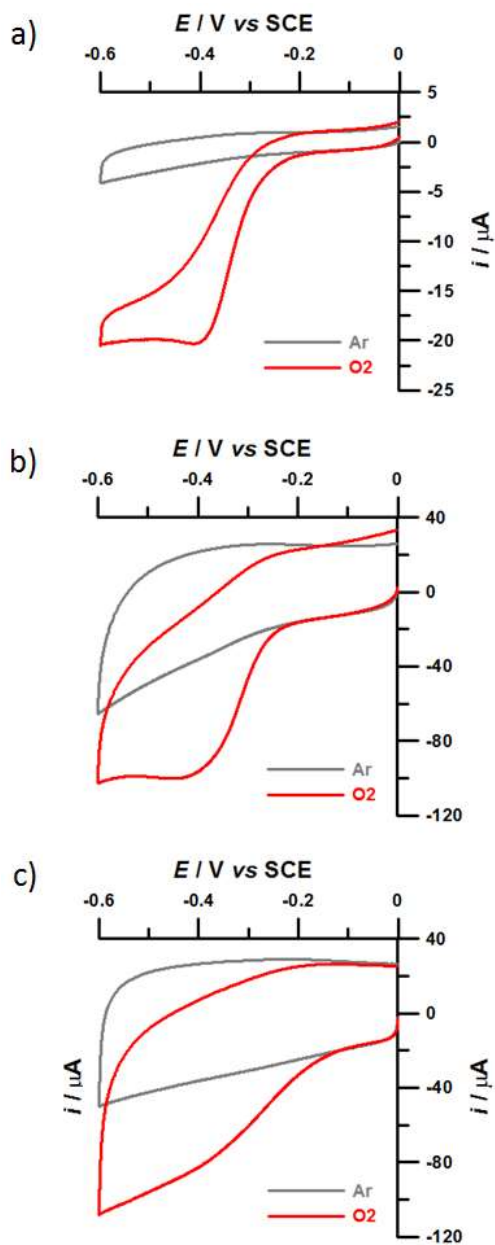


Fig. 53 Cyclic voltammograms in KOH 0.1M solution (pH=13), in presence of Argon (grey) and O₂ atmosphere (red) of a) GO, b) rGO and c) rGO-N; 40 μl of 1 mg/ml EtOH dispersion dropcasted onto GC electrode; scan rate: 25 mV/s; T= 298K

Reduced GO and rGO-N show an impressive increase, one order of magnitude, of current respect GO; moreover the doped material shows a lower overpotential for ORR (-0,18 V vs SCE).

3.1.2.2.2 Rotating Disc Electrode Voltammetry

Cyclic voltammetry with Rotating Disc Electrode (RDE) was performed in order to obtain Koutecky-Levic plots. Rotating the electrode with dropcasted catalyst at different rotation rates ω , produces different limiting current values (I_L). The plot of the dependence of I_L versus ω allows to obtain the number of electrons involved in the ORR processes.

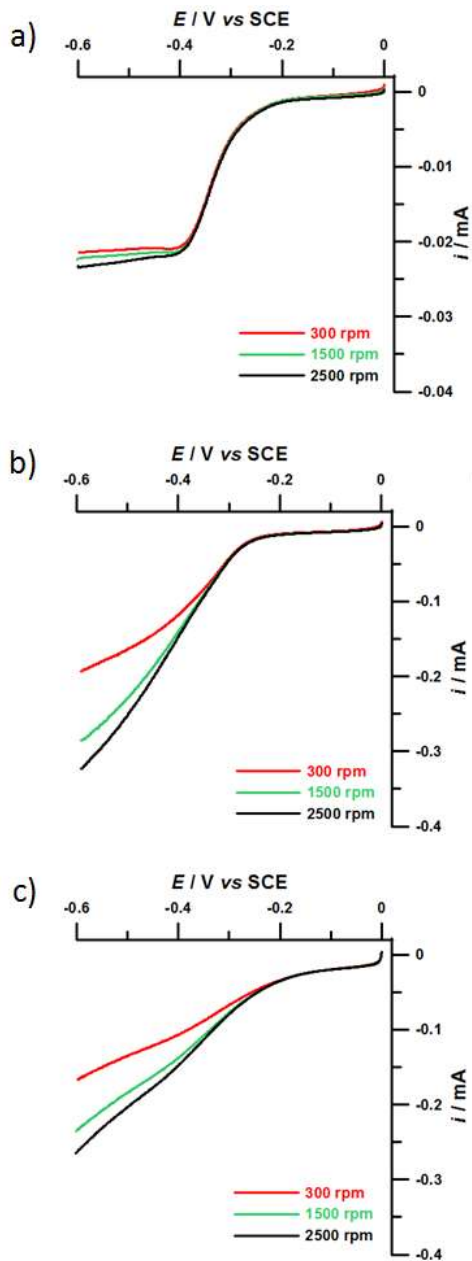
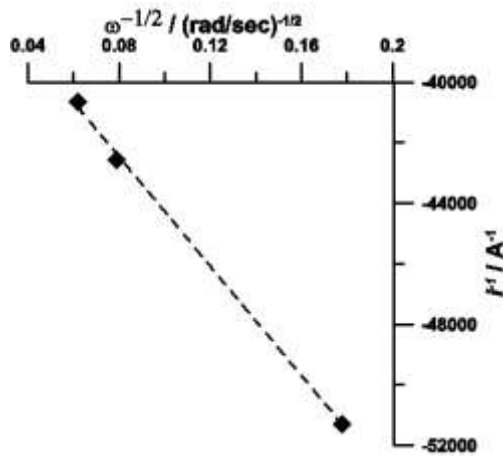


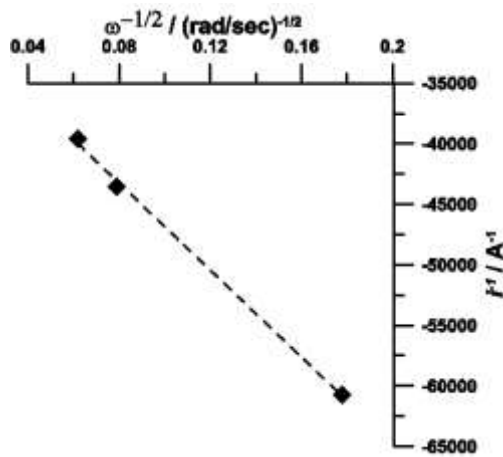
Fig. 54 RDE Voltammeteries for a) GO, b) rGO and c) rGO-N; 40 μ l of 1 mg/ml EtOH dispersion dropcasted onto GC; scan rate: 25 mV/s



ω	300	1500	2500
$\omega^{-1/2}$	0,178	0,079	0,062
$1/i$	-51282	-42553	-40651

Slope	1.0×10^5
n	1,8

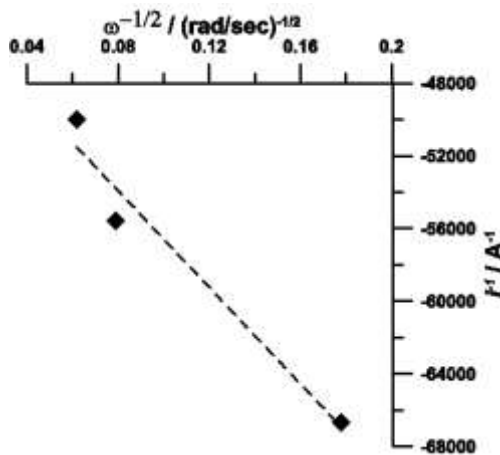
Fig. 55 Koutecky-Levich plot and Tab. 5 Values obtained for GO



ω	300	1500	2500
$\omega^{-1/2}$	0,178	0,079	0,062
$1/i$	-60745	-43544	-39570

Slope	1.19×10^5
n	2,1

Fig. 56 Koutecky-Levich plot and Tab. 6 Values obtained for rGO



ω	300	1500	2500
$\omega^{-1/2}$	0,178	0,079	0,062
$1/i$	-66598	-55587	-50015

Slope	1.30×10^5
n	2,3

Fig. 57 Koutecky-Levich plot and Tab. 7 Values obtained for rGO-N

The rGO-N, compared to GO and rGO, gave the best results with a mechanism, at -0,5 V, that is compatible with a two-electron pathway. This demonstrates that the oxygen reduction catalysed by rGO-N, at such a potential, proceeds by 2-electrons, generating oxygen peroxide.

It is worth to notice that during the voltammetric measurements in Ar atmosphere the current changes until reaching a stable value with time. This effect, visible both at oxidative and reductive potentials, was reproducible and reversible, in fact, alternating reductive and oxidative cycles there is a complete reconstruction of previous voltammetric behaviour.

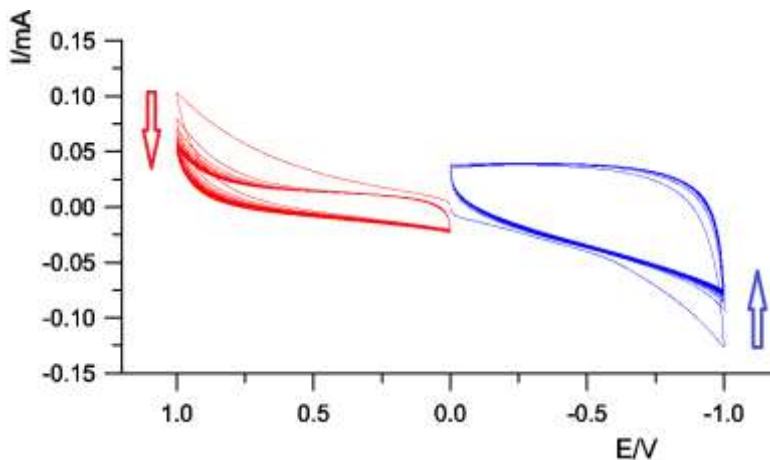


Fig. 58 Oxidative (red) and reductive (blue) voltammetric cycles showing current changes for rGO-N 40 μ l of 1 mg/ml EtOH dispersion dropcasted onto GC electrode; Ar atmosphere; KOH 0,1M; scan rate: 0,05 V/s

After the material underwent a reductive cycling, down to -1.0 V, at least, as reported above in the Figure 58, it shows a slightly higher catalytic efficiency towards the oxygen reduction, especially for what concerns the onset current. This phenomenon can be considered as a sort of “conditioning”, probably due to a partial electrochemical reduction of carbonyl groups and defects, still remaining after the chemical reduction. At opposite, in Figure 59 is possible possible to observe that, when the “conditioning” is carried out in oxidation, there is a little worsening in the rGO-N ORR catalytic performances.

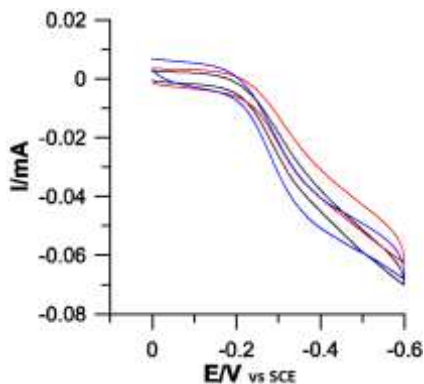


Fig. 59 CVs of unconditioned material (black), material after positive (red) and negative conditioning (blue); rGO-N dropcasted on GC WE in KOH 0,1 M, scan rate: 0,05 V/s

3.1.2.3 Scanning electrochemical microscopy

Generation-Collection SECM mode on rGO-N

Scanning Electrochemical Microscopy (SECM) was used in order to identify products of 2-electrons reaction, i.e., ROS,. The first step consisted in performing a substrate-generation/tip-collection experiment. Using a bipotentiostat two different potentials can be applied to the substrate and the tip, to produce a product that can be analysed and quantified with the electrochemical probe, represented by the UME, positioned just few μm on top of the material.

Substrate potential was varied from 0 to -0,7 V, in order to have different H_2O_2 production rates, while the Platinum tip potential, in close proximity of the substrate surface, was linearly scanned between +0,1 and +0,7 V, which is the most suitable potential range to re-oxidate the most probable product, H_2O_2 .

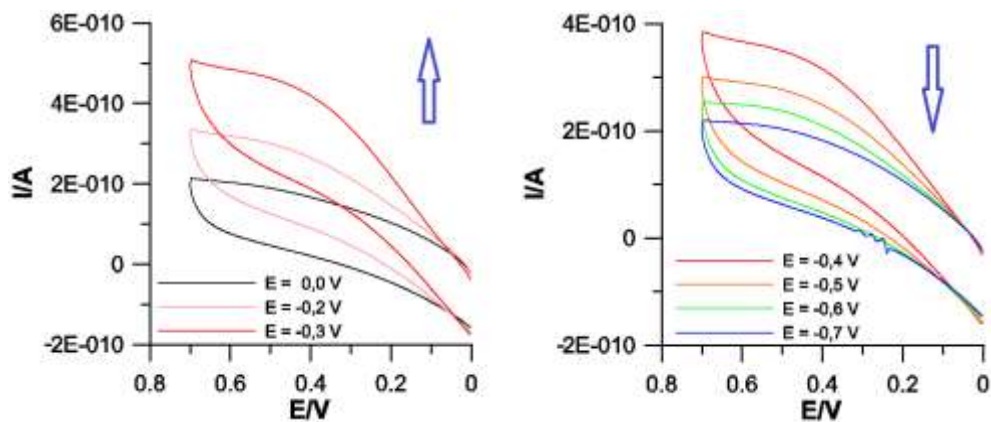


Fig. 60 Cyclic Voltammetric curves recorded at Pt 10 μm tip for different substrate potentials, from 0,0 V to -0,3 V (left) and from -0,4 V to -0,7 V (right). rGO-N dropcasted on Highly Oriented Pyrolytic Graphite (HOPG), scan rate = 0,05 V/s, KOH 0,1 M, Ag/AgCl 3M reference electrode

After an initial increase of tip current with the negative increase of the substrate potentials down to -0.3 V, at more negative potentials (from -0.4 V to -0.7 V), there is a constant decrease in the current recorded by the UME tip.

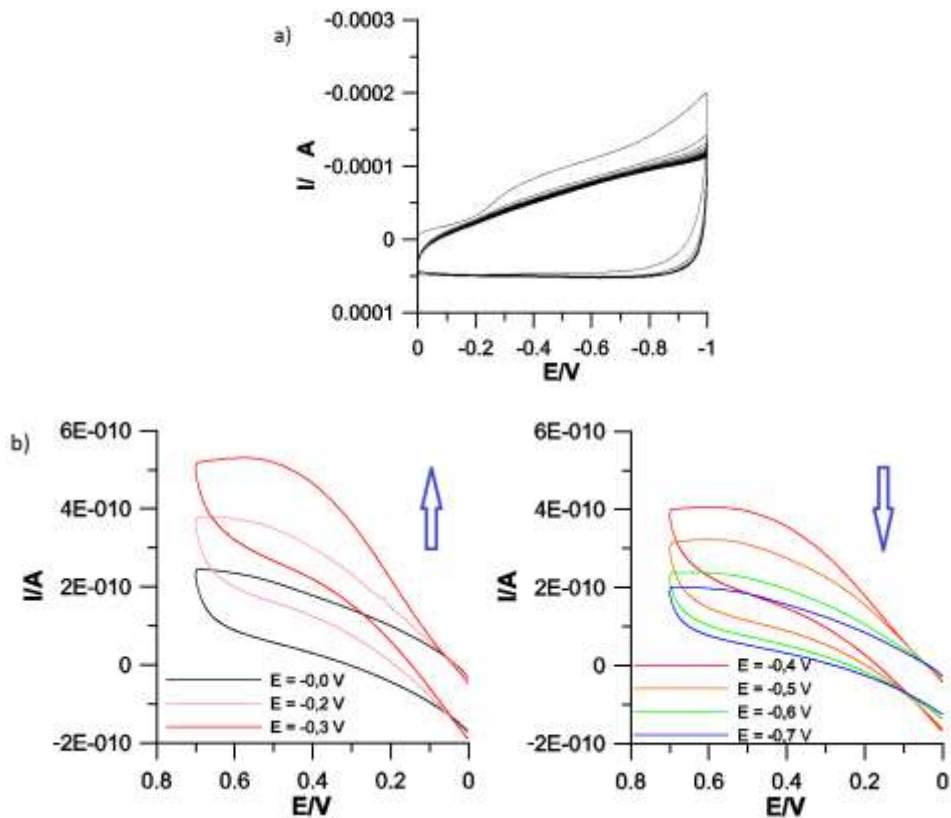


Fig. 61 a) Voltammetric reductive conditioning of rGO-N in KOH 0,1 M, 20 cycles, scan rate 0,05 V/s, RE Ag/AgCl 3M; b) Cyclic Voltammetric curves recorded at Pt 10 μm tip at different substrate potentials, from 0,0 V to -0,3 V (left) and from -0,4 V to -0,7 V (right); rGO-N dropcasted on HOPG, scan rate 0,05 V/s, KOH 0,1 M, RE: Ag/AgCl 3M

Fig. 61 shows that reductive conditioning of the rGO-N material does not affect the trend described above, regarding the production of H_2O_2 . In fact, it is possible to see an increase for substrate potentials up to -0,3 V followed by a current decrease for potentials between -0,4 V and -0,7 V.

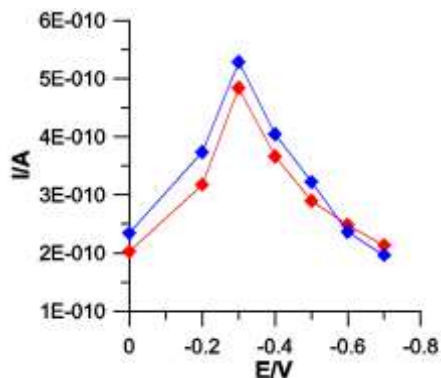


Fig. 62 Comparison between tip currents before (red) and after (blue) the electrochemical conditioning

Such a trend and the difference between negatively and positively conditioned rGO-N has been plotted as tip current versus potential. The increase, followed by the decrease in the current is related to the quantity of H_2O_2 recorded at the tip. The two trends, shifted in current, highlights what has been said above, i.e., that the electrochemical “conditioning” at negative potentials makes the rGO-N more catalytically effective than the pristine rGO-N and even more than the positively “conditioned” one. Moreover, in Figure 62 it is possible to see two potential regions. The falling part in the diagram can be rationalized with a consumption of H_2O_2 by the substrate itself at potentials more negative than -0.3 V. The only explanation for this stems from a further reduction of H_2O_2 at the substrate. Hydrogen peroxide produced in proximity of the catalyst could, in fact, be further reduced to H_2O , with overpotentials higher than -0,3 V.

By using scanning electrochemical microscopy, the maximum number of H_2O_2 moles detectable is 7.3×10^{-16} for unconditioned material and 7.7×10^{-16} after conditioning.

Kinetic electron transfer constant

In order to extract the electron transfer kinetic constant, before and after electrochemical conditioning, a *redox competition mode SECM* experiment has been performed. In this experiments negative potentials are applied both at the substrate and at the tip, in order to reduce Oxygen at both two working electrodes. ^[10]

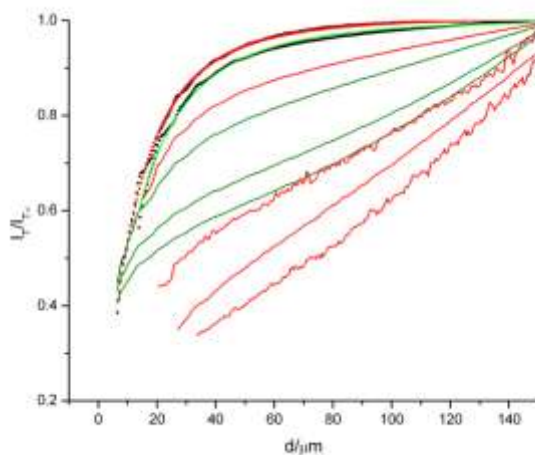


Fig. 63 Approach curves for competition mode SECM (descending negative potentials from 0 to -0,5 V), rGO-N approach curves before (green) and after conditioning (red)

The fitting of the approach curves allows to have the electron transfer kinetic constant that has a value of 0,015 for unconditioned material and 0,030 after conditioning by negatively cycling.

3.2 Fullerene based photoelectrochemical conversion system

As previously mentioned, one of the most important applications of nanomaterials could be in the field of photoelectrochemical energy conversion. Mimicking natural photosynthesis starts with choosing the suitable chromophore, able to absorb light and transfer energy to a reaction centre. At this point a series of electron transfer processes generate a charge separated state between the electron donor and the final acceptor. If charge separation does not recombine rapidly and its lifetime is sufficiently long, photoelectrochemical conversion is highly exploitable. One of the most interesting molecules for this purpose are dyads that joint antenna and charge separation properties. We focused our attention on a Bodipy-fullerene dyad because of the generally high absorption coefficients, emission quantum yields and tuning spectral properties of BF₂-chelated dipyrromethene compounds, together with C₆₀ electronic delocalization efficiency.

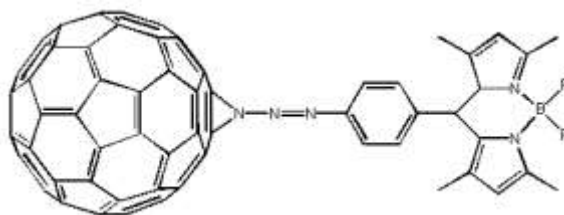


Fig. 64 Our Bodipy-C₆₀ dyad

3.2.1 Absorption and fluorescence measurements

The comparison between isolated Bodipy and Bodipy-C₆₀ absorbance spectra shows the appearance of a band at 330 nm, due to C₆₀ moiety, but no alteration on the 500 nm Bodipy band.

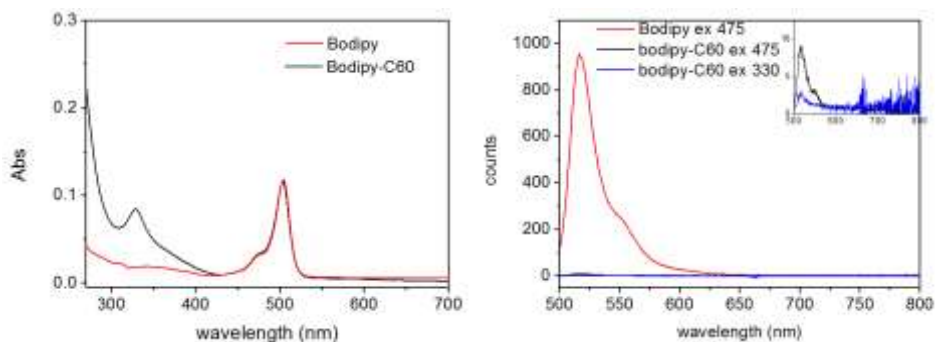


Fig. 65 a) Absorption spectrum of the Bodipy- C_{60} bichromophore in chloroform (black) and isolated Bodipy moiety (red) recorded using a Perkin Elmer LAMBDA 950; b) fluorescence spectra of the isolated Bodipy excited at 475 nm (red) and of Bodipy- C_{60} excited at 475 nm (black) and 330 nm (blue) recorded with Jasco FP-750 fluorimeter

On the other hand fluorescence spectrum of isolated Bodipy is completely different than that of the adduct; in fact, the presence of C_{60} almost completely quenches the fluorescence band of the dye at 516 nm, thus suggesting an electron or hole transfer process in the dyad. However, the fluorescence quenching can be due either to excitation energy transfer or to electron/hole transfer. C_{60} excitation band, centred at 330 nm, also induces Bodipy fluorescence, suggesting that excited state energy transfer from C_{60} to Bodipy is not the main path for the observed emission quenching.

3.2.2 Electrochemistry of Bodipy- C_{60}

3.2.2.1 Voltammetric Investigation

The voltammetric investigation of the Bodipy- C_{60} dyad revealed three reduction and two oxidation processes. The first two reduction processes are completely reversible and one-electron processes that can be

attributed exclusively to C_{60} reduction.^[11] The third voltammetric peak, at higher potentials, is completely irreversible at sweep rate of 1 V/s.

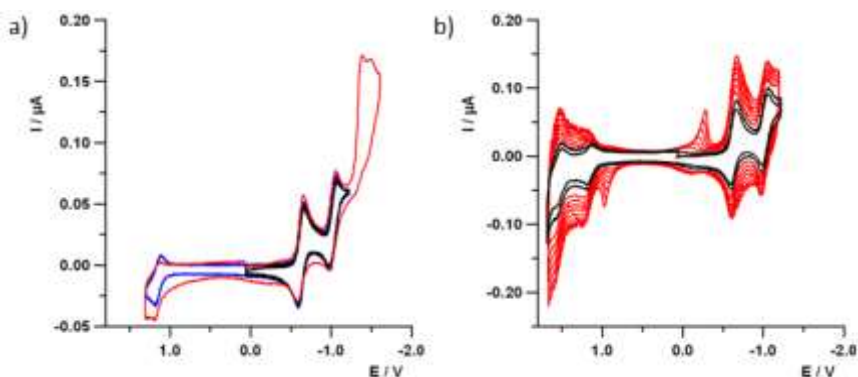


Fig. 66 Cyclic voltammetric curves of species Bodipy- C_{60} 0.6 mM in 0.08 M TBAH/DCM solution, sweep rate 1 V/s, working electrode: Pt (125 μm diameter), $T=25^\circ C$; a) the three reduction (black, red) and first oxidation (blue, red) processes b) The first two reductions and oxidations of Bodipy- C_{60} , show an increase in current (from black to red CV)

On the oxidative part, the first reversible process (at sweep rate of 1 V/s) can be assigned to Bodipy moiety, in fact, its $E_{1/2}$ potential (about +1.2 V) is very close to oxidation potentials of both Phenyl-Bodipy (Bodipy-Ph) and p-azidephenyl-Bodipy (Bodipy-N3) recorded in similar experimental conditions.

At higher potentials, a process with some chemical irreversibility is visible and further cycles show a constant increase in peaks current together with the appearance of a new peaks in the voltammetric curve. Such a behaviour is not visible when scans are reversed before the second oxidative peak and can be explained with the Bodipy- C_{60} bond breaking and the formation of a C_{60} conducting polymer depositing onto the electrode surface.^[12]

To better characterize the dyad and to safely attribute the localization of redox processes to the different moieties of the system, electrochemical investigation of Bodipy-N3 and of Bodipy-Ph was performed.

The voltammetric study of Bodipy-N3 revealed that the apparently irreversible reduction at -1.3V, at room temperature, becomes reversible at faster scan rates and lower temperatures.

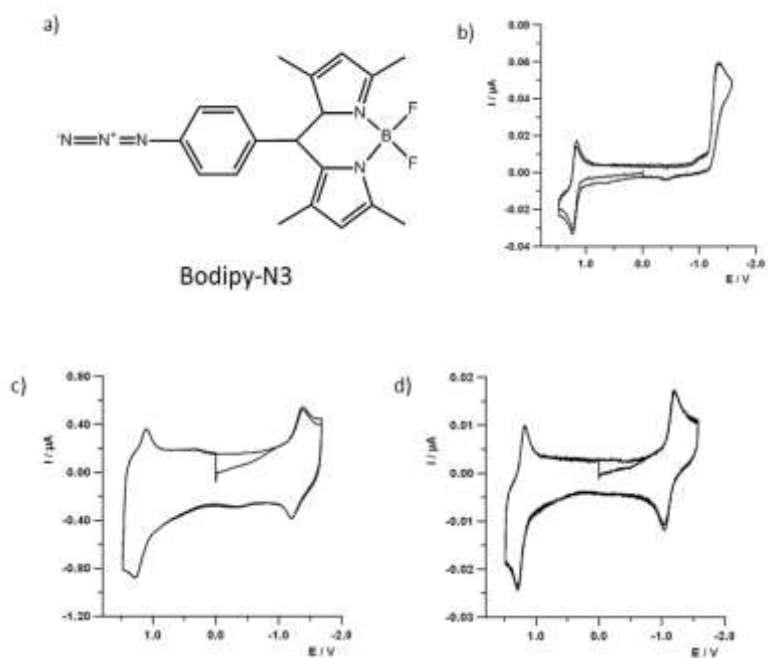


Fig. 67 a) Chemical structure of 10-(4-azidophenyl)-5,5-difluoro-1,3,7,9-tetramethyl-9a,10-dihydro-5H-5H,6H-dipyrrolo[1,2-c:2',1'-f][1,3,2]diazaborinine (Bodipy-N3) and b) Cyclic Voltammetric curves of Bodipy-N3 moiety 0,8 mM in 0.08 M TBAH/DCM solution, working electrode: Pt (125 μm diameter), sweep rate 1 V/s; b) T=25 °C; c) sweep rate 100 V/s, T=25 °C; d) sweep rate 1 V/s, T= -60 °C

The electrochemical investigation of Bodipy-Ph reveals that the reversible oxidation process falls at the same potential of Bodipy-C₆₀, while at higher negative potentials the presence of an irreversible peak (second reduction) that does not change its reversibility either at fast sweep rates or low T.

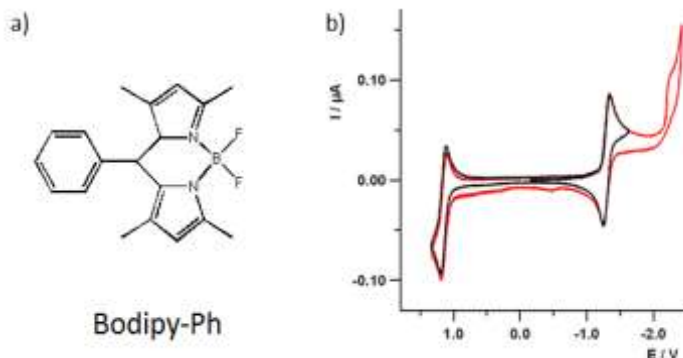


Fig. 68 a) Chemical structure of 5,5-difluoro-1,3,7,9-tetramethyl-10-phenyl-9a,10-dihydro-5H-5l4,6l4-dipyrrolo[1,2-c:2',1'-f][1,3,2]diazaborinine (Bodipy-Ph); b) Bodipy-Ph CV 1 mM in 0.08 M TBAH/DCM solution, working electrode: Pt (125 μm, diameter), scan rate 1 V/s, T=25 °C, reference electrode SCE.

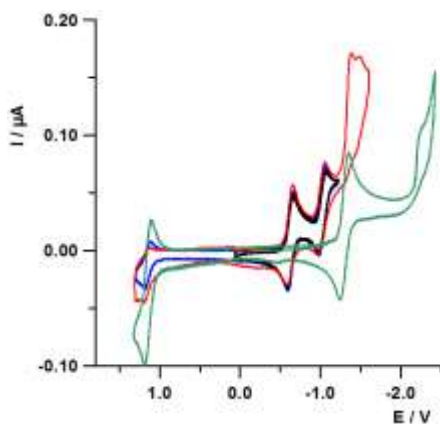


Fig. 69 Bodipy-C₆₀ (black, blue red) is compared with Bodipy-Ph (green). Bodipy-C₆₀ 0.6 mM in 0.08 M TBAH/DCM solution, sweep rate 1 V/s, working electrode: Pt (125 μm diameter), T=25 °C; reference electrode SCE. Bodipy-Ph 1 mM in 0.08 M TBAH/DCM, working electrode: Pt (125 μm, diameter), sweep rate 1 V/s, T=25 °C, reference electrode SCE

Finally, we can assign the following localization: (i) the first oxidation to Bodipy moiety, (ii) the partially reversible second oxidation to C₆₀, with the electrochemically induced reaction localized on the aza-cyclopropane bridge (iii) the first two reductions to C₆₀ and (iv) the completely irreversible third peak can be attributed to the Bodipy moiety.

Species	(Ox.) - E _{1/2} / V		(Red.) - E _{1/2} / V		
	I	II	I	II	III
C₆₀-Bodipy	1.16	1.54	-0.63	-1.02	-1.38 ^b -1.49 ^b
Bodipy-Ph	1.14	--	-1.30	-2.26 ^b	--
C₆₀^c	1.69	2.16	-0.64	-1.04	-1.47

Tab. 8 Half-Wave (E_{1/2}) Redox Potentials^a (vs SCE) of all compounds at 25°C; a) in 0,08 M TBAAsF₆/DCM solution: WE Pt disc (125 μM); b) irreversible process peak potential; c) potentials from ^[13]; all referred in a 0.08 M TBAAsF₆/DCM solution

3.2.2.2 UV-Vis-NIR Spectroelectrochemistry

In order to assess the localization of the charge transfer state of the dyad, UV-Vis-NIR Spectroelectrochemistry (Uv-Vis-NIR SEC) was performed.

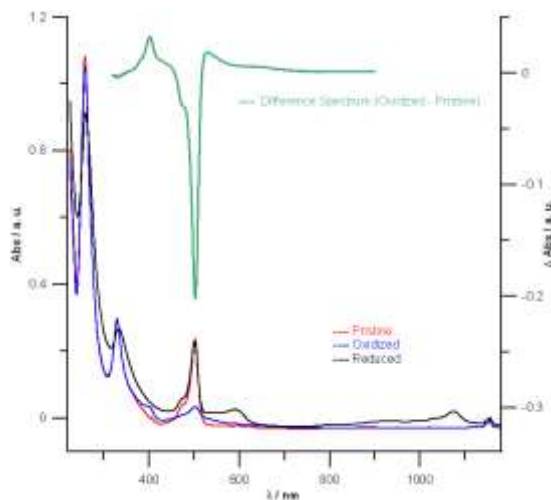


Fig. 70 UV-Vis-NIR SEC of Bodipy-C₆₀ and difference spectrum of oxidized minus pristine form (green)

The absorbance spectra of pristine, oxidized and reduced Bodipy-C₆₀ show different features. In the absorption spectrum of the pristine form is possible to distinguish bands attributed both to fullerene (at about 260 nm and 330 nm) and Bodipy (at about 500 nm). A complete reduction of the dyad at -0.7 V causes a decrease and a red shift of the two C₆₀ bands together with the appearance of a NIR band (centred at 1000 nm), giving a spectrum that matches with that observed for C₆₀ mono-anion (black trace in fig. 70).^[14] On the contrary, when the dyad is oxidized its spectrum shows a progressive disappearance of the 500 nm Bodipy band (blue trace in fig. 70).

Difference spectrum obtained by subtraction of the oxidized minus pristine spectrum emphasizes the oxidative variations, with a sharp decrease at 500 nm and minor increases corresponding to shorter and longer wavelengths.

Thus, the spectroelectrochemistry results confirm the voltammetric ones about the main localization of the various redox processes: first reduction centred on fullerene and oxidation on Bodipy.

3.2.3 Time resolved spectroscopy

In collaboration with the group of prof. Paolo Foggi at the LENS of Firenze, transient absorption measurements have been performed at three different wavelengths, exciting mainly the Bodipy moiety at 475 nm, both chromophores at 400 nm and C₆₀ unit at 266 nm.

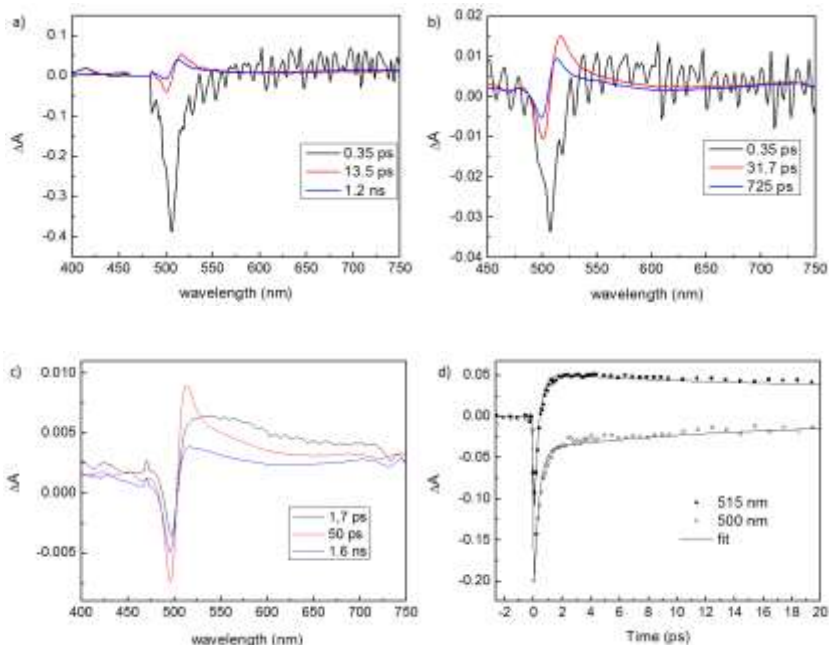


Fig. 71 Time resolved spectra were recorded by an assembled system made with a Ti:sapphire laser oscillator (Spectra Physics Tsunami) pumped by the second harmonic from a Nd:YVO (Spectra Physics Millennia) with a pulse duration of 100 fs. The repetition rate of the output beam was reduced by a mechanical chopper. Excitation pulses at 475 nm was obtained by mixing the output signal of an optical parametric generator-amplifier (OPG-OPA) based on a BBO crystal (TOPAS by Light Conversion, Vilnius, Lithuania) with the residual laser fundamental, while pulses at 266 nm and 400 nm have been obtained respectively by third and second harmonic generation of the fundamental 800 nm laser output.

Excitation at all different wavelengths induces, in time resolved differential spectra, a negative band at 505 nm that can be attributed to Bodipy, as shown by the absorption bleaching, almost completely recovered in 0.35

ps. In all cases the following spectral component is characterized by a small differential signal between 501 and 517 nm that can be attributed, in agreement with SEC measurements, to Bodipy⁺ formation as a consequence of an ultrafast ET occurring in the Bodipy-C₆₀ dyad. The simultaneous fit of all kinetic traces have been analyzed with exponential decay functions, giving a bi-exponential result having a shorter lifetime component of 45 ps and a longer one of 1.7 ns. The total signal bleaching at longer time scales is due to charge recombination.

By cross-checking electrochemical and photophysical measurements, it is possible to notice a good agreement between differential SEC spectrum and photoexcitation transient spectrum, thus implying the occurrence of photoinduced electron transfer from Bodipy to C₆₀, even if at the moment it is not possible to completely exclude alternative mechanisms.

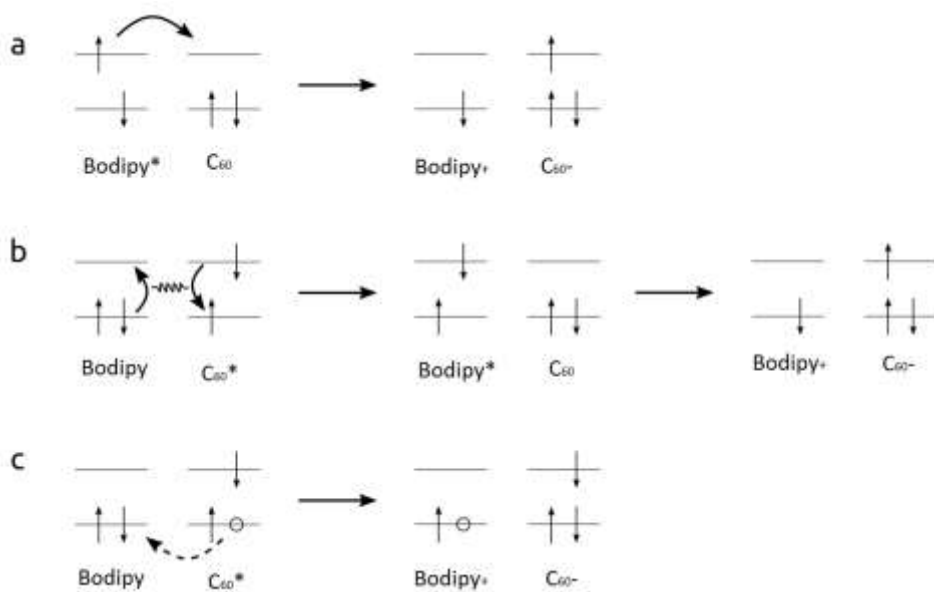


Fig. 72 Four-orbital models of the possible electronic process mechanisms: a) Electron Transfer (ET) from excited Bodipy to C₆₀ moiety; b) Electronic Energy Transfer from the excited C₆₀ to Bodipy moiety, followed by evolution to ; c) Electron Transfer from Bodipy to C₆₀ excited state, interpreted as a hole transfer (HT) from excited C₆₀ to Bodipy

References

- 1 Winter M., Brodd R.J., *CHEM REV*, **2004**, *104*, 4245
- 2 Lee J.-S. et al., *ADV ENERGY MATER*, **2011**, *1*, 34
- 3 Chorkendorff I., Niemantsverdriet J. W., **2003**, *Concepts of Modern Catalysis and Kinetics*, Weinheim, WILEY-VCH Verlag GmbH & Co
- 4 a) Morcos I., Yeager E., *ELECTROCHIM ACTA*, **1970**, *15*, 953; b) Feng X. (Ed.), **2015**, *Nanocarbons for advanced energy conversion*, Vol.2, Weinheim, Wiley-VCH Verlag-GmbH & Co.
- 5 a) Wang S. et al., *ANGEW CHEM INT EDIT*, **2012**, *51*, 4209; b) Dai L. et al., *CHEM REV*, **2015**, *115*, 4823; c) Zeng Y. et al., *ANGEW CHEM INT ED*, **2013**, *52*, 3110; d) Yang Z. et al., *ACS NANO*, **2012**, *6*, 205; e) Sun X. et al., *ACS CATAL*, **2013**, *3*, 1726; f) Tuci G. et al., *ACS CATAL*, **2013**, *3*, 2108
- 6 a) Gong K. et al., *SCIENCE*, **2009**, *323*, 760; b) Panomsuwan G., Saito N., Ishizaki T., *ACS APPL MATER INTERFACES*, **2016**, in press; c) Qu L. et al., *ACS NANO*, **2010**, *4*, 1321
- 7 Wu J. et al., *ACS APPL MATER INTERFACES*, **2015**, *7*, 14763
- 8 a) Maldonado S., Stevenson K.J., *J PHYS CHEM B*, **2005**, *109*, 4707; b) Shao Y. et al., *APPL CATAL B-ENVIRON*, **2008**, *79*, 89
- 9 Ref. 6 Chap 2
- 10 Eckhard K. et al., *PHYS CHEM CHEM PHYS*, 2006, *8*, 5359
- 11 Paolucci F. et al., *JACS*, **1995**, *117*, 6572
- 12 Bruno C. et al., *JACS*, **2008**, *130*, 3788
- 13 Bruno C. et al., *JACS*, 2003, *125*, 15738
- 14 Dubois D. et al., *JACS*, **1991**, *113*, 4364

4 Principles and techniques

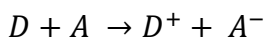
4.1 Principles of Electrochemistry

In order to deeply understand the fundamental role played by electrochemistry in nanotechnology and to better approach problems and possible solutions in this field, it is necessary to give an overview of its basic principles. The aspects of electrochemistry that primary need to be discussed are: electron transfer theory, electron transfer kinetic at the electrode surface (heterogeneous electron transfer) and cyclic voltammetry.

Redox site, made of one or more atoms, is the domain where redox orbital is delocalized and is responsible for molecules electrochemical behavior. Redox states simplification permits to discuss the electrochemical behaviour of families of compounds through localised redox processes and to simply evaluate interactions between different redox centers. Molecules, supermolecules or complexed structures, as proteins, may contain from one to several redox sites spread in different parts of the molecular structure.

4.1.1 Electron Transfer

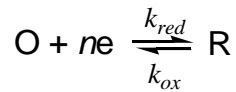
As previously mentioned, ET is an electronic exchange occurring between an electron donor (D) and an electron acceptor (A). When the process involves only two different free in solution species, ET is a bimolecular process.



4.1.2 Kinetic and Mass transport at the Electrode Surface

Kinetic at the electrode surface

The equilibrium between free species close to the working electrode (WE) is perturbed by the applied potential.



Eq. 1 A generic electrochemical reaction, k_{red} and k_{ox} represent rate constants for reduction and oxidation half-reactions and n is the number of exchanged electrons

For a generic O/R electrochemical reduction that has ET rate faster than v , the relationship between species concentration and potential difference ($E-E^0$) is defined by Nernst equation.

$$E = E^{0'} + \frac{RT}{nF} \ln \frac{C_O^*}{C_R^*}$$

Eq. 2 Nernst equation. $E^{0'}$ is the formal potential, a potential adjusted from standard potential (E^0) that takes in account activity coefficients and chemical effects of the medium as ionic strength and complexation; T is the temperature; F the Faraday constant; R the gas constant; $C_{o/r}^*$ is the bulk concentration of species

In this situation total flowing current (i) is the difference between reductive i_r and oxidative i_o currents.

$$i = i_r - i_o = nFAk_{red}C_{O,0} - nFAk_{ox}C_{R,0}$$

Where A is the electrode area and $C_{O/R,0}$ are the concentration at electrode surface-solution interface, where concentrations differ from the bulk. Applied electrode potential affects the kinetic of reactions occurring on its surface, in fact, when energy barriers of both oxidation and reduction are the same the reaction rates are equal and the systems is at equilibrium ($E = E_{eq}$). If the potential is changed in one direction the energy of relative reaction decreases and the net current flows in that direction. Switching to more positive potentials than E_{eq} gives an anodic current, on the contrary a more negative potential than E_{eq} gives a cathodic current. Half-reaction constants depend exponentially on the changing of electronic potential and the equation that describes current response to potential changes is Butler-Volmer equation.

$$i = i_0 \left\{ \frac{C_{O,0}}{C_O^*} e^{\frac{\alpha n F (E - E^{0'})}{RT}} - \frac{C_{R,0}}{C_R^*} e^{\frac{(1-\alpha) n F (E - E^{0'})}{RT}} \right\}$$

Eq. 3 In Butler-Volmer equation α is the charge transfer coefficient, a measure of the activation barrier symmetry, K_0 is the rate constant at the equilibrium and i_0 is the exchange current

Mass Transport

Another limiting factor towards electrode reactions is the transfer of species to and from its surface. This transfer can occur by migration, convection or diffusion processes. Migration is short range electric field effect that can be easily removed using inert electrolyte excess that substitutes consumed charge at interface, decreasing also solution resistance. Convection, forced by stirring or naturally due to thermal gradients, increases the transport of species but, difficult to control, has to be avoided working under thermal-controlled conditions. Differently than

previous cases, diffusion, the movement of neutral and charged species driven only by concentration gradient, cannot be removed but can be treated using Cottrell equation that in the case of conventional spherical electrodes supplies the diffusion-limited current value. If electrode radius is extremely small, comparable or smaller than diffusion layer thickness, mass transport to and from electrode have maximum efficiency and steady state current is reached. These micro or ultra-micro electrodes (UME) are used for fast scan analysis and for low conductive media or biological investigation.

$$\mathbf{a} \quad I_d = nFADC^* \left[\frac{1}{(\pi Dt)^{1/2}} + \frac{1}{r_0} \right] \qquad \mathbf{b} \quad I_{ss} = 4nFD_0C_0^*r_0$$

Eq. 4 a) Diffusion limited current for a spherical electrode with radius r_0 , D is the diffusion coefficient and C^* is bulk concentration; b) steady state current for an UME disk

4.1.3 Techniques and equipments

4.1.3.1 Voltammetry

The simplest technique used to study electron transfer processes is Voltammetry, a potential sweep method that consists in the application, at the working electrode, of a time varying potential. The resulting curve highlights current relative to oxidation and reduction processes. Together with electroactive species behavior it is possible to study double layer capacitance * and absorption-desorption phenomena. Voltammetry can be

* Double layer capacitance is a phenomenon happening at the interface between an electrolytic solution and an electrode when a potential is applied. In this condition close to the electrode two layers of ions of different polarity, separated by a layer of solution, are formed. The accumulation and removal of electrical charges at the interface results in a current flowing through the electrochemical cell. This current, not involved in any reaction, is named double-layer or non-Faradic current.

made with a linear sweep method (LSV) and in cyclic mode, Cyclic Voltammetry (CV).

Linear Sweep Voltammetry

In LSV, the potential is scanned from an initial (E_i) to a final (E_f) chosen value. The slope, defined by dE and dt ratio, defines the potential scan rate (v) that changes when time, necessary to cover the sweep, changes. Resulting voltammograms display the current (I) response as a function of potential (E). Potential scan rate is only one of the factors influencing linear sweep voltammograms shape, which are affected also by ET rate and by the chemical reactivity of electroactive species.

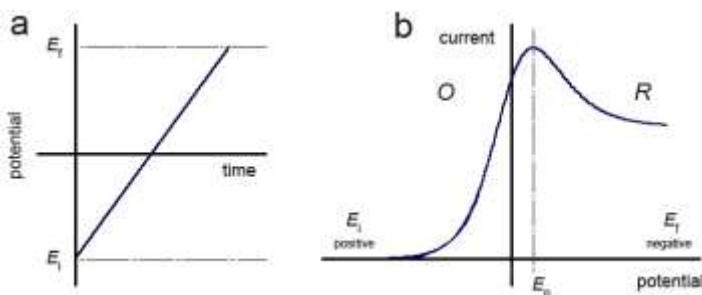


Fig. 73 a) Variation of the applied potential during time in LSV b) typical shape of a linear sweep voltammogram for a reversible reaction

As previously mentioned, for a generic O/R reaction, having ET rate faster than the potential sweep rate, the equilibrium is reached and Nernst equation is valid. When E is swept from its initial value E_i , the equilibrium position at the electrode surface is shifted and the reactant (O) is gradually converted to the product (R) with an electron flow that determines a current. Continuous sweep of the potential is followed by a current flow

that increases until diffusion layer has grown enough to prevent fresh reactant to reach electrode surface with a consequent decrease of current. LSV can show the influence of scan rate on current response. Curves registered at different scan rates maintain the same shape but their total current is proportional to scan rate. Reacted species has more time to diffuse and diffusion layer grows much further in comparison to faster scans, with the result of smaller flux to the electrode and smaller currents. Reaction with a fast ER rate are named reversible and display, at different scan rates, different currents but unvarying position of maximum current (E_p). Reactions characterized by an ET slower than potential scan rate are named quasi-reversible or irreversible electron transfer reactions, the equilibrium is not rapidly established and current response to the applied potential is slower than reversible case, with a shift of E_p .

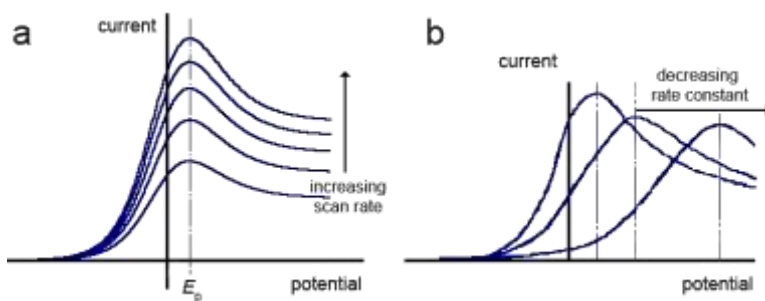


Fig. 74 a) Linear Sweep Voltammograms of a reversible specie (same K_{red}) recorded at different scan rates; b) Linear Sweep Voltammograms for different values of rate constant (K_{red})

Cyclic Voltammetry

Cyclic Voltammetry (CV) is probably the most used technique in electrochemistry and consist in two following and reverse LSV steps.

Potential is cycled from E_i to E_f and, during the following step, back to E_i , in order to form the product and to convert it back to the reactant.

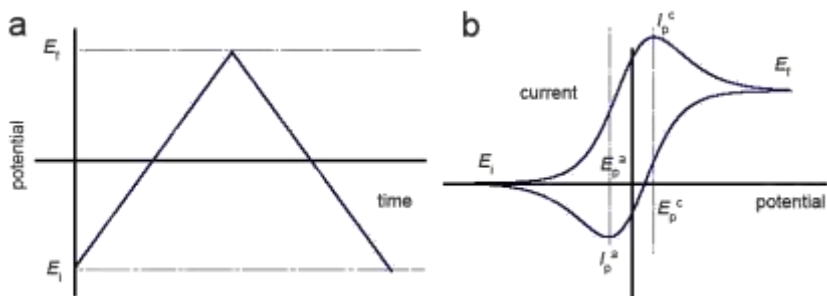


Fig. 75 a) Typical CV potential sweep; b) cyclic voltammetric response for a reversible ET process

Everything mentioned for LSV is still valid but this technique is more powerful because more information can be resumed.

Reversible electrochemical reactions has a potential peak separation defined by the following equation and E_p position is not function of the potential scan rate.

$$\Delta E = E_p^a - E_p^c = \frac{59}{n} mV$$

Moreover peak currents are proportional to the square root of the scan rate and their ratio is equal to one.

$$I_p^a \equiv I_p^c \propto \nu^{1/2} C^* D^{1/2} A \qquad \frac{I_p^a}{I_p^c} = 1$$

As previously mentioned for LSV, also in this case reversible reactions current are proportional to scan rate, while quasi-reversible reactions have

different values of reduction and oxidation rate constants with a shift of E_{eq} to more reduced and oxidized potentials; thus peak separation between forward and back reactions is not fixed but changes as a function of the scan rate. In these cases current is not function of the square root of scan rate but an accurate analysis of the variation in peak position can estimate ET rate constant ^[1].

Rotating Disc Electrode Voltammetry

Rotating Disc Electrodes is basically a common working electrode assembled at the end of a motor that permits its tunable and constant rotation, providing an hydrodynamic system. During rotation, solution is subjected to a forced convective mass transport, perpendicular to electrode surface but parallelly deflected in its close proximity.

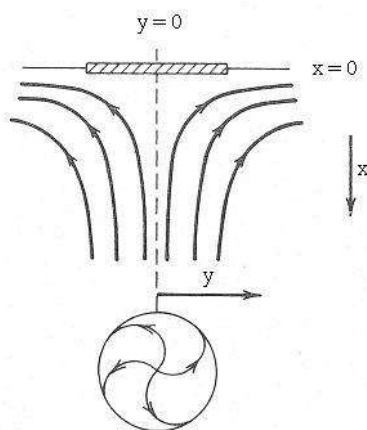


Fig. 76 Representation of a liquid flux in proximity of WE during its rotation

Such operating system presents several advantage, in fact, it provides continuous fresh analyte to the electrode, which is immediately displaced from the surface after electrochemical reaction, quickly reaching steady

state. Moreover, double layer charging as well as mass transfer contribution to electron transfer kinetic are minimized, because mass transfer is higher than diffusion rate. The variation of analyte concentration for RED experiments is expressed by a reaction that put in relation analyte concentration in time with its distance to the electrode, giving the intensity of current in function of time.

$$\frac{\partial[C]}{\partial t} = D_c \frac{\partial^2[C]}{\partial x^2} - v_x \frac{\partial[C]}{\partial x}$$

Eq. 5 Equation relating analyte concentration in time to distance; x is electrode distance, v_x is the rate of liquid flux in x direction and D_c is analyte diffusion coefficient

Alternatively to this complicate equation it is possible to consider analyte diffusion profile at the RDE surface and correlate it to electrode centre distance. When a solid surface is immersed in a liquid, the speed profile forms the so called Prandtl layer, in which speed increases going far from the electrode until reaching the maximum value in the bulk.

$$\delta^* = \left(\frac{\nu y}{u_0} \right)^{1/2}$$

Eq. 6 Prandtl value δ^* , with ν cinematic viscosity of the solution, y is distance from impact point that in this case is the central point of disk electrode, u_0 maximum speed value

In close proximity of electrode surface solution to previous equation gives the relation between impact point and maximum speed value involving electrode rotation angular frequency.

$$\frac{y}{u_0(y)} = 2,62 \omega^{-1}$$

Taking in account common values for D_c , ν and considering current intensity for a plane electrode in stationary conditions, it is possible to obtain Koutecky-Levich equation, which, in limited current condition can be written as:

$$I_{lim} = 0,62 n F A D^{\frac{2}{3}} \omega^{\frac{1}{2}} \nu^{-\frac{1}{6}} C_{bulk}$$

Eq. 7 Koutecky-Levich equation in terms of limiting current, with n number of exchanged electrons, F is Faraday constant, A is electrodic area, D is diffusion coefficient, ω is electrode rotation angular frequency and ν is cinematic viscosity

Koutecky-Levich plot, obtained plotting limiting current versus electrode rotation angular frequency (I_{lim} vs $\omega^{1/2}$), gives several important informations, especially on the number of electrons exchanged during electrochemical processes. The slope of the koutecky-Levich plot is, in fact, in relation with the number of exchanged electrons. [2]

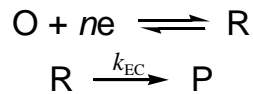
$$b = \frac{1}{0,62 n F C^0 D^{\frac{2}{3}} \nu^{-\frac{1}{6}}}$$

$$n = \frac{1}{0,62 b F C_0 D^{\frac{2}{3}} v^{-\frac{1}{6}}}$$

Eq. 8 *b* is the slope value obtained from Koutechy-Levich equation and *n* the number of exchanged electrons

Electrochemical Induced Reactions

One of the most important application of CV is the study of electrochemically induced reaction that happens when the electrochemical reaction generates as a product the reactant for a sequent chemical reaction.



The mass transport of O and R, in absence of further reactions, is identical but if a chemical reaction that subtract R occurs, this product won't be free for back reaction. For this reason, voltammetric responses for such cases are significantly different from that observed in absence of chemical reactions and can be studied to resume information about k_{EC} .

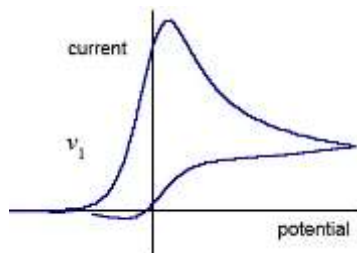


Fig. 77 Example of voltammogram for electrochemically induced reaction

The biggest difference between these and conventional CV is in back peak shape, it depends, in fact, on the amount of product further reacted. If k_{EC} is very small compared to CV timescale, R has no time to react and no difference in shape is visible; at k_{EC} increasing R is subtracted to back electrochemical reaction and back peak decreases, the absence of a back peak can be due to the complete consumption of R. In these cases performing CV at faster scan rates is very useful, in order to give R less time to chemically react during measurement. Moreover, varying the scan rate and analyzing back peak height is possible to calculate k_{EC} value.

4.1.3.2 Electrochemical equipment

The equipment used to perform CVs and electrochemical induced reactions is an home-made fast potentiostatic system controlled by an AMEL model 568 function generator. Measurements performed with ultra-micro electrodes were conducted using a copper homemade Faraday cage in order to minimize electrical noise. The rotating disc voltammetries were performed using a Radiometer Analytical RDE.

Cyclic voltammetries of enzymes were performed using an Autolab PGSTAT20 potentiostat controlled by Nova software, the electrochemical cell was housed in an anaerobic glovebox (Vacuum Atmospheres, $O_2 < 2$ ppm) and gas flow was controlled using mass flow controllers of Sierra Instruments.

Electrochemical cell

The main components of a conventional electrochemical cell are essentially the three electrodes, Working electrode (WE) through which potential is

applied, Counter electrode (CE) that permits current flow, and Reference electrode (RE) that gives the exact potential. Experiment were performed using, as WE, a Pt 125 μm UMEs or ITO glass strips for optical, surface or electrochromic investigation. Different reference electrodes were used for different experiments, Ag quasi reference electrode (QRE), Standard calomel electrode (SCE) or Ag/AgCl 3M electrode, while in all cases a Pt spiral was used as counter electrode. Other fundamental components are, of course, the electrolyte and the solvent. The choose of the correct solvent for our reaction is extremely important, it determines, in fact, the potential window for the electrochemical reaction. The more solvent window is extended the bigger is the possibility to see all the electrochemical processes of the molecule.

Solvent and electrolytes treatments

To avoid any water contamination, that would narrow organic solvents potential window, in our group a suitable technique to obtain dry conditions was developed. Electrolytes are heated under vacuum in sealed electrochemical cells and solvents are previously treated. Solvent treatments consist in dehydrate them on activated Al_2O_3 and store them under vacuum on molecular sieves. Solvent pouring in the cell is performed using trap to trap method and electrochemical measurements are performed in the sealed cell.

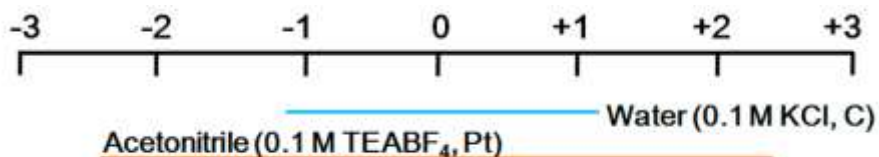


Fig. 78 Example of the potential windows of two different solvents, water and Acetonitrile in different electrolyte solutions whit different WE. The great possible changes are highlighted.

4.1.4 Spectroelectrochemistry

Spectroelectrochemistry (SEC) couples two different techniques, electrochemistry and spectroscopy [3]. SEC is largely used in chemistry, biochemistry and material science. This powerful tool exploits all the spectral changes induced by changing the oxidation state of species. Addition or removal of electrons from an analyte cause electronic and, in some cases, conformational changes; the electronic distribution of the molecule slightly changes and its interaction with incident light changes simultaneously. Such experiments are carried on using a quartz OTTLE (optical transparent thin layer electrode) cell. This particular cell integrates three electrodes, in order to change the potential, and the possibility of register all spectral changes of the electrogenerated species. The problem of thin layer design is the presence of an high uncompensated resistance, due to the distance between working and counter electrode that are not in close proximity. This causes an unhomogeneous distribution of redox species in the OTTLE cell that can be partially overcome using very slow potential scans ($< 5 \text{ mV/s}$).

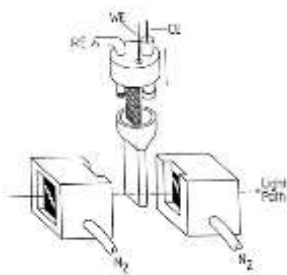


Fig. 79 Sketch of the homemade spectroelectrochemical cell used for our experiments. WE is a Platinum mesh, CE is a Platinum wire separated by a glass frit and RE is an Ag/AgCl 3M

4.1.4.1 SEC Equipment

For SEC experiments the potentiostatic equipment, previously described, was interfaced with a VARIAN Cary 5 UV-Vis-NIR spectrophotometer, used also for electronic absorption spectra recording.

4.2 Raman Spectroscopy

Raman Spectroscopy is a technique born in twentieth century based on the intuition of the Indian physicist Sir Raman. This technique, complementary to infrared spectroscopy, uses laser sources to excite vibro-rotational energies of the molecules. If the sample can be anisotropically polarized, incident energy won't be absorbed but scattered, returning a map of energy transitions, which is typical for a certain molecule [4].

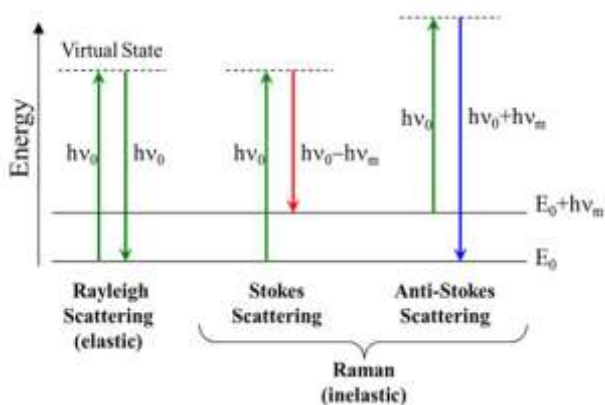


Fig. 80 Sketch of Raman scattering effect

4.2.1 Raman Spectroscopy equipment

Raman Spectra have been recorded using a Ventana 532 Raman Spectrophotometer of Ocean Optics equipped with a 532 nm laser or using an Horiba XploRA One Raman microscope, equipped with 532 and 785 nm lasers.

4.3 LD-TOF Mass Spectroscopy

Laser Desorption Time of Flight Mass Spectroscopy is a soft ionization technique used to determine mass of compounds. The source, usually CO₂ or Argon laser, is addressed to the sample in order to ionize and fragment it. Desorbed charged fragments are generally accelerated by an electric field, deflected and then addressed to a time of flight (ToF) detector. The acceleration impressed to all fragments is the same but different mass/charge ratio cause molecules to have different speed and so a different ToF, which is used to quantify masses [5].

$$P = \gamma m v$$

Eq. 9 In this equation, valid for all particles, P is the pulse impressed to a particle, γ is Lorentz coefficient, m and v are particle mass and velocity

4.3.1 LD-Tof Equipment

LD-Tof have been recorded using a 4800 Plus MALDI TOF/TOE Analyzer of Applied Biosystems.

4.4 Atomic Force Microscopy

Atomic Force Microscopy (AFM) is a scanning probe technique, born thirty years ago, based on Van Der Waals interactions between sample and probe atoms. Since AFM first experiments, it was clear that its reconstruction of surfaces morphology has a nanometric resolution, far below optical diffraction limit, that in some positive cases can reach and atomic resolution. The tip, a tiny probe (ideally mono-atomic ending), is brought

almost in contact with the substrate and during the scan of the sample it is deflected by intermolecular forces. The tip is assembled at the end of a flexible cantilever and each tip bending, due to attraction or repulsion forces, is transmitted to the cantilever which position is monitored by a laser beam with nanometric precision. [6]

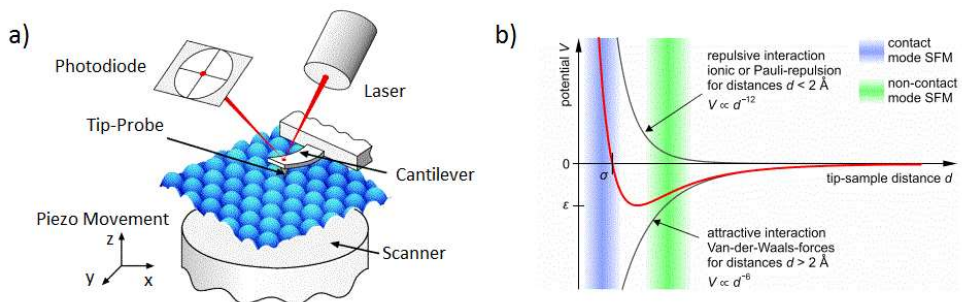


Fig. 81 a) AFM simplified operation mode and b) main forces involved in tip deflection

During sample scan, tip position is continuously adjusted keeping laser beam centred with a feedback system that controls z-movements, of the tip or of the scanner, through a piezoelectric stage. AFM can work in three different modes, contact, non-contact and tapping mode. Contact mode is useful for revealing adhesion properties of the sample but is very dangerous for sample integrity and, for this reason, not commonly used; on the contrary non contact mode gives less information on nanometric structure. The best compromise between these two modes is tapping-mode, which is, in fact, the most used. In tapping mode AFM measurements the tip is subjected to oscillations that allow the tip to interact with the surface without being totally attracted but subjected to an average force.

AFM is an extremely versatile technique that needs no specific sample preparation, coating or vacuum systems and, differently than STM, does

not necessary need a conductive substrate. Together with sample topography, AFM gives important information about its profile distributions and roughness and recently it has been used for surface manipulation, using the probe to modify substrate in specific places. [7] The great advantage of AFM respect to STM is that the substrate is not necessarily conductive.

4.4.1 AFM Equipment

AFM imaging and analysis were performed in air using a Digital NanoScope IIIa Multimode (Veeco, USA), operating in tapping mode with Phosphorous (n) doped Silicon probes.

Samples for AFM imaging were prepared on ultra-flat ITO electrodes as described in previous chapters.

4.5 Scanning electrochemical Microscopy

Scanning electrochemical microscopy (SECM) is a relatively young scanning probe technique, which uses UMEs as probes for collecting amperometric signals. [8] SECM is an extremely versatile technique that is used for analyzing electron, ion and molecule transfer using a wide range of substrates and interfaces. It can be successfully used with glass, metals and polymer substrates in liquid/liquid or liquid/air interfaces, becoming also a powerful tool for biological investigation. [9]

The probe is scanned in close proximity of a surface in order to provide an electrochemical response and identify interfacial physicochemical processes with the great advantage of obtaining both topographical and reactivity informations. [10]

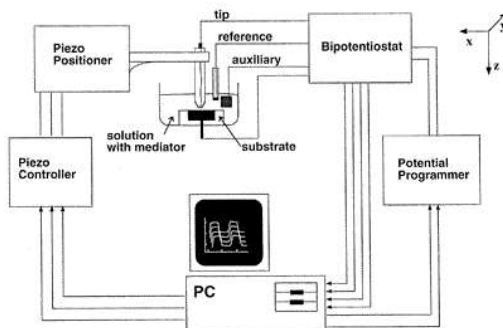


Fig. 82 Simplified plan for SECM set up

Apart from the UMEs, the most important part of this technique is the three dimension positioning system, which actuate tip movements. This system is composed by three stepper motors, used for coarse positioning, and an xyz piezoelectric system that guarantees fine placement and precise repositioning. Spatial resolution of this technique is 1,6 nm versus a maximum travelling distance of 2,5 cm. SECM can operate in different modes:

- a) Tip-generation/Substrate collection mode, in which the probe electrode generates a specie detected by the substrate.
- b) Substrate generation/Tip collection mode where the tip collects current changes due to a specie generated by the substrate, which is extremely useful for studying concentration profiles at the substrate.
- c) Feedback mode that uses current changes due to a redox mediator in solution. Probe is influenced by substrate presence and when carefully approached to the substrate it could detect and higher or lower value for redox current (i_T) respect to steady state current ($i_{T,\infty}$). When electroactive species diffusion is obstructed there would be a decrease in current and a negative feedback, on the contrary if the redox current is regenerated by a

conductive substrate it produces a positive feedback. This mode is particularly useful in the study of heterogeneous samples because it is able to discriminate conductive and insulating regions on the same substrate.

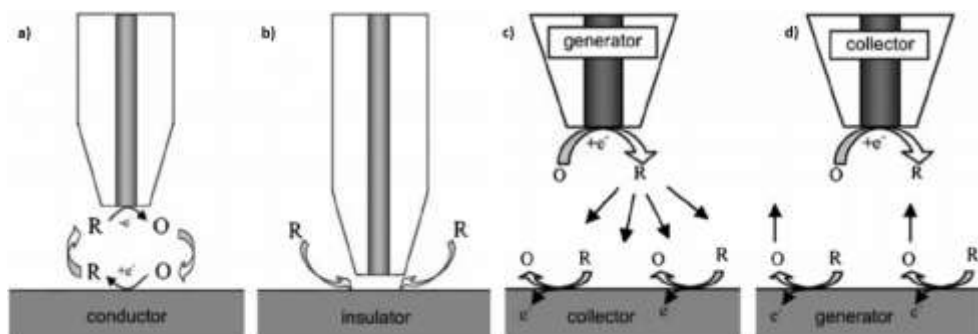


Fig. 83 SECM working modes: feedback mode in presence of a) a conductive and b) an insulating substrate, c) tip-generation/substrate collection and d) substrate-generation/tip-collection

The current obtained during the approach of the tip to the substrate ($i_T = i_T/i_{T,\infty}$) can be related to the approach distance ($L = d/a$) obtaining steady-state current-distance curves, called approach curves. Approach curves gives information about electron transfer constant of substrate reactions thanks to a relationship between limiting current and applied potential.

$$K = \frac{K^0 \exp[-\alpha f(E - E^0)]}{\frac{i_T(L)}{\pi a^2 n F C_0}}$$

Eq. 10 Equation relating diffusion-limited tip current at the normalized tip/substrate distance L [$i_T(L)$] with potential, K is the homogeneous rate constant, K^0 is the standard rate constant, C_0 the redox active specie bulk concentration, α is transfer coefficient and f is a parameter equal to F/RT

4.5.1 SECM Equipment

For SECM experiments a CH Instruments CHI910B apparatus was used with a 10 μm UME Pt tip of CH Instruments, U.S..

4.6 X-ray Photoemission Spectroscopy

X-ray photoemission spectroscopy (XPS), is a surface spectroscopy technique, developed by Siegbahn, that allows sensitive investigation on sample atomic composition, giving information also on its chemical and electronic state. The under vacuum irradiation of the sample, with a suitable energy electromagnetic radiation, causes simultaneous emission of photoelectrons from the first nanometric volume of the sample. Electrons emission is reached only if the energy absorbed by the sample is higher than the electron binding energy, at this point electrons are addressed to an electron multiplier and amplified in order to allows sample identification.

$$E_{binding} = E_{photon} - E_{kinetic} + \phi$$

Eq. 11 $E_{binding}$ is the binding energy of the sample electrons, E_{photon} is the energy of x-ray beam, $E_{kinetic}$ is the measured energy for escaped electrons and ϕ is a parameter depending on the material and the spectrometer

Electron binding energy is typical of every electron ejected from a specific atom (e.g.: 286 eV for Carbon) and can be determined using the already known energy of incident x-rays and the measured kinetic energy of collected electrons. During their way out electrons can interact elastically with the matrix giving peak signals or can have inelastic interactions giving background noise, which increase with the increasing thickness of crossed sample. Each peak area is proportional to the number of atoms present on

the surface and can be expressed in terms of atomic percentage of surface composition. [11]

When an atom is bind to a different one the binding energy of their core electrons is influenced by their chemical bond. Addition or removal of electrons from valence band (reduction or oxidation of the atom) causes, in fact, changes in electrostatic shielding that is translated in a decrease or increase of binding energy with a sequent chemical shift of its original value.

4.6.1 XPS Equipment

X-Ray Photoemission spectra were recorded at room temperature in ultra-high-vacuum conditions (10^{-10} mbar) using a modified VG ESCALAB MKII experimental chamber. Photoelectrons were excited by means of Mg K α photons and collected with a 150 mm hemispherical analyzer in normal emission geometry (overall energy resolution of about 0.8 eV). Samples were pretreated with a mild annealing (50 °C) to remove adsorbed contaminants. All binding energies are referred and calibrated to the Fermi edge of Au plate in electrical contact with the sample.

References

- 1 Bard A.J., Faulkner L.R., **2001**, *Electrochemical methods-Fundamentals and applications*, 2nd ed., New York, John Wiley & Sons, Inc.
- 2 Ref.1
- 3 Kuwana T., Darlington R.K., Leedy D.W., *ANAL CHEM*, **1964**, *36*, 2023
- 4 Raman C.V., *The molecular scattering of light, Noble lecture*, December 11, **1930**
- 5 Chamberlain O., *The early antiproton work, Nobel lecture*, December 11, **1959**
- 6 a) Benning G.K., **1986**, *Atomic force microscope and method for imaging surfaces with atomic resolution*, US4724318A, (Engl.); b)Binning G., Quate C.F., Gerber Ch., *PHYS REV LETT*, **1986**, *56*, 930
- 7 Liu H., Hoepfner S., Schubert U.S., *ADV FUNCT MATER*, **2016**, *26*, 614
- 8 a) Bard A.J., Fan F.-R.F., Lev O., *ANAL CHEM*, **1989**, *61*, 132; b) Kwak J., Bard A.J., *ANAL CHEM*, **1989**, *61*, 1794
- 9 a) Sun P., Laforge F.O., Mirkin M.V., *PHYS CHEM CHEM PHYS*, **2007**, *9*, 802; b) Mirkin M.V. et al., *PHYS CHEM CHEM PHYS*, **2011**, *13*, 21196
- 10 Bard A.J. & Mirkin M.V. (Eds), **2001**, *Scanning electrochemical microscopy*, New York, Marcel Dekker
- 11 a) Turner D.W., Jobory M.I.Ai., *J CHEM PHYS*, **1962**, *37*, 3007; b) Siegbahn K., *Electron spectroscopy for atoms, molecules and condensed matter, Nobel lecture*, December 8, **1981**

5 Conclusions

The aim of this thesis was the investigation and exploitation of some of the less studied properties of Carbon nanomaterials by electrochemistry. Nanomaterials, especially Carbon based ones, are getting more and more importance, thus nanotechnology requires supports from other sciences as electrochemistry.

In the first part of this work the possibility to find a novel pathway for the synthesis of Carbon nanostructures has been investigated. One of the most used way to synthesize polyaromatic hydrocarbons is the intra or intermolecular cyclization of their precursors promoted by chemical oxidation. Using electrochemistry, the simplest way to oxidize species, it is possible to obtain similar results. Chemical and morphological characterization of the obtained aggregates confirm, in fact, the generation of small Graphenic structures and that such an approach is successful.

The second part of my thesis focused on the application of doped and functionalized nanocarbons for energy applications. The extraordinary properties of Fullerene and Graphene can be, in fact, tuned in order to enhance specific properties. Doping Graphene with Nitrogen atoms enhances its electrocatalytic activity towards Oxygen reduction reaction (ORR) with respect to undoped material. This effect is highlighted both by an increase of the reductive current and the decrease of the required overpotential. Coupling Fullerene with an efficient chromophore, as Bodipy, promotes photoinduced electron transfer and the formation of a charge separated state that can be useful to generate an electron current in the external circuit.

Even though electrochemistry is usually identified with the aim of exploring electrical and catalytic properties of materials, it can be also used to investigate other fundamental processes and modify or synthesize new

structures, thus becoming an interface between nano and macroscopic world.